GEOLOGIC AND HYDROLOGIC STUDIES OF SITES HU1A AND HU1B IN HUDSPETH COUNTY, TEXAS

by

C. W. Kreitler, J. A. Raney, W. F. Mullican III,
E. W. Collins, and R. Nativ

Bureau of Economic Geology
W. L. Fisher, Director
The University of Texas at Austin
Austin, Texas 78713

Final report prepared for the
Low-Level Radioactive Waste Disposal Authority
under contract no. IAC(86-87)-1061

April 1987

CONTENTS

FIGURES

Appendix Figures

Tables

Plate (in pocket)

EXECUTIVE SUMMARY

The Bureau of Economic Geology, The University of Texas at Austin, conducted preliminary investigations of the geology and hydrology of northern Hudspeth County for the Texas Low-Level Radioactive Waste Disposal Authority. The Authority had previously identified two sites, HU1A and HU1B, as possible sites for an above-ground disposal facility for low-level radioactive wastes.

Regional and site-specific investigations were conducted to characterize the geology and hydrology of HU1A and HU1B. The two sites are underlain by different bedrock lithologies covered by alluvium, which necessitated drilling for site-specific investigations. Because of the lack of exposed bedrock, studies of the regional geologic setting were used to infer the probable nature of the bedrock geologic environment at each site. Hydrologic studies were predominantly regional because of the limited data available at either site and the availability of water-level data and water samples from previously drilled wells in the region.

Subsurface lithologies at HU1A and HU1B are Precambrian rhyolite porphyry and Cretaceous limestone interbedded with some silty and muddy interbeds, respectively. The rhyolite porphyry is very fractured; the fractures strike in many directions and dip from vertical to horizontal. Most fractures contain no mineral fillings, indicating that they are not sealed. Cretaceous limestone at HU1B is not as fractured as the rhyolite porphyry at HU1A. There is evidence of carbonate dissolution and formation of some solution permeability.

The Babb flexure is north of both sites; however, fractures that are evident away from the inferred margins of the flexure may be related to flexure deformation. The flexure may be the Permian or post-Permian expression of a major pre-Permian strike-slip fault (Hodges, 1975). It is unknown if Cretaceous rocks have been warped

by recurrent movement along the structure.

Regional ground-water flow is from southwest to northeast. The ground-water divide is not located along the Babb flexure but is close to the southern edge of the Diablo Plateau, an escarpment that overlooks the Rio Grande basin. Two aquifers are present, a shallow aquifer in the southwestern area with depths to water generally less than 200 ft (61 m) and a deeper aquifer through most of the region with depths to water of as much as 700 ft (213 m).

Recharge occurs over the entire study area and is not restricted to the updip part of the potentiometric surface in the areas of higher elevation. Tritium occurs in nearly all wells regardless of their location within the regional water table. Most recharge probably occurs during flooding of the arroyos that traverse the plateau. Recharge along fractures permits recently recharged water to move rapidly through a thick unsaturated section. Three separate fracture sets were identified during pumping tests (PT) no. 1 and no. 6 of of this study. Because of the fracture control on ground-water flow, flow velocities cannot be estimated but are expected to be high. Discharge is either by evaporation on the salt flats or through pumping wells.

The shallower aquifer may or may not be present at either site, though it is not used in the vicinity of either site. Depth to ground water in the deeper aquifer beneath the sites is probably greater than 600 ft (183 m). Fractures in bedrock beneath the arroyos are important pathways for recharge in the vicinities of the sites as has been documented through chloride analysis and vadose permeability tests.

Flooding down Antelope Draw, which bounds site HU1A, may be very intense for short durations, and consideration should be given to any siting with respect to this potential flooding.

INTRODUCTION

In June 1986 the Bureau of Economic Geology (BEG) was asked by the Texas Low-Level Radioactive Waste Disposal Authority to conduct a preliminary study of the geology and hydrology of two sites being considered for construction of a low-level radioactive waste repository. Both sites are located in northern Hudspeth County, Texas.

The rocks below potential sites are Precambrian rhyolite porphyry and Cretaceous limestone interbedded with some sandstone and mudstone. The geologic investigations provide data for evaluation of the general geologic framework of the proposed sites and provide site-specific data for evaluation of the physical and structural character of the rock units.

The hydrologic investigations address the following questions:

(1) Are there any regional aquifers below these sites? Aquifers are defined as water-bearing formations capable of producing water from a well.

(2) What is the thickness of the unsaturated zone (the depth to the uppermost regional ground-water table) at each site? What is the permeability of the unsaturated zone? Are there fracture zones in the unsaturated zone in which water and solute migration could be rapid?

(3) What are the flow directions of ground water in the aquifers?

(4) What is the residence time of water in the regional aquifers?

(5) What are the methods and rates of recharge to these aquifers? How much of the recharge comes from direct precipitation and surface flooding? How much recharge water could percolate through the vadose zone?

(6) Where are the discharge points (natural and wells) of these aquifers, and what is their distance from the site?

Hydrogeologic study of both the unsaturated and saturated zones at each site was conducted to provide an initial assessment of these questions.

C. W. Kreitler and J. A. Raney are co-principal investigators for the hydrologic and geologic studies. W. F. Mullican III investigated the hydrology of the sites and supervised drilling programs. E. W. Collins studied the geology of the area. R. Nativ assisted with the interpretation of the chemical and isotopic analysis and the pumping tests. We are appreciative of the cooperation of the local landowners during our investigations.

SITE INVESTIGATIONS

Location

The Texas Low-Level Radioactive Waste Disposal Authority selected two sites (HU1A and HU1B) within an area in Hudspeth County, Texas, for consideration as the location of a low-level radioactive waste repository. The sites are on land owned and administered by The University of Texas System and are located approximately 15 mi (24 km) west of the Salt Basin in the vicinity of the Pump Station Hills on University Block K, sections 5, 6, 7, and 8, and University Block N, sections 16, 17, 31, 32, and 33, respectively (fig. 1). HU1A and HU1B are in the Hueco Station and Scratch Ranch 7.5-minute quadrangles, respectively. Site HU1A is 2 mi (3 km) south of the intersection of U.S. Highway 62-180 and Ranch-to-Market Road 1111. Site HU1B is about 1.5 mi (2.4 km) south of Scratch Ranch. Precambrian rhyolite porphyry bedrock is partly covered by alluvium at HU1A, whereas at HU1B alluvium covers Cretaceous limestone interbedded with some sandstone and mudstone. Both sites can be accessed from Ranch-to-Market Road 1111.

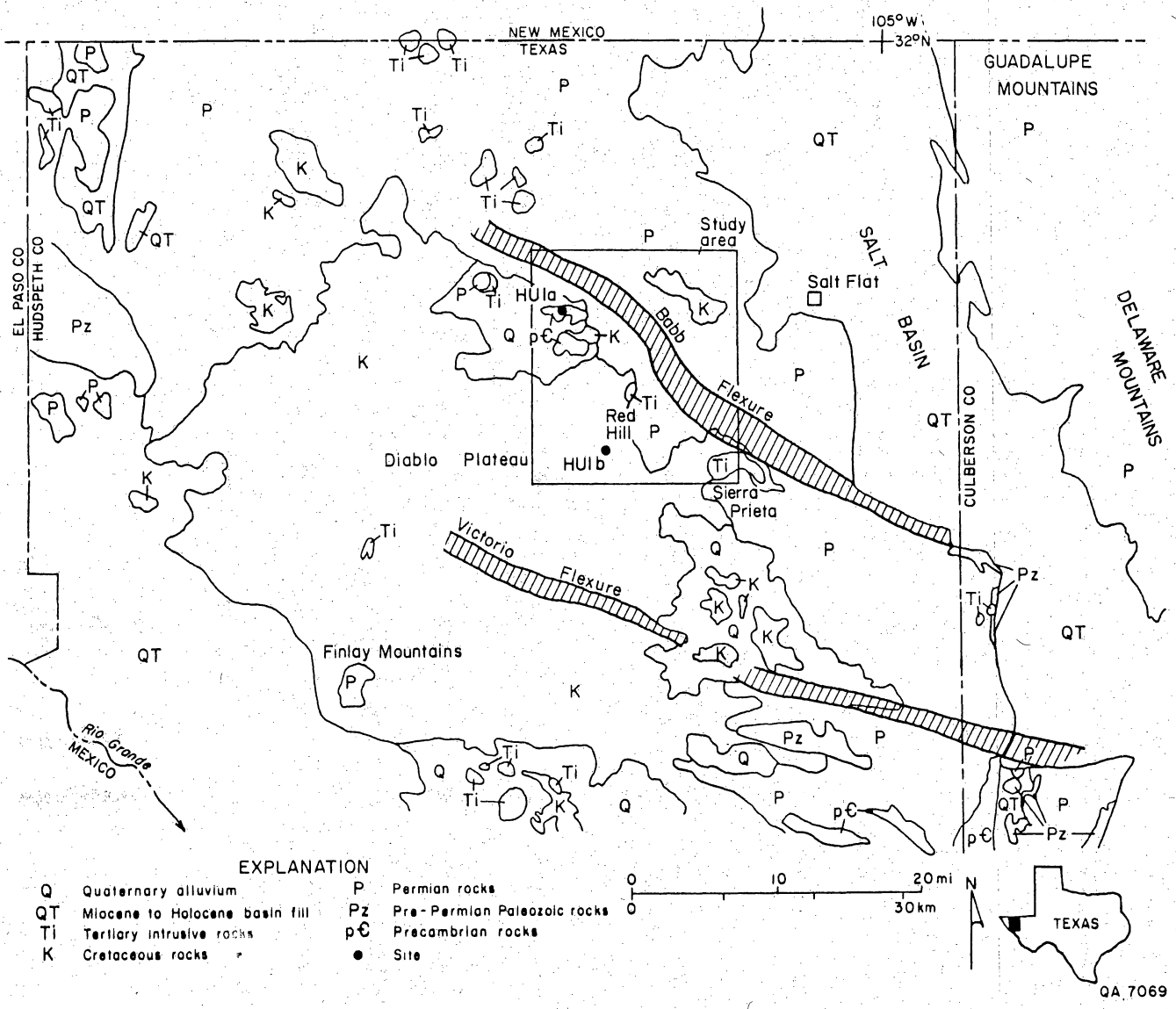

Figure 1. Location and regional setting of Pump Station Hills study area, Hudspeth County, Texas. Geology from Henry and Price (1985).

Methods

Aerial photographs at a scale of 1:12,000 (1 inch = 1,000 ft, 1 cm = 120 m) were acquired for a large area in the vicinity of the sites. The interpretations of the aerial photographs were compared with published maps. Field studies refined interpretations made from aerial photographs, and fracture data were collected.

Water-level data for the regional aquifers near the proposed sites were collected from several sources and are presented in appendix 1. Thirty-five static water-level values were obtained either by direct measurement using an electric water probe and steel tape, or from information provided by the well owner (fig. 2). Data for the Dell City and Salt Basin areas were taken from Texas Natural Resources Information System (TNRIS) computerized data base and from Nielson and Sharp (1985) and Boyd and Kreitler (1986). Information on the Fort Hancock area, southwest of the study sites, had previously been collected by BEG personnel (Kreitler and others, 1986b).

No data were available on porosities, hydraulic conductivities, or transmissivities of the unsaturated or saturated zones at the sites.

Drilling Programs

The first drilling program, conducted in July-August 1986 at sites HU1A and HU1B, was designed to provide data on the subsurface stratigraphy and rock characteristics at the sites and to drill boreholes for hydrologic testing. The second drilling program, accomplished in January 1987, was designed specifically for chloride profile investigations at HU1B. This second program was performed with the BEG drilling rig. Results of these investigations are included in the recharge section of this report and in appendix 9.

Byrl Binkley, drilling contractor, drilled four test holes to complete initial drilling objectives. At each site a 150-ft (45.7-m) deep stratigraphic test hole was drilled (HU1A-BEG#1 and HU1B-BEG#1), and continuous core from top of bedrock to total depth was recovered to characterize the nature of the subsurface bedrock. The top of unweathered bedrock was determined at each site, and 15 ft (4.5 m) west of each stratigraphic test hole, a permeability test hole was cored (HU1A-BEG#2 and HU1B-BEG#2) to the top of unweathered bedrock. Casing was run to bottom and cemented to surface in each permeability test hole, and an additional 30 ft (9.1 m) was cored below casing. Constant head permeability tests were conducted for the intervals below casing to determine the hydraulic conductivity of the unweathered section of the unsaturated zone (appendix 2).

The permeability test holes were drilled with fresh water circulated only once instead of using a gel-based mud system. This procedure was used to reduce potential contamination by mud-cake buildup on the walls of the borehole. The nature of the rhyolite and dense limestone prevented use of air for circulation as tremendous heat buildup occurred on the coring bit while drilling with compressed air. It was determined that drilling with compressed air was not feasible, and the system was converted to fresh water.

Previous drilling of the shallow subsurface (Dames and Moore, 1985) at both sites documented variability in thickness of bedrock cover and depths of weathered bedrock. Permeability tests on such heterogeneous units may be of only local significance and not applicable to the site as a whole. Unweathered rhyolite penetrated at HU1A, however, may be very homogeneous (assuming uniform fracture distribution), and permeability tests on this interval could be applicable to a larger area. The heterogeneity of alluvial cover and weathered bedrock strata at HU1B also indicates that permeability tests on these units are of only local significance.

Figure 2. Surface drainage and location of wells within the study area. Thirty water level measurements were taken, as were 30 ground-water samples that were analyzed for general chemistry, $\delta^{18}O$, δD, tritium, $\delta^{34}S$, $\delta^{13}C$, and ^{14}C. Water level data and chemical analyses of ground water in the Del City area taken from Texas Natural Resources Information System (TNRIS), Nielson and Sharp (1985), and Boyd and Kreitler (in press).

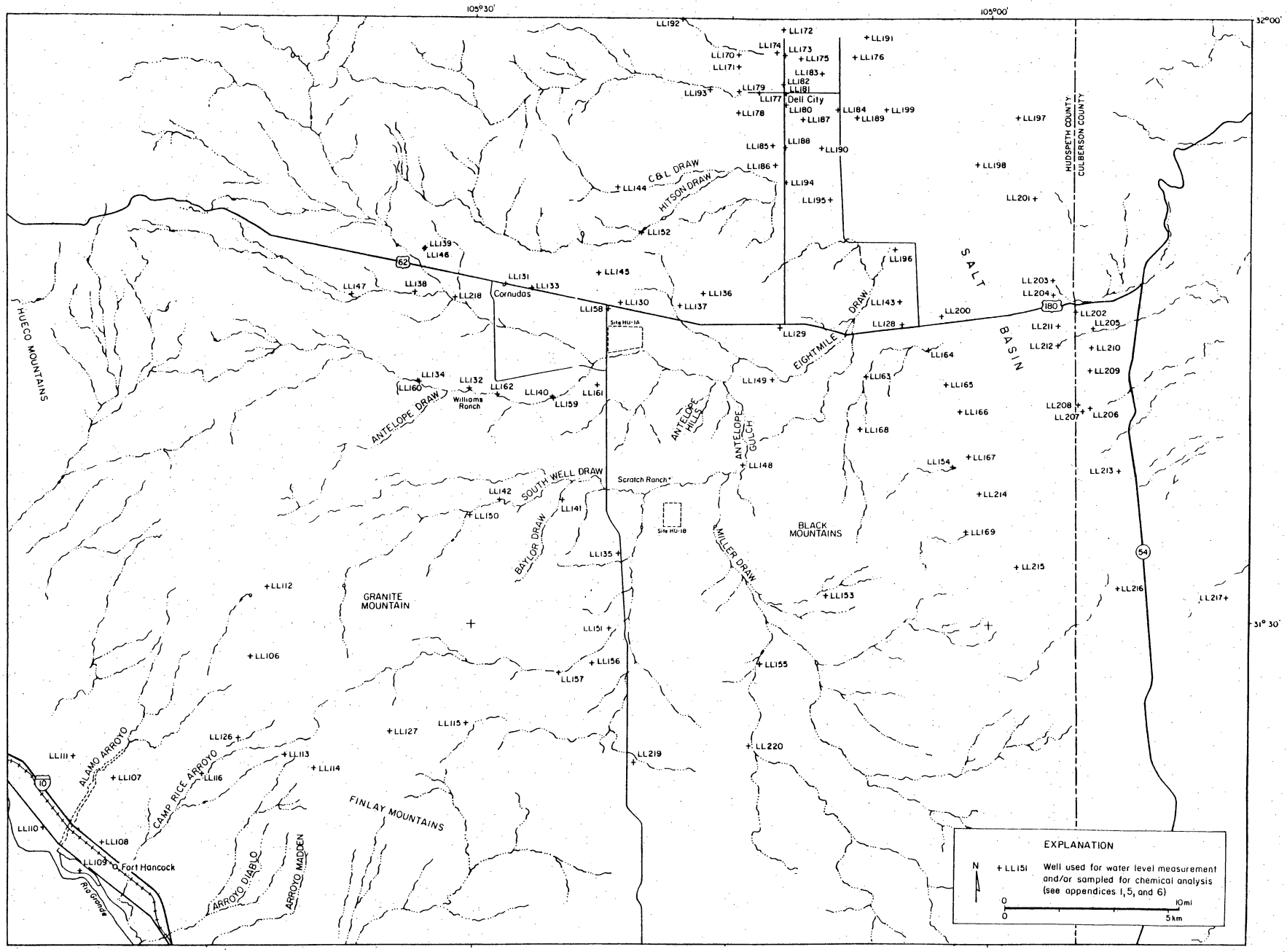
105°30'
105°00'
32°00'
31°30'
LL192
LL172
LL191
LL174
LL173
LL175
LL176
LL170
LL171
LL183
LL182
LL181
LL179
LL193
LL177
Dell City
LL180
LL178
LL184
LL199
LL187
LL189
LL197
LL185
LL188
LL190
LL186
LL198
C&L DRAW
LL144
HITSON DRAW
LL194
LL195
LL201
HUDSPETH COUNTY
CULBERSON COUNTY
LL152
LL139
LL146
62
LL196
SALT
DRAW
LL147
LL138
LL131
LL133
LL145
LL203
LL204
180
LL218
Cornudas
LL136
LL130
LL137
LL143
LL200
LL202
LL205
LL158
Site HU-1A
LL128
LL129
LL211
LL212
LL210
HUECO MOUNTAINS
EIGHTMILE DRAW
BASIN
LL164
LL209
LL134
LL160
LL132
LL162
LL140
LL161
LL149
LL163
LL165
Williams Ranch
LL159
ANTELOPE DRAW
ANTELOPE HILLS
ANTELOPE GULCH
LL208
LL207
LL206
LL166
LL168
LL148
LL154
LL167
LL213
SOUTH WELL DRAW
Scratch Ranch
LL142
LL214
LL141
LL150
Site HU-1B
BLACK MOUNTAINS
LL169
BAYLOR DRAW
MILLER DRAW
LL135
54
LL215
LL112
LL216
GRANITE MOUNTAIN
LL153
LL217
LL151
LL106
LL156
LL155
LL157
LL115
LL126
LL127
LL111
LL113
LL219
LL220
ALAMO ARROYO
LL114
LL107
LL116
CAMP RICE ARROYO
10
FINLAY MOUNTAINS
LL110
LL108
LL109
Fort Hancock
Rio Grande
ARROYO DIABLO
ARROYO MADDEN
EXPLANATION
N
+ LL151 Well used for water level measurement and/or sampled for chemical analysis (see appendices 1, 5, and 6)
0
10mi
0
5km

Two permeability tests were performed during this study in the unsaturated zone. At HU1A the tested interval is the upper 30 ft (9 m) of unweathered rhyolite, and at HU1B the tested interval is the upper 30 ft (9 m) of unweathered Cretaceous Campagrande limestone. Seven pumping tests in the saturated zone of the Diablo Plateau (assumed to be in Permian Victorio Peak - Bone Spring strata) were conducted. Data from the permeability tests and pumping tests are presented in appendices 2 and 3, respectively.

Geologic and hydrologic data were obtained from eight water wells drilled and operated by the El Paso Natural Gas Company (EPNG) for their now-abandoned Pump Station #2 (appendix 4). Pump Station #2 is located 7.5 mi (12.2 km) west-southwest of site HU1A.

Chemical and Isotopic Analysis

Chemical analyses of ground water from wells in the Dell City area and in the Salt Basin were obtained from Texas Water Commission files. Data for wells near sites HU1A and HU1B were unavailable, but 30 active water wells within the study region were sampled. All samples were analyzed for general chemistry, $\delta^{18}O$, δD, tritium, $\delta^{34}S$, $\delta^{13}C$, and ^{14}C. Chemical analyses were performed by Mineral Studies Laboratory (BEG); ^{14}C analyses, by Radioisotopes Laboratory, Balcones Research Center (UT-Austin); other isotopic analyses ($\delta^{18}O$, δD, tritium, $\delta^{34}S$, and $\delta^{13}C$), by Environmental Isotope Laboratory, University of Waterloo, Ontario, Canada. Methods and applications of isotopic data ($\delta^{18}O$, δD, $\delta^{34}S$, $\delta^{13}C$, tritium, ^{14}C) are discussed in Kreitler and others (1986b; appendix 3). Water temperatures were measured at the sampling sites. All chemical and isotopic data collected during this study are reported in appendix 5. Additional data used in this report from Kreitler and others (1986b) and Texas Water Development Board (1985) are in appendix 6.

REGIONAL SETTING AND SEISMICITY

The study area lies within the Diablo Plateau region, Hudspeth County, Trans-Pecos Texas, at the eastern part of the Basin and Range structural province (fig. 1). This province consists of topographically high ranges separated by major normal faults from adjacent topographically low basins. Structural development of the province began about 24 million years ago (mya) during east-northeast-oriented extension. Faulting and associated relative subsidence of the basins began at that time and continue to the present. The basins were progressively filled by detritus eroded from the adjacent ranges. The study area lies about 15 mi (24 km) west of the Salt Basin, a large Basin and Range graben at the eastern edge of Hudspeth County.

No detailed studies of seismicity are available for Hudspeth County. Information on possible seismic activity in these areas is based on a consideration of the tectonic setting of Trans-Pecos Texas, including the presence of Quaternary fault scarps, and on recent seismicity in adjacent areas and in the Basin and Range structural province. Quaternary fault scarps occur throughout much of Trans-Pecos Texas and are abundant in the Salt Basin (Muehlberger and others, 1978; Henry and Price, 1985). Quaternary scarps have not been found within the study area, although some parallel the eastern part of the Babb flexure in the Salt Basin (Goetz, 1977). The west-northwest-trending Babb flexure extends from the Salt Basin across the study area (fig. 1).

Recent compilations of regional seismicity data include (1) the entire Basin and Range province (Askew and Algermissen, 1983), (2) southeastern New Mexico (Sanford and Toppozada, 1974), and (3) southern Culberson County and adjacent areas (Dumas, 1980). Askew and Algermissen (1983) show six epicenters in the Trans-Pecos region between 1803 and 1977, two with Richter magnitudes (surface waves) of

5 and 6. Both of these latter earthquakes occurred near Valentine, Texas; one, the 1931 Valentine earthquake, had a modified Mercalli intensity of VIII and was the strongest reported earthquake in Texas. The 1955 earthquake near Valentine had a modified Mercalli intensity of IV (Reagor and others, 1982). Dumas (1980) detected about 300 earthquakes, all with magnitudes less than 3.7, between 1976 and 1980 near the site of the Valentine earthquake. Dumas (1980) also identified a seismically active area along the eastern margin of the Salt Basin near abundant Quaternary fault scarps. However, this area could not be located precisely because it was outside the seismic network. Sanford and Toppozada (1974) listed 11 felt earthquakes prior to 1961 and 6 instrumentally detected quakes between 1961 and 1972 in southeastern New Mexico and West Texas. Askew and Algermissen (1983) identified a swarm of earthquakes, all having Richter magnitudes of less than 4, centered near Juarez, Chihuahua, Mexico, about 45 mi (70 km) west of Hudspeth County.

Geology

The sites lie on the Diablo Plateau, west of the Salt Basin. Rocks in the area range in age from Precambrian to Recent (fig. 1 and plate). Strata most important to this investigation are Precambrian rhyolite porphyry at site HU1A and Cretaceous limestone interbedded with sandstone and mudstone at site HU1B.

Precambrian rhyolite porphyry crops out in the northwestern part of the study area in low rounded hills (plate). The petrology and age of the rhyolite porphyry were discussed by King and Flawn (1953), Stead and Waldschmidt (1953), Flawn (1956), Masson (1956), and Wasserburg and others (1962). The dark red rhyolite porphyry has pink feldspar and clear glassy quartz phenocrysts that range in size from

0.1 to 0.4 inches (0.2 to 1.0 cm). Chlorite is a common alteration product. It is unknown if the rhyolite is intrusive or extrusive. Masson (1956) suggested that a complex of both extrusive and intrusive Precambrian rocks is present. The general age determined by strontium isotopic analysis is 1,060 mya, whereas the age determined by the lead-uranium method on zircon is 1,150 to 1,200 mya (Wasserburg and others, 1962). Lithologic descriptions of core from HU1A are in appendix 7. Core and good exposures in an abandoned quarry indicate that fractures are locally abundant. The fractures are discussed in the structure section of this report.

Permian strata that crop out in the study area include the Victorio Peak limestone and undivided Leonardian rocks (plate). These thin- to thick-bedded fossiliferous limestones and dolomites have interbeds of sandstone and siltstone (King, 1965). The Permian Cutoff shale also crops out in the eastern part of the study area, and the Hueco limestone is present on the south side of Sierra Prieta in the southeastern part of the area.

Cretaceous strata include the Campagrande Formation, Cox sandstone, and Finlay Formation (plate). Washita Group marl and fossiliferous shale also crop out at Sierra Prieta. The Campagrande Formation in the study area consists of thin-bedded, nodular, partly conglomeratic limestone with marl and clay interbeds (Barnes, 1983). It is commonly mottled yellow and red. The Cox conformably overlies the Campagrande Formation and consists of siltstone, sandstone, shale, and fossiliferous limestone (Barnes, 1983). Throughout most of the study area the Campagrande and Cox are poorly exposed and are undivided (plate). Test holes at site HU1B penetrate both Cox and Campagrande strata. Core descriptions are in appendix 7. Overlying the Cox are thick- to thin-bedded fossiliferous limestone interbedded with marl, shale, and sandstone of the Finlay Formation (Albritton and Smith, 1965; Barnes, 1983).

Two Tertiary intrusive bodies are present in the study area. The Red Hills (Antelope Hills) intrusion lies in the central part of the area and is about 6 mi (10 km) southeast of HU1A and 4 mi (6 km) north of HU1B (plate). The quartz trachyte intrusion is locally discordant but generally resembles a sill (Sullins, 1971). The intrusion has a Rb-Sr age of 28.2 $\pm$ 3.2 mya (Haley, 1971). The Sierra Prieta syenite intrusion (Black Mountains) lies 6 mi (10 km) east of HU1B. Hodges (1975) described Sierra Prieta as a "trap door" intrusion overlain by Permian strata and floored by Cretaceous rocks. Emplacement of the syenite intrusion was 35.0 $\pm$ 2.0 mya (Hodges, 1975).

Quaternary alluvial deposits cover much of the bedrock in the area. The alluvium consists of silt and sand with some pebbles and cobbles derived from local bedrock. Caliche layers up to 3 ft (1 m) thick occur near the surface.

Structure

Babb Flexure

The Babb flexure is a west-northwest-trending monocline with downward displacement of strata on the north side of the flexure (King, 1949, 1965). It can be traced about 40 mi (65 km) northwestward from the Salt Basin across the study area and is approximately 1 to 2 mi (1.5 to 3 km) wide (fig. 1 and plate). Permian rocks exposed on the flexure usually dip 10° to 15° north. The Victorio Peak Formation is displaced about 1,000 ft (305 m), and the Cutoff shale occurs only on the north side of the flexure (east of the study area). An angular unconformity exists between Permian and Cretaceous strata. Cretaceous rocks are not well enough exposed to determine if they have been warped by recurrent movement along the structure. Hodges (1975) mentioned that the flexure may be the Permian or post-Permian expression of a major pre-Permian strike-slip fault. Basement relief across the flexure could be greater than 4,500 ft (1,370 m) based on the difference in

elevation between exposed Precambrian rhyolite porphyry and the Jones No. 1 Mowry test hole, located 12 mi (19 km) northeastward, that bottomed in Ordovician strata at 500 ft (150 m) below sea level. The great amount of basement relief across the flexure indicates that the basement may be faulted.

Faults, Folds, and Joints

Faults present in outcrop are associated with the two Tertiary intrusions and do not extend far from the extrusive bodies. An east-west-trending anticline occurs west of Sierra Prieta. The anticline could have been caused by an unexposed intrusion that warped the overlying strata during emplacement. The buried intrusion may be related to the nearby Sierra Prieta intrusion.

Minor faults, flexures, and zones of closely spaced joints are mapped in well-exposed Permian strata in the northeastern part of the study area (plate). Displacement across the minor normal faults and flexures is commonly a few feet. Joint spacing in the fractured zones is as great as 10 joints per 3 ft (1 m) for limestone beds 1.5 ft (0.5 m) thick. Most of the fractured zones are about 6 ft (2 m) wide. These minor structures are probably related to the regional deformation along the Babb flexure but occur in strata well beyond the margins of the regional flexure.

Joints and minor normal faults also occur in the Precambrian rhyolite porphyry. Joint spacing of nearly vertical joints locally approaches 6 joints per 3 ft (1 m). Many of the joints extend vertically throughout the 15 to 20 ft (6 m) height of available exposures. Subhorizontal joints with dips of less than 30° also are abundant. Iron staining is a common feature on the joint surfaces, indicating that the joints have acted as ground-water conduits. Limonite and hematite stains also occur on fracture surfaces in core, and some fractures are filled with dolomite and/or

calcite (appendix 7). Fifty percent of the rhyolite porphyry core from site HU1A is fractured (appendix 7). Fractures in the core have dips ranging from horizontal to vertical, similar to fractures observed in outcrop.

Nearly vertical joints in the Precambrian rhyolite porphyry have multiple strike orientations (station 2 on the plate, and fig. 1). Three minor normal faults present in the rhyolite strike west-northwestward, similar to the regional trend of the Babb flexure. Permian and Cretaceous strata usually have two major joint sets that vary in strike regionally across the area (plate). Across most of the study area, nearly vertical joints strike northwest at 300° to 340° and northeast at 050° to 070° (stations 2, 3, 4, and 5, plate). North of Sierra Prieta, joints striking 010° to 030° are also common (station 6, plate). West of Sierra Prieta, joints strike north-northwest at 330° to 000° and east-west at 250° to 290° (stations 7 and 8, plate). The east-west trend parallels the anticline axis and faults at Sierra Prieta. Joints at site HU1B may strike in the same direction as joints in bedrock at stations 7 and 8 (plate). Core from test holes at HU1B was not as fractured as core from HU1A.

HYDROLOGIC SETTING

Surface Flow

HU1A

All surface streams in this region are ephemeral and, except for small local depressions, discharge east of the sites into the Salt Basin (fig. 2). Antelope Draw, one of the larger ephemeral streams in the area, is located 1.5 mi (2.4 km) south of

HU1A. Dames and Moore (1985) report that this draw drains more than 650 mi^2 of the Diablo Plateau west of the site. Final discharge of Antelope Draw is into Eight Mile Draw, which discharges into the Salt Basin approximately 18 mi (28.9 km) east.

During field activities for this study, several thunderstorms occurred. Flooding of Ranch-to-Market Road 1111 created a body of water 2 ft (0.6 m) deep and as much 200 to 300 ft (60 to 91 m) across (fig. 3). Duration of the flooding was very brief, and the road became passable almost as soon as rainfall terminated.

A smaller unnamed draw in the northern part of this site drains a very small area and is not considered as potentially hazardous as the larger draws. The National Flood Insurance Rate Map (FIRM) for HU1A (Community-panel number 480361 0400 B) (fig. 4) classifies both Antelope Draw and this smaller unnamed draw as Zone A, defined as areas of 100-year flood; base flood elevations and flood hazard factors were not determined. The site itself is classified as Zone C, defined as areas of minimal flooding.

HU1B

The northern and western portions of HU1B are within the mapped floodplain of Antelope Gulch, a large ephemeral draw that discharges into Antelope Draw several miles to the north (FIRM, Community-panel number 480361 0550 B) (fig. 5). This draw is also classified as Zone A, and the remaining area is mapped as Zone C (U.S. Department of Housing and Urban Development, 1985).

Methodologies utilized by the National Flood Insurance Program (NFIP) to classify potential areas of flooding may be divided into three basic types: (1) existing sources, such as the U.S. Army Corps of Engineers; (2) USGS flood-prone area quadrangles; and (3) normal depth equations actually calculated for specific areas.

Figure 3. Photograph of flooding at Antelope Draw where it crosses Ranch-to-Market Road 1111. The flood created a body of water 2 ft (0.6 m) deep and as much 200 to 300 ft (60 to 91 m) across. Duration of flooding was very brief, and the highway became passable almost as soon as rainfall terminated.

Extensive field investigations were conducted during January 1987 to determine the extent of flooding at HU1B, which resulted from heavy precipitation events observed in 1986. The main area of interest was Antelope Gulch, to the west and north of HU1B. Observations in this area did not locate any physical evidence of a previous flood event outside of the rather poorly defined arroyo. Other than the presence of the arroyo itself, no real evidence was recorded of flooding within the arroyo. Evidence indicates that actual flooding within the site boundary of HU1B would be of only minimal impact and engineering barriers constructed at the site would be sufficient to control future flood events.

Unsaturated Zone

The thickness of the unsaturated zone in the study area ranges from 3 ft (0.9 m) in the salt flats to 790 ft (240 m) in well LL138 (fig. 6). The unsaturated zone is made up of Cenozoic alluvium and colluvium, Cretaceous sandstones and limestones, Paleozoic carbonates and clastics, and Precambrian rhyolites.

Vertical permeabilities of cores through the alluvial cover at HU1A range from 2×10^{-4} to 2×10^{-5} cm/sec (63.072 to 6.3072 m/yr)(Dames and Moore, 1985). In situ horizontal permeability measurements from the upper 30 ft (9.1 m) of unweathered bedrock (Precambrian rhyolite) indicate a hydraulic conductivity value of 2.59×10^{-5} cm/sec (8.19 m/yr) (appendix 2). This value falls within the range of fractured igneous and metamorphic rocks as reported by Freeze and Cherry (1979, their table 2.2).

Vertical permeabilities of cores through the alluvial cover at HU1B range from 7×10^{-4} to 4×10^{-6} cm/sec (220.752 to 1.2614 m/yr)(Dames and Moore, 1985). In situ horizontal permeability measurements taken on the upper 30 ft (9.1 m) of

Figure 4. Flood Insurance Rate Map (FIRM) for area around site HU1A (Community-panel number 480361 0400 B). Both Antelope Draw and a smaller unnamed draw are enclosed as Zone A, defined as an area of 100-year flood. Base flood elevations and flood hazard factors were not determined. The site itself is classified as Zone C, defined as area of minimal flooding (U.S. Department of Housing and Urban Development, 1985).

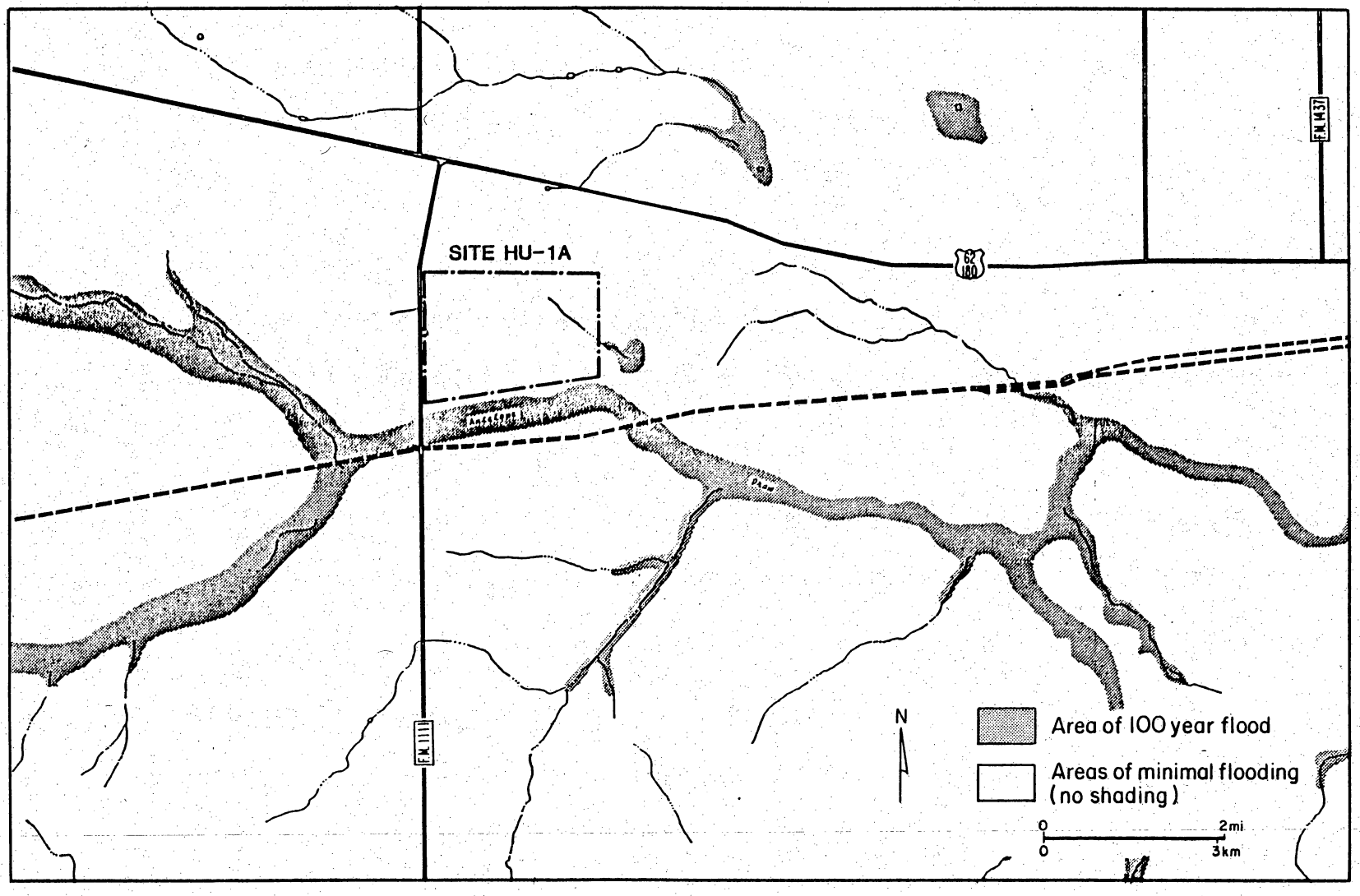
SITE HU-1A
F.M. 1437
62
180
F.M. 1111
N
Area of 100 year flood
Areas of minimal flooding
(no shading)
0
2mi
0
3km

Figure 5. Flood Insurance Rate Map (FIRM) for area around site HU1B. The northern and western portions of HU1B are within the mapped floodplain of Antelope Gulch, a large ephemeral draw that discharges into Antelope Draw several miles to the north (FIRM, Community-panel number 480361 0550 B). This draw is also classified as Zone A, defined as area of 100-year flood. The remaining area is mapped as Zone C, defined as area of minimal flooding (FIRM, 1985).

SITE HU-1B
N
Area of 100 year flood
Areas of minimal flooding
(no shading)
0
2mi
0
3km

Figure 6. Map showing potentiometric surface elevations in the study area. Land surface elevation changes from 3,450 ft (1,050 m) at the salt flats and Dell City area to greater than 4,500 ft (1,370 m) in higher regions in the west, but the elevation of the water table in Aquifer A rises only 200 ft (61 m) (from 3,445 ft to 3,650 ft, or 1,050 to 1,113 m) across the same region, resulting in increasing depth to water at higher elevation. Thickness of the unsaturated zone in the study area ranges from 3 ft (0.9 m) in the salt flats to 702 ft (214 m) in well LL132 in the west.

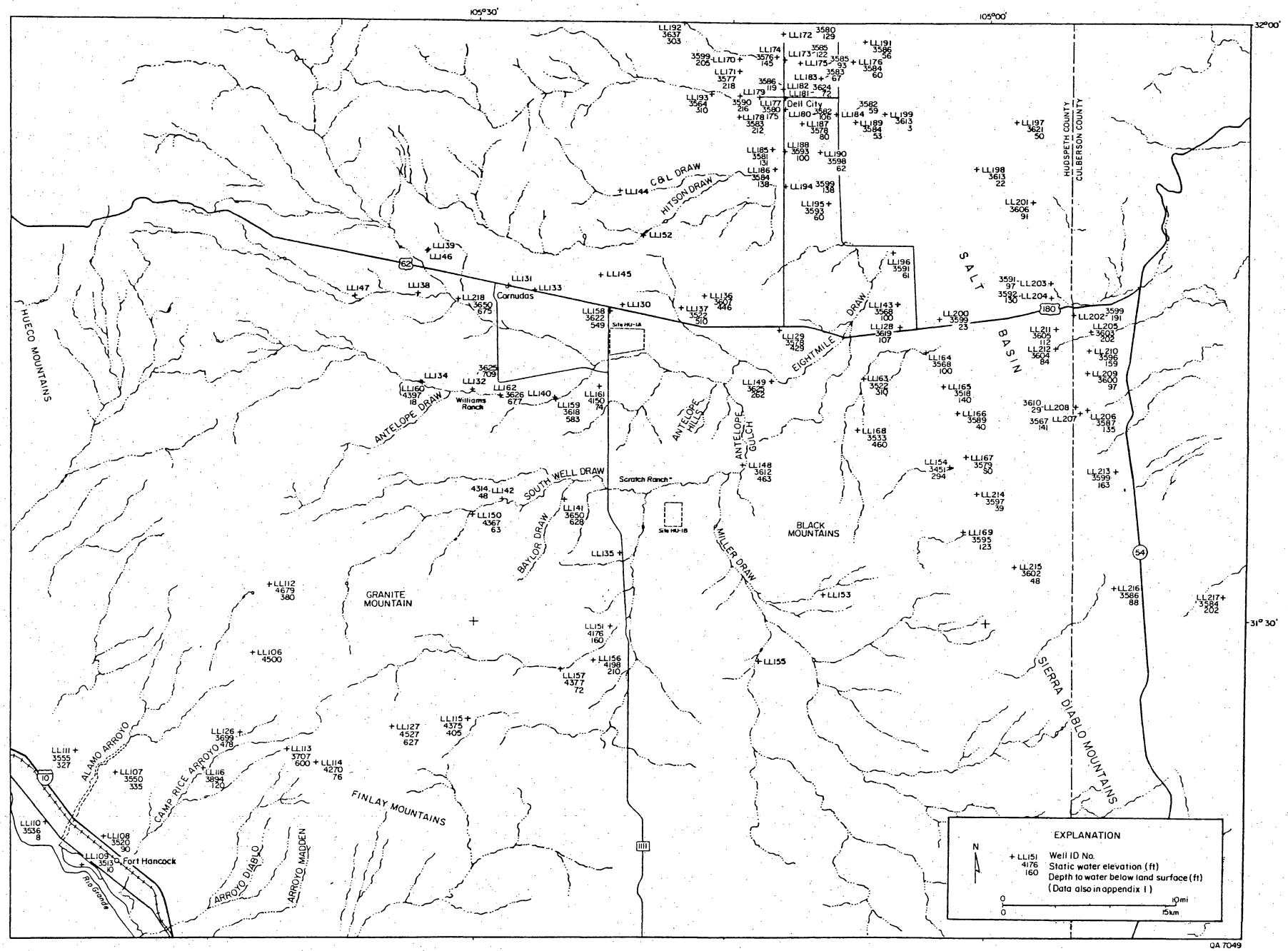
105°30'
105°00'
32°00'
31° 30'
HUDSPETH COUNTY
CULBERSON COUNTY
HUECO MOUNTAINS
GRANITE MOUNTAIN
BLACK MOUNTAINS
FINLAY MOUNTAINS
SIERRA DIABLO MOUNTAINS
SALT BASIN
EIGHTMILE DRAW
C&L DRAW
HITSON DRAW
ANTELOPE DRAW
ANTELOPE HILLS
ANTELOPE GULCH
SOUTH WELL DRAW
BAYLOR DRAW
MILLER DRAW
ALAMO ARROYO
CAMP RICE ARROYO
ARROYO DIABLO
ARROYO MADDEN
Rio Grande
Dell City
Cornudas
Williams Ranch
Scratch Ranch
Site HU-1A
Site HU-1B
Fort Hancock
EXPLANATION
+ LL151 Well ID No.
4176 Static water elevation (ft)
160 Depth to water below land surface (ft)
(Data also in appendix 1)
0 10mi
0 15km
N
QA 7049

Cretaceous Cox sandstone and Cretaceous Campagrande limestone below the alluvium indicate a hydraulic conductivity of 1.226×10^{-4} cm/sec (38.6 m/yr). This value is within the range of limestones, dolomites, and sandstones (Freeze and Cherry, 1979).

Natural fracturing occurs in cored bedrock at both sites and in an abandoned quarry southeast of the test holes at HU1A. Natural fractures are more abundant in the rhyolite. Most of the fractures in the rhyolite are still open with only thin layers of limonite and hematite lining the fractures and providing no appreciable restriction to ground-water flow. Fractures in the limestones of HU1B, however, are partially to totally occluded by brown calcite and dolomite cements. The degree of restriction to ground-water flow that results from these cements is unknown. At least two examples of fracture enlargement by solutioning were recorded from the limestone core. In addition to fracture solutioning, partially occluded biomolds, initially a result of solutioning, were also observed. The apparent increase in fracturing from HU1B to HU1A may be a result of closer proximity to the Babb flexure. Higher permeabilities at HU1B, however, could result from more efficient connection of fracture systems due to the effects of solutioning. Permeability tests on the unsaturated zone at HU1A (appendix 2) also confirmed the presence of fracture systems in the subsurface rhyolite.

Saturated Zone

The primary aquifer, Aquifer A, (see Potentiometric Surface section for a detailed discussion) in the study area is part of a regional aquifer that extends across much of the Diablo Plateau. Previous studies of the Dell City area have reported that locally the water-bearing formation is the Bone Spring limestone of the Leonard series of Permian age (Scalapino, 1950; Peckham, 1963; Young, 1976; Gates and others,

1980; Logan, 1984). In the nearby Guadalupe Mountains, the Bone Spring limestone attains a thickness of several thousand feet (King, 1948). In the Dell City area, the Victorio Peak and Bone Spring limestones crop out, and locally the aquifer is referred to as the Victorio Peak - Bone Spring aquifer. Peckham (1963) reports that the Bone Spring limestone is a black, cherty, dense, fine-textured, thin-bedded limestone at least 500 ft (152 m) thick, and the Victorio Peak limestone is a thick-bedded succession of gray limestone with a total thickness of about 800 ft (243 m). Ground water has been reported to be encountered at depths from 200 ft (61 m) to 1,500 ft (457 m)(D'Appolonia, 1978).

Lithologic control for this aquifer outside the Dell City area is extremely limited. Two driller's logs were obtained from El Paso Natural Gas Company records (appendix 4) for water wells drilled at Pump Station #2. These logs record lithologies that could reasonably be correlated with Permian strata of the area.

The shallow aquifer, Aquifer B (fig. 7), is a local aquifer located in the southwestern portion of the study area. Although no previous studies report aquifer host rock, stratigraphic thicknesses, coring at HU1B, and discussions with local well drillers make possible some inferences. Aquifer B is probably a Cretaceous limestone aquifer with permeabilities controlled by the presence of fracturing and solutioning. Cretaceous rocks in the area are typically reported to have minimum thicknesses of 200 ft (61 m) and because all but one of the wells producing from Aquifer B are shallower than 200 ft (61 m), a Cretaceous host rock seems reasonable.

Figure 7. Potentiometric surface map, Aquifers A and B. Ground water flows predominantly to the northeast. A ground-water divide is located north of the Diablo Plateau scarp. The abrupt change of the potentiometric surface together with the difference in gradients and depth to water suggests the presence of two separate aquifers: The primary deep aquifer, Aquifer A, and a shallower aquifer, Aquifer B.

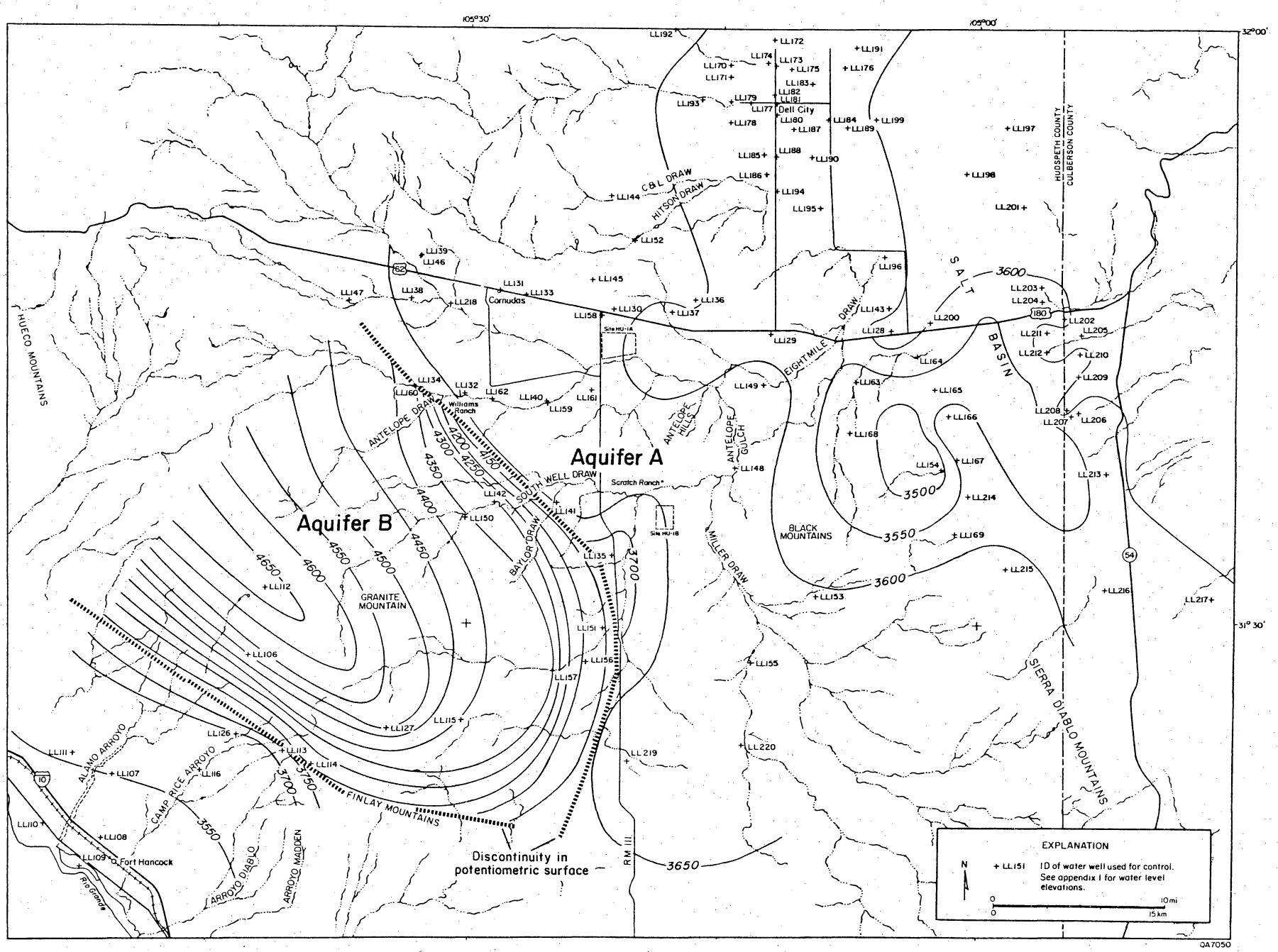
105°30'
105°00'
32°00'
31°30'
Aquifer A
Aquifer B
Discontinuity in potentiometric surface
EXPLANATION
+ LL151 ID of water well used for control. See appendix I for water level elevations.
N
0 10 mi
0 15 km
QA7050
Dell City
Cornudas
Williams Ranch
Scratch Ranch
Site HU-14
Site HU-18
Fort Hancock
HUECO MOUNTAINS
GRANITE MOUNTAIN
FINLAY MOUNTAINS
BLACK MOUNTAINS
SIERRA DIABLO MOUNTAINS
ANTELOPE DRAW
ANTELOPE HILLS
ANTELOPE GULCH
SOUTH WELL DRAW
BAYLOR DRAW
MILLER DRAW
EIGHT MILE DRAW
C&L DRAW
HITSON DRAW
SALT BASIN
ALAMO ARROYO
CAMP RICE ARROYO
ARROYO DIABLO
ARROYO MADDEN
RIO GRANDE
RM 111
HUDSPETH COUNTY
CULBERSON COUNTY
3600
3550
3500
3650
3700
4650
4600
4550
4500
4450
4400
4350
4300
4250
4200
4150

Water-bearing Characteristics

The occurrence and quantity of ground water both in the Dell City area and throughout this regional aquifer appear to be controlled by fractures. Subsurface joints and fractures, caused by structural movement along the Babb and Victorio flexures (fig. 1), have contributed to both porosity and permeability development of the aquifer. Logan (1984) reports that in the Dell City area, ground water occurs in open joints and fractures under both water table and confined conditions. Stratigraphic or facies controls on transmissivity values have not been reported.

Fractures in the carbonate rock may be enhanced by solution from the flow of fresh ground water through primary and secondary porosity. The presence of recent sinkholes 12 ft (3.6 m) deep and 12 ft (3.6 m) in diameter (Young, 1976) is evidence of active solution in the Dell City area. Well drillers in the area also report the regular occurrence of lost circulation zones indicative of large openings or caverns (Scalapino, 1950). Although the extent of fractures has not been clearly defined, inferences of highly permeable fracture zones may be drawn from the low hydraulic gradients recorded for Aquifer A.

Seven pumping tests have now been completed on wells spaced across the Diablo Plateau for this study. Six of the pumping tests were on water wells producing from Aquifer A while one was producing from Aquifer B. Water wells tested were (in the order of testing) LL162, LL156, LL155, LL148, LL141, LL132, and LL138 (fig. 2). Pumping test (PT) no. 1 at well LL162 was the only test where monitoring of observation wells was possible due to nearby wellbores LL219 and LL220 (figs. 2 and A3-1). No drawdown was observed, however, in these observation wells. Data collected from these tests are included in appendix 3. Values of transmissivity calculated by the methods of Walton, Jacob, and Theis and Logan's method of approximation for both semiconfined leaky aquifer and confined nonleaky aquifer

conditions range from 2.39 gpd/ft of drawdown to 1,713.9 gpd/ft of drawdown (0.32 ft^2/d, or 0.03 m^2/d to 229.1 ft^2/d, or 21.3 m^2/d) for Aquifer A whereas Aquifer B had significantly higher transmissivity values, ranging from 37,163.1 gpd/ft of drawdown (4,968.3 ft^2/d, or 461.5 m^2/d) to 49,986 gpd/ft of drawdown (6,683 ft^2/d, or 621 m^2/d). The mean transmissivity calculated from 26 separate interpretations for Aquifer A was 228.2 gpd/ft of drawdown (30.5 ft^2/d, or 2.8 m^2/d), with a large standard deviation of 343 gpd/ft of drawdown (45.8 ft^2/d, or 4.2 m^2/d). At present, these are the only known pumping tests for the study region outside of the Dell City area. In the Dell City area, specific capacity data range from 5 to 64 gpm/ft (93 to 1,141 m^2/d) of drawdown (Peckham, 1963).

In each of the seven pumping tests, the data either directly or indirectly recorded the importance of fracture flow within the aquifers of the Diablo Plateau. Transmissivity within an individual water well is partially or totally dependent on the number and size of fractures encountered while penetrating the saturated section. Three of the seven tested water wells tested during this study were observed to be underproducing from both Aquifer A and Aquifer B. In these wells, drawdown stabilized after a few minutes of pumping with no more than a couple of feet of drawdown. This initial drawdown probably results from well bore storage (Driscoll, 1986) and does not reflect the hydrologic conditions of the aquifer. These pumping tests curves illustrate a short-term drawdown and then only minimal additional drawdown throughout the rest of the pumping tests. Only an approximation of a minimum transmissivity can be made by using Logan's method (Kruseman and De Ridder, 1976). Larger discharge pumping tests are needed on these wells to determine their true transmissivities.

Tectonic events on the Diablo Plateau that have been responsible for the creation of fracture systems have been numerous throughout the geologic history of the area. Successful siting of 11 water wells was achieved based on the location of lineaments and fractures mapped using aerial photographs of the Dell City area (H. Logan, Soil Conservation Service, personal communication, 1987). Only 1 out of 11 wells failed to encounter a sufficient amount of fractures to meet injection well transmissivity requirements of 2,000 gpm/ft of drawdown (267.4 ft^2/m, or 24.8 m^2/m). Additional studies to better understand the unexpected water-bearing potentials of both Aquifer A and Aquifer B on the Diablo Plateau should include comparative studies between surface fractures and lineaments recorded on aerial photographs and the location of successful water wells (a successful water well being one capable of delivering acceptable quantities of water to the surface economically). Preliminary investigations indicate a potential for finding additional transmissive zones with good water quality for a large portion of the Diablo Plateau.

Potentiometric Surface

The potentiometric surface (fig. 7) on the Diablo Plateau shows that regional ground water flows predominantly to the northeast. A ground-water divide is located just to the north of the Diablo Plateau scarp. No divide is evident in the region of the Babb flexure as had been postulated during previous studies (Dames and Moore, 1985). Recharge from either site HU1A or HU1B would flow in the general direction of the Dell City irrigation region and toward the salt flats.

Two separate aquifers may exist. Aquifer A is located in the northeast section of the study area and includes the Dell City irrigation and salt flat areas (fig. 7).

Elevations of the water table range from 3,445 ft (1,050 m) in the Dell City and salt flat regions in LL154 to 3,650 ft (1,112 m) for wells LL141 and LL218. Depth to water varies from 3 ft (1 m) on the salt flats to more than 700 ft (213 m) in areas of higher land elevations (fig. 6). Land surface elevation changes approximately 1,000 ft (305 m) from ≃ 3,450 ft (1,051 m) at the salt flats to more than 4,500 ft (1,372 m) in higher regions of the Diablo Plateau, but the elevation of the water table only rises 200 ft (61 m) across the same region. This explains why the depth to water increases significantly at higher elevations. The maximum hydraulic gradient measured between LL218 and LL154 is 6.9 ft/mi (1.3 m/km). A more typical gradient for the area, however, is 2.5 ft to 5 ft/mi (0.5 to 0.9 m/km), as measured between several wells.

Southwest of Aquifer A is a local aquifer (referred to as Aquifer B) with water-table elevations that are significantly higher than in Aquifer A (fig. 7). Aquifer B is bounded on the southwest by the escarpment of the Diablo Plateau. Water elevations for this area range from 4,397 ft (1,340 m) in LL160 to 4,176 ft (1,272 m) in LL151. The depth to ground water at Aquifer B is significantly less than that observed at Aquifer A; depth of water ranges from 18 to 210 ft (5 to 64 m), and the water depth for most wells is less than 100 ft (30 m). Ground water flows predominantly to the northeast. Limited flow is southwestward toward the Rio Grande valley. The hydraulic gradients measured for Aquifer B are higher than those of the regional Aquifer A, values being as high as 90 ft/mi (17 m/km) between wells LL156 and LL157.

The two different potentiometric surfaces in Aquifer A and Aquifer B suggest two permeable zones beneath the Diablo Plateau. Aquifer B represents a perched aquifer; Aquifer A is predicted to lie beneath Aquifer B in the southwestern part of the study area. In the north-northeastern part of the study area there are three examples of

Aquifer B overlying Aquifer A: (1) The water elevation of well LL161, a geothermal test well drilled on the flanks of one of the Pump Station Hills, is 4,150 ft (1,265 m), which is similar to water-table elevation of the shallow aquifer. This well was not used in potentiometric mapping of Aquifer A because of its apparently anomalous nature. (2) Wells LL160 and LL134 are located 100 ft (30 m) apart from each other on the Williams' Ranch at Hobo Tank, west of HU1A, and have significantly different water levels. LL160, a shallow windmill located in the bottom of an arroyo, has a depth to water of 18 ft (5.4 m), whereas the water depth in LL134, a deep pumpjack in the same area, was greater than 750 ft (229 m) (as reported by the owner). (3) The driller's logs for the abandoned El Paso Natural Gas Company Pump Station #2 well, which was used as an observation well for the pumping test (appendix 3), indicate that three water-bearing zones were encountered during drilling. During this study, water was always observed on the electric-line probe at depths of less than 200 ft (60.9 m), although static water level was recorded at 673 ft (205.1 m). In addition, water could be heard cascading down the borehole. (There was no casing below 100 ft (30.5 m) depth).

The difference in water levels, the difference in gradients, and the abrupt change in water levels that exist between the deep water table (Aquifer A) and the shallow water table (Aquifer B) found in the southwestern part of the study area suggest a change in hydrologic properties between the two regions. Aquifer A may be more fractured because of its location over or proximate to the Babb flexure. Fractures would permit greater leakage through possible aquitards between Aquifer A and Aquifer B and drain any ground water in overlying permeable zones. Greater fracture permeability would also permit a lower hydraulic gradient for Aquifer A than for Aquifer B. The Jacob plots for the aquifer tests of Aquifer A at wells LL132 and LL162 shows a segmented drawdown curve with time, which indicates drawdown in a

fractured medium (appendix 3). In the plot for well LL162 the first straight-line segment (a) represents drawdown in the fracture(s) penetrated by the well. These fractures have a transmissivity of 111 gpd/ft (1.38 m^2/d). A barrier was hit at 40 minutes. The cone of depression hit another set of fractures at ≃ 80 minutes. Transmissivity measured at the second set of fractures is 84 gpd/ft (1.05 m^2/d); a higher transmissivity (158.6 gpd/ft; 1.97 m^2/d) representing a third set was intersected at 900 minutes. The different transmissivities measured with increased time do not represent transmissivity values specific to each fracture set but do represent the cumulative value for the area affected by the cone of depression. The increased transmissivity evident at the end of the test may only indicate that more fractures are being intersected by the cone of depression, not that the fractures are more permeable. There was no drawdown in either of the adjacent observation wells, further indicating fracture control of ground-water flow and distribution. A similar pattern was also observed during the drawdown of well LL132. The abrupt change in water-table elevations between Aquifer A and Aquifer B may be due to a structural feature that functions as a hydrologic drain from Aquifer B into Aquifer A.

Recharge

Tritium levels measured on Diablo Plateau ground waters (Kreitler and others, 1986a; this report) indicate that a majority of the sampled wells (26 of 30, 87%) contain recently recharged water. The major process responsible for this current recharge is infiltration of runoff in arroyos during occasional flash flooding (appendix 9). In the Dell City area, another probable source of current recharge is the recirculation of irrigation waters.

Several wells, particularly in the southwestern portion of the study area, also were found to contain high NO_3 levels. High nitrate levels may also be used as a qualitative tool for the documentation of local recent recharge. A detailed discussion of NO_3 in the study area and its implications for recharge appears in the Ground-Water Geochemistry section of this report.

Previous studies of the Diablo Plateau have dealt specifically with the identification of potential zones of recharge for the Dell City area. Peckham (1963) reported recharge zones to the west of Dell City and to the north in New Mexico. Principal recharge for the Dell City area has been attributed to the Sacramento River drainage basin located to the northwest of Dell City (Young, 1976). Peckham (1963) and Young (1976) also noted that to a lesser extent, recharge may occur in the Dell City area by the infiltration of precipitation on the land surface but apparently most of this evaporates (Dougherty, 1975; Boyd and Kreitler, 1986). Gates and others (1980) estimate annual recharge in the Dell City area as 31,000 acre-ft (3.8×10^7 m^3). The unsaturated section in the Dell City area consists of 5 to 150 ft (1.5 to 45 m) of alluvial cover. Recharge through the alluvium in the interarroyo areas is expected to be minor. Vegetation changes observed during field work may also influence or indicate active surface recharge. Preliminary studies dealing with climate and vegetation are presented in appendix 8.

Studies of recharge methods at HU1B

Reconnaissance field work in the study area indicates that recharge on the Diablo Plateau probably occurs by infiltration of runoff water in arroyos where erosion has transected Cretaceous bedrock. Detailed sampling of soil profiles for chloride analysis was conducted both in arroyos and in interarroyo areas to determine the relative recharge in each of these geomorphic areas. The recharge equation of Allison and

Hughes (1978) was then used to estimate the amount of precipitation and runoff that moves through the vadose zone annually.

Ten hollow-stem auger holes were drilled along two transects oriented east-west and north-south across HU1B (fig. 8). One additional auger hole was drilled in a closed depression located southwest of the site. Two boreholes, C1 and C6, were located within the drainage channel of Antelope Gulch, west and north of the site respectively, and C4 was located within a minor unnamed north-south drainage channel along the eastern boundary of HU1B. Each bore hole was drilled to auger refusal, which at all but one location could be confirmed to be the top of Cretaceous bedrock. Two cores drilled during previous investigations (Kreitler and others, 1986a, plate 1) and limited outcrops in the area indicate the Cretaceous units encountered at the top of bedrock are limestones of the Finlay and Campagrande Formations and the Cox Sandstone.

Data specific to chloride concentration profiles at HU1B are present in appendix 9. The following discussion will be based on the Midland value of 0.79 mg/L chloride in rainfall. Borehole locations and chloride profiles are presented in figure 8.

Chloride profiles and calculated annual recharge document the very strong influence of the presence of arroyos on the amount of water moving in the vadose zone in the area of HU1B. Calculated annual recharge calculations for boreholes located in arroyos ranged from 0.0688 to 0.0041 inches/yr (0.1747 to 0.0104 cm/yr). Boreholes located in the interarroyo areas however recorded significantly lower annual recharge rates ranging from .0022 to .0008 inches (.0056 to .0020 cm). Rates of recharge within a closed depression closest in the site region resembled those of arroyo areas, having an estimated annual recharge rate of 0.0501 inches/yr (0.1272 cm/yr). Recharge to bedrock within the boundary of HU1B, based on chloride

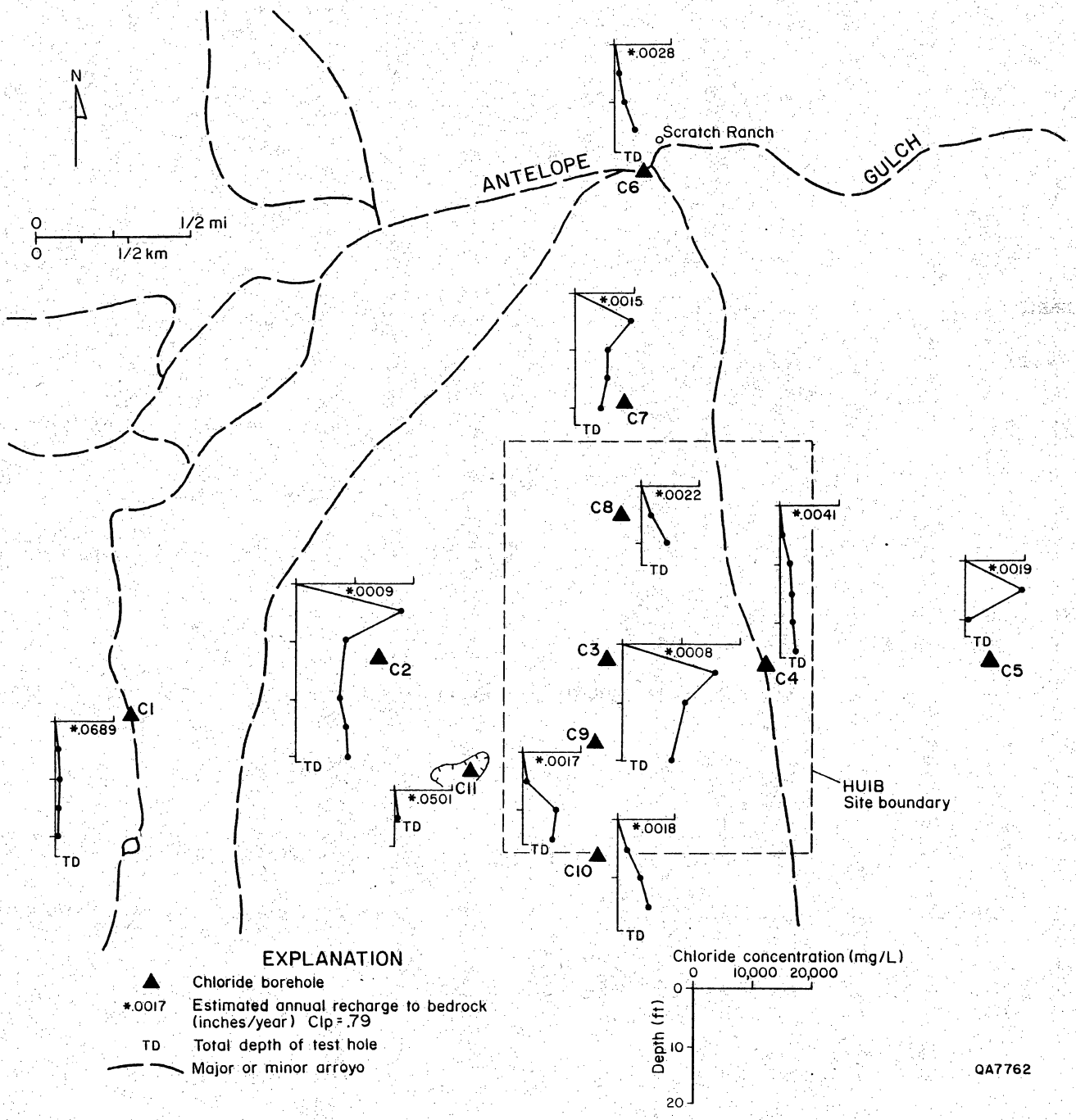

Figure 8. Map showing location of boreholes augered for chloride analysis at HU1B. Adjacent to borehole location is vertical profile of chloride concentrations measured in soil samples.

concentration investigations, was found to be very small. These rates of recharge are similar to rates measured in the area of the Fort Hancock site to the southwest, which ranged from 0.009 to 0.0005 inches/yr (0.023 to 0.0013 cm/yr) (Kreitler and others, 1986b).

Flood management and recharge in the Dell City area

Currently, a large flood-control program is under construction in the Dell City area. The flood control program is under the direction of the Soil Conservation Service (SCS), an agency of the U. S. Department of Agriculture (USDA). Major arroyos responsible for drainage through the Dell City area have only minor topographic definition and often fail to confine runoff during periods of heavy precipitation. Four retarding dams will eventually be completed to reduce costly damages resulting from flash flooding in the Dell City area. Currently, three dams have been completed and one is still under construction.

Man-induced ground-water recharge of floodwaters through a series of large-diameter (20-inch) recharge wells below each retarding dam is a secondary benefit of the flood control measures (Logan, 1984). The number of injection wells required per dam is dependent on the size of the drainage area above each structure. Current plans specify a total of 11 injection wells based on a ratio of 1 well per 30 mi^2 (77.7 km^2) of drainage area. Injection is to be by gravitational flow. Three possible benefits from this effort, in addition to the obvious control of floodwaters, include (1) improved ground-water quality, which has steadily been declining since the inception and recycling of irrigation waters, (2) reduction or reversal of declining water levels due to the intensive ground-water production during peak irrigation periods, and (3) a better understanding of aquifer characteristics and potential for the area through geophysical logging, videologging, and pumping tests conducted in each injection well.

Discharge

The potentiometric map of Aquifer A (fig. 7) indicates that ground water flows toward the salt flats. Peckham (1963) and Young (1976) also reported that ground-water flow is in the direction of the salt flats. Discharge occurs naturally by evaporation in geographically extensive areas where depths to water may be as shallow as 3 ft (0.9 m) in the salt flats. Boyd and Kreitler (1986) and Chapman (1984) consider the salt flats to be the major discharge zone for the area. The potentiometric map of the study region confirms this hypothesis.

Abundant ground water was discovered in Dell City in 1947. By 1949, 32 water wells had been completed and 6,000 acres of farm land were under irrigation (Scalapino, 1950). The magnitude of irrigation continued to increase until as much as 40,000 acres of land had been converted to irrigated farming. According to D'Appolonia (1979), this represented the highest concentration of irrigated farm land within the state of Texas. Soil Conservation Service records indicate that as much as 150,000 acre ft (1.8×10^8 m^3) of irrigation water was produced in Dell City during 1979 (Logan, 1984).

Water levels measured in 1961 in the Dell City area had dropped an average of 18.5 ft total (5.6 m) since irrigation became prominent in the area around 1948. Young (1976) reports that water levels in the Dell City area have declined an average of 1.5 to 1.7 ft/yr (0.45 to 0.51 m/yr) from 1948 to 1968. During the same period of record, water salinity at Dell City tripled because of return flow from irrigation that leached salts from the soil. Production yields from these wells range from 160 to

2,240 gpm (875 to 12,250 m^3/d) (Peckham, 1963). In 1960, about 200 wells pumped 100,000 acre-ft (123 x 10^6 m^3) of water from the aquifer. This decline of the potentiometric surface in the Dell City area has caused the wells in the Dell City area to be discharge points for the northern part of Aquifer A. It is uncertain whether flow from site HU1A would be toward Dell City. Based on the potentiometric map (fig. 7), however, flow from HU1B is expected to discharge at the salt flats.

Discharge of the aquifer has also occurred through naturally flowing springs. Crow Springs, located east-northeast of Dell City, was an important water oasis until the 1950's when an irrigation well was drilled adjacent to the spring. Flow of the spring terminated overnight (Brune, 1981). Other springs in the area that dried up due to pumpage are Washburn and Persimmon Springs north of Cornudas, Cove Spring on the south side of the Paint Waterhole Mountains, Shot Springs in the Antelope or Red Hills, Sulphur Springs on the east side of salt flat, Cottonwood Springs southeast of salt flat, and Aparejo or Harness Springs on the south side of Black Mountain (Brune, 1981).

No exterior drainage from Aquifer A was recorded during this study. Nielson and Sharp (1985) offer the possibility, however, that intrabasinal flow to the east may occur in the southern portion of the Salt Basin.

Ground-water Geochemistry

Chemical and isotopic analyses of ground-water samples from Hudspeth County collected during this study are presented in appendix 5. Additional chemical and isotopic analyses used during the evaluation of the southern site in Hudspeth County (Kreitler and others, 1986b) and chemical analyses from the Texas Water Development Board (1985) are presented in appendix 6.

Figure 14. Map of NO_3 distribution. Higher NO_3 concentrations (mg/L) exist in Aquifer B than in Aquifer A. Shallower depth to ground water in Aquifer B permits more rapid recharge. The source of nitrates may be anthropogenic, and contaminant can rapidly reach water table through fracture permeability. Some of the wells with high NO_3, however, contain no tritium, suggesting other sources of NO_3.

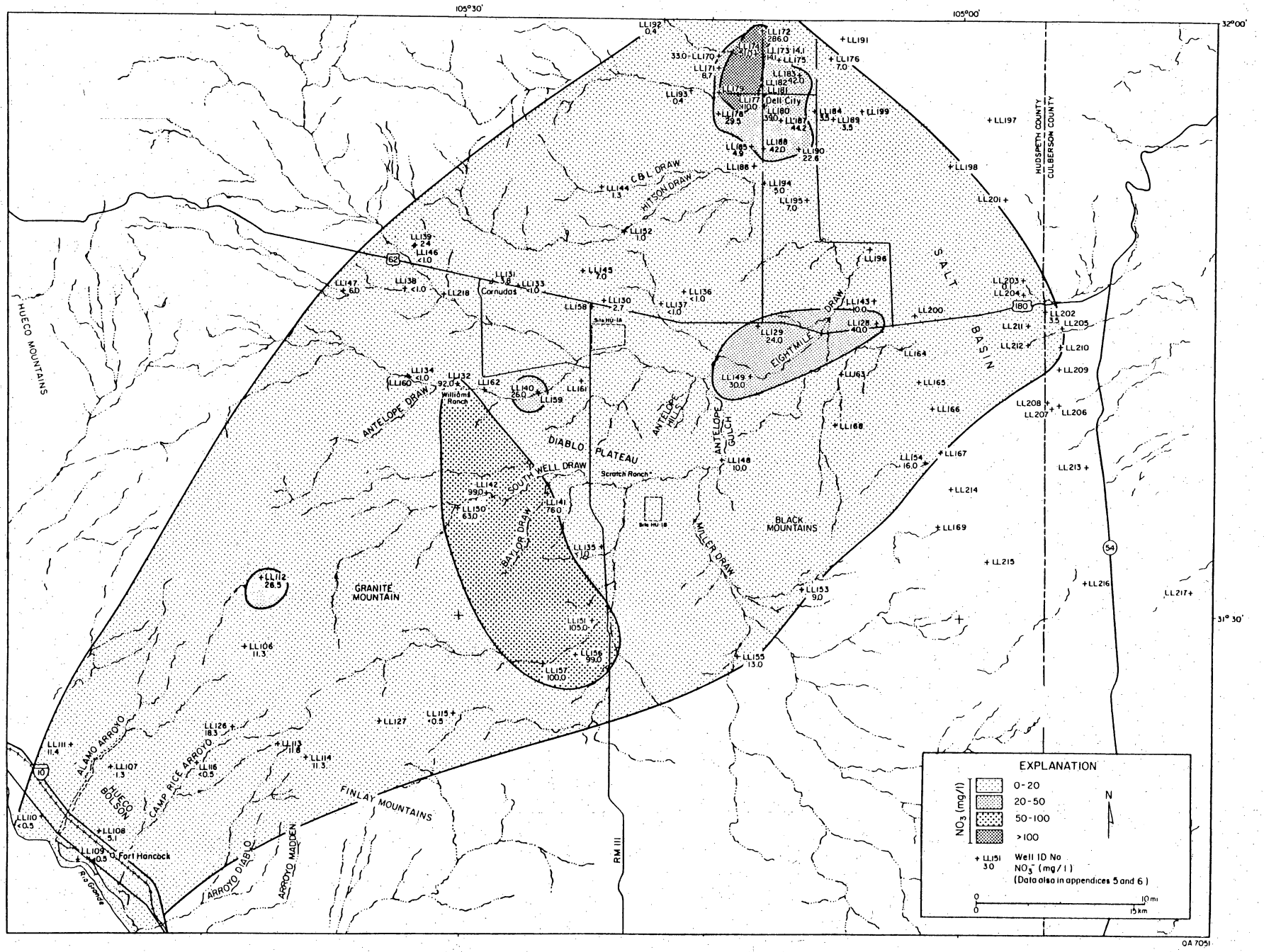
105°30'
105°00'
32°00'
31°30'
HUECO MOUNTAINS
GRANITE MOUNTAIN
FINLAY MOUNTAINS
BLACK MOUNTAINS
DIABLO PLATEAU
Scratch Ranch
Williams Ranch
Cornudas
Fort Hancock
Rio Grande
ANTELOPE DRAW
ANTELOPE GULCH
ANTELOPE HILLS
SOUTH WELL DRAW
BAYLOR DRAW
MILLER DRAW
CBL DRAW
HITSON DRAW
EIGHT MILE DRAW
ALAMO ARROYO
BLUEGO BOLSON
CAMP RICE ARROYO
ARROYO DIABLO
ARROYO MADDEN
RM 111
HUDSPETH COUNTY
CULBERSON COUNTY
U S A L T
B A S I N
Dell City
Site HU-1A
Site HU-1B
EXPLANATION
NO_3 (mg/l)
0-20
20-50
50-100
>100
N
+ LL151 30 Well ID No NO_3^- (mg/l)
(Data also in appendices 5 and 6)
10 mi
15 km
OA 7051

Figure 15. Map of ^{14}C and tritium distribution. Tritium activity data range from 0 to 32 TU and, except for four ground-water samples, all samples had varying amounts of tritium, indicating active recharge into both Aquifer A and Aquifer B. Ground water ages determined by ^{14}C ranged from recently recharged modern water to 22,831-yr-old water. Presence of tritium in water with old ^{14}C corrected age may indicate mixing of very young water with older waters, or it may indicate that the calculated ^{14}C ages are erroneous. Tritium and ^{14}C activities vary significantly within short distances and do not show a clear distribution pattern, suggesting the importance of fracture flow.

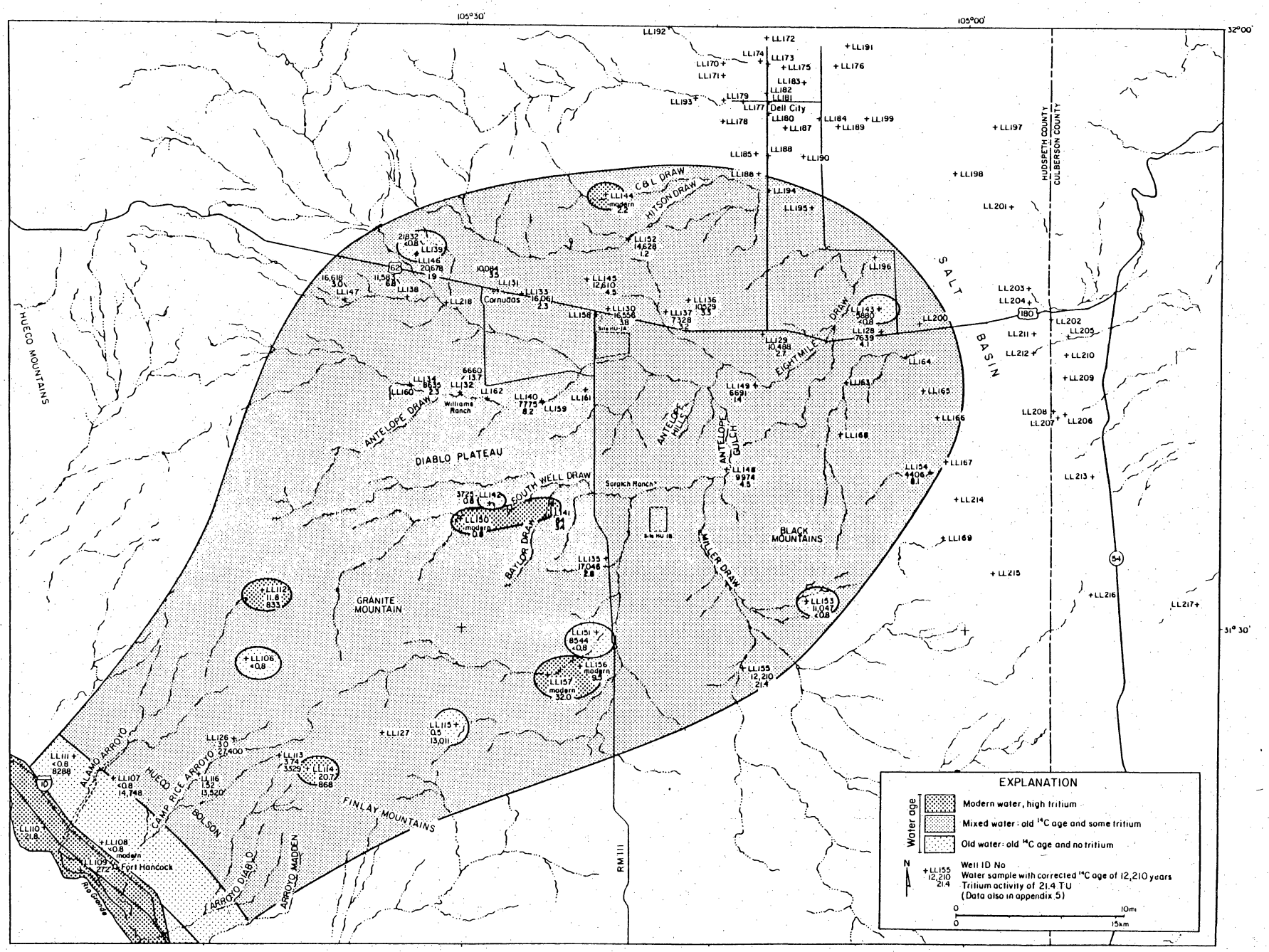
105°30'
105°00'
32°00'
31° 30'
HUECO MOUNTAINS
DIABLO PLATEAU
GRANITE MOUNTAIN
FINLAY MOUNTAINS
BLACK MOUNTAINS
SALT BASIN
HUDSPETH COUNTY
CULBERSON COUNTY
Dell City
Cornudas
Williams Ranch
Sorgach Ranch
Fort Hancock
ANTELOPE DRAW
ANTELOPE HILLS
ANTELOPE GULCH
EIGHT MILE DRAW
HITSON DRAW
C&L DRAW
SOUTH WELL DRAW
BAYLOR DRAW
MILLER DRAW
ALAMO ARROYO
HUECO
CAMP RICE ARROYO
BOLSON
ARROYO DIABLO
ARROYO MADDEN
RM 111
Rio Grande
EXPLANATION
Water age
Modern water, high tritium
Mixed water: old 14C age and some tritium
Old water: old 14C age and no tritium
Well ID No
Water sample with corrected 14C age of 12,210 years
Tritium activity of 21.4 TU
(Data also in appendix 5)
10mi
15km

Figure 16. Map of $\delta^{18}O$ and δD distribution. Ground-water samples vary in $\delta^{18}O$ values from -6.90 to -10.53 °/oo, and δD values vary from -46.4 to -81.5 °/oo (with the exception of well LL141). Enriched values, which resemble current annual mean rainfall values in Midland, are encountered at the west and southwest parts of the study area (in both Aquifer A and Aquifer B), where ground-water salinities are relatively low, tritium activities are high, and the age of the water is young. The most depleted values of δ^{18} and δD occur in the north, where water has the oldest ^{14}C dates and lacks tritium.

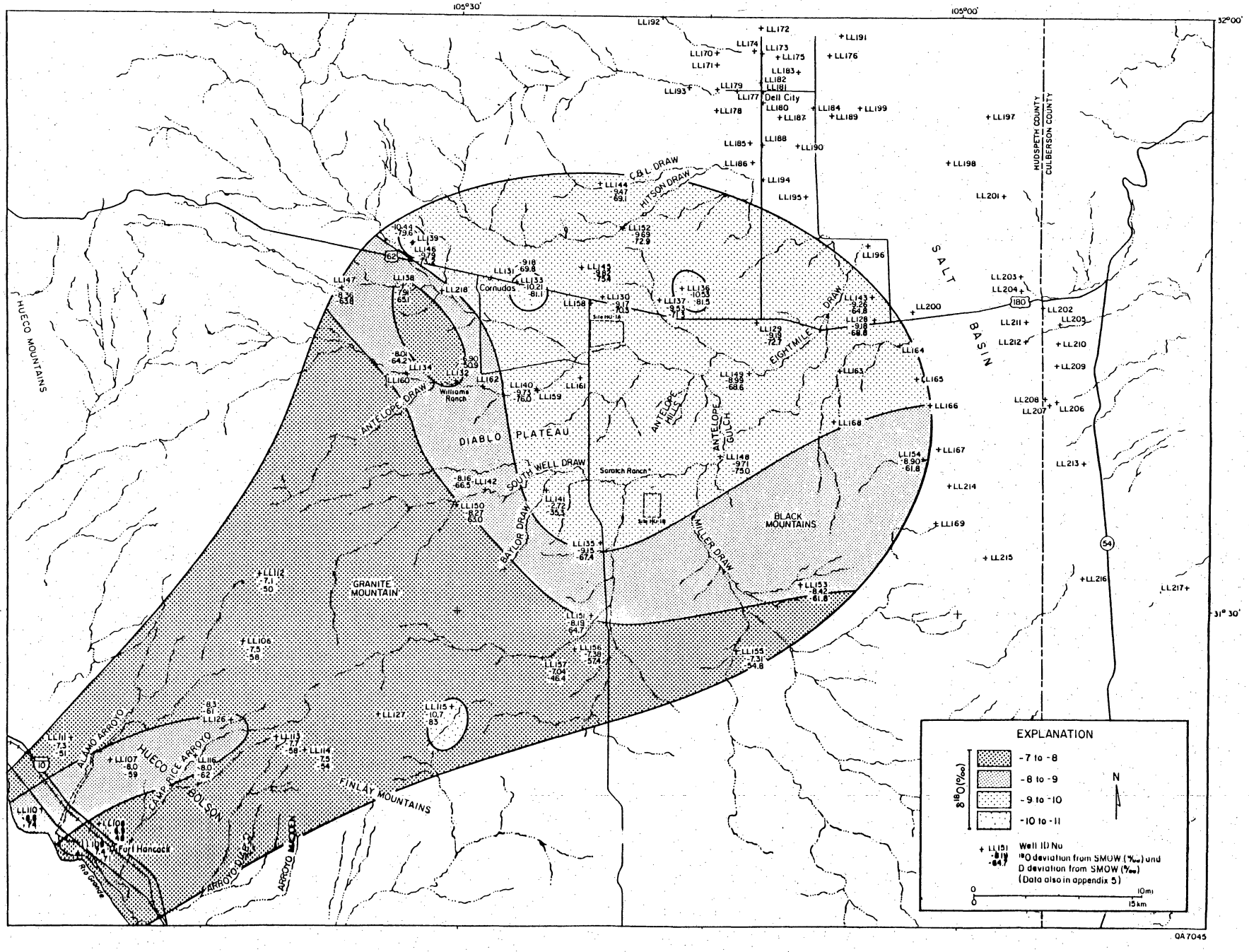
105°30'
105°00'
32°00'
31°30'
HUECO MOUNTAINS
DIABLO PLATEAU
GRANITE MOUNTAIN
FINLAY MOUNTAINS
BLACK MOUNTAINS
SALT BASIN
HUDSPETH COUNTY
CULBERSON COUNTY
C&L DRAW
HITSON DRAW
EIGHTMILE DRAW
ANTELOPE DRAW
ANTELOPE HILLS
ANTELOPE GULCH
SOUTH WELL DRAW
BAYLOR DRAW
WILLER DRAW
ALAMO ARROYO
HUECO TANKS ARROYO
CAMPBELL ARROYO
BOLSON
ARROYO BLANCO
ARROYO MACHO
Rio Grande
Fort Hancock
Dell City
Cornudos
Williams Ranch
Scratch Ranch
EXPLANATION
-7 to -8
-8 to -9
-9 to -10
-10 to -11
δ18O (‰)
N
Well ID No
18O deviation from SMOW (‰) and
D deviation from SMOW (‰)
(Data also in appendix 5)
10mi
15km
QA7045

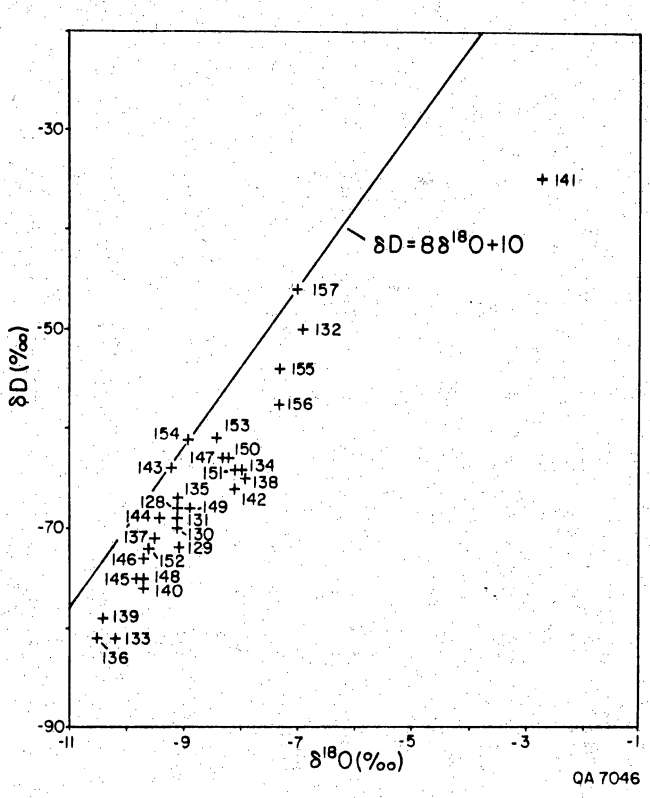

Figure 17. Plot of $\delta^{18}O$ versus δD. Values of $\delta^{18}O$ and δD in ground water in the study area generally plot parallel to and below the meteoric water line (Craig, 1961), similar to ground water in the southern Hudspeth County and Culberson County sites (Kreitler and others, 1986b). These data may reflect a local version of the meteoric water line, controlled by high temperatures and evaporation rates prevailing in the study area.

local version of the world meteoric line. Stable isotope data of ground water from Roswell basin, eastern New Mexico (Hoy and Gross, 1982), indicate a shift of the local line to fit the line equation $\delta D = 7.27\delta^{18}O + 5.36$, rather than Craig's equation (1961) $\delta D = 8\delta^{18}O + 10$. Hoy and Gross (1982) related this shift to the higher temperatures and increased evaporation rates that prevail in eastern New Mexico. However, isotope data from the Ogallala, Dockum, and Cretaceous aquifers of the Texas Panhandle (Nativ and Smith, 1985), where climatic conditions are similar, plot along the world meteoric line, rather than below it.

Values of $\delta^{34}S$ range from -1.24 to +16.11°/oo, (fig. 18); two-thirds of the samples have values above +6°/oo. Heavier values (9.28 to 16.11°/oo) were encountered in the north and northeast of Aquifer A toward the discharge zone (fig. 7) and suggest that the dissolved SO_4 in ground water in this area is from dissolution of anhydrite in the host rock. These $\delta^{34}S$ values of dissolved sulfate are typical of Permian sulfate minerals (10 to 15°/oo) (Hoefs, 1973; Claypool and others, 1980). The $\delta^{34}S$ of the ground water SO_4 from Block 46 and S-15 (Culberson County) occupies a narrow range of +9 to +11°/oo and indicates simple Permian evaporite dissolution. In other parts of the study area, values are less enriched, possibly because of shorter reaction time with the host rock, or in the case of Aquifer B because of either different $\delta^{34}S$ values of sulfate minerals in the Cretaceous host rock or a mixing of sulfates from Cretaceous and Permian rocks. The most depleted $\delta^{34}S$ values are found in the northern part of Aquifer A, where ground water has other unique features regarding ^{14}C, tritium, $\delta^{18}O$, and δD values.

Values of $\delta^{13}C$ range from -10.35 to -3.64°/oo (fig. 17). These values are heavier than those encountered in the southern Hudspeth County site (Kreitler and others, 1986b). Most marine carbonate rocks have $\delta^{13}C = 0$°/oo, whereas common values for organic material and CO_2 in soil are -25 to -20°/oo. The concentration of

Figure 18. Map of $\delta^{34}S$ and $\delta^{13}C$ distribution. Values of $\delta^{34}S$ range from -1.24 to $+16.11^{o}/oo$; two-thirds of the samples have values above $+6^{o}/oo$. Values of $\delta^{13}C$ range from -10.35 to $-3.64^{o}/oo$ and are heavier than those in the southern Hudspeth County site (Kreitler and others, 1986b). Old ground water in the north has the most depleted $\delta^{13}C$ values, whereas young water in the south and southwest has enriched values.

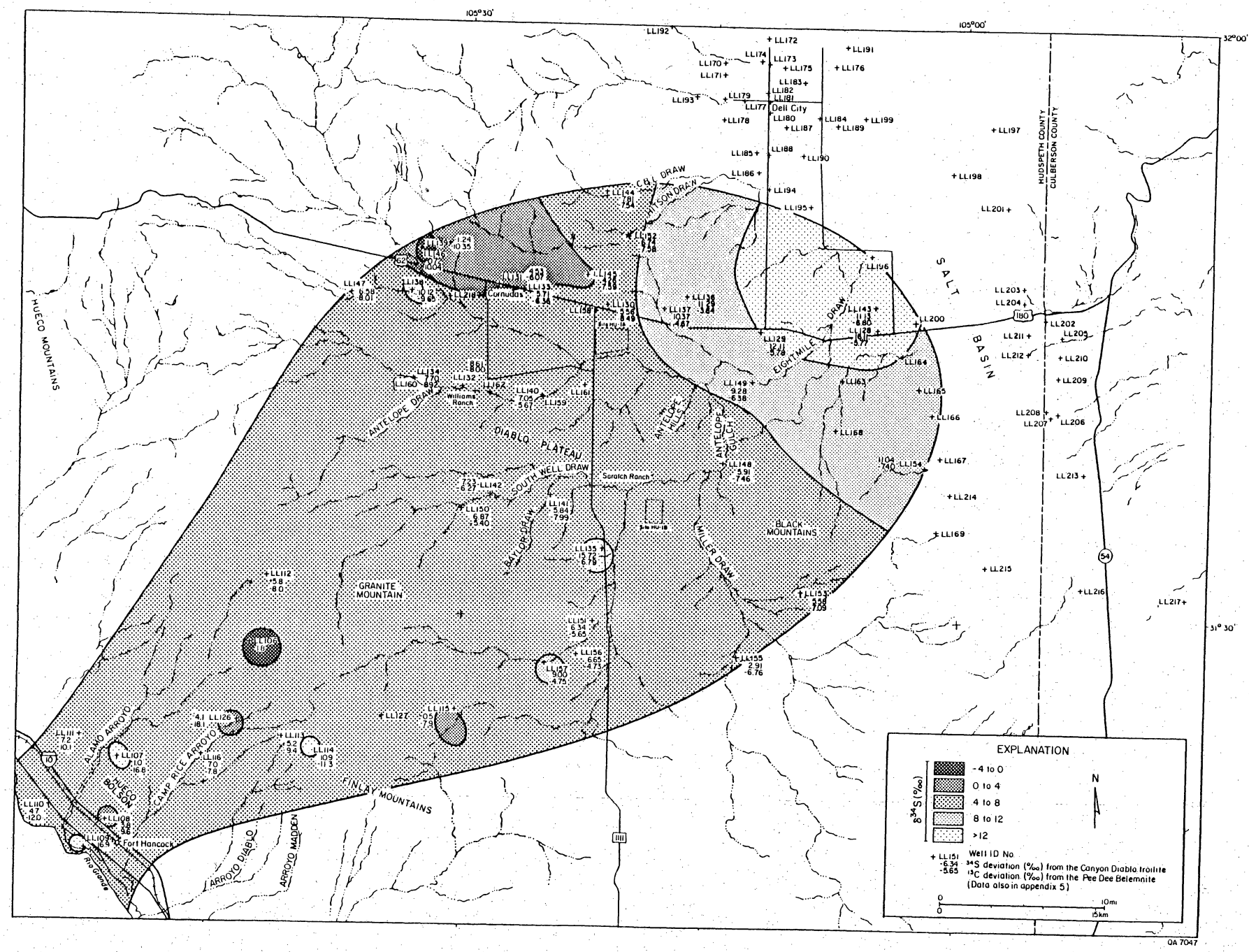
105°30'
105°00'
32°00'
31°30'
HUECO MOUNTAINS
GRANITE MOUNTAIN
DIABLO PLATEAU
BLACK MOUNTAINS
SALT BASIN
HUDSPETH COUNTY
CULBERSON COUNTY
Dell City
Cornudas
Fort Hancock
Rio Grande
ANTELOPE DRAW
EIGHT MILE DRAW
SOUTH WELL DRAW
ALAMO ARROYO
CAMP RICE ARROYO
ARROYO DIABLO
ARROYO MADDEN
EXPLANATION
-4 to 0
0 to 4
4 to 8
8 to 12
>12
δ34S (‰)
N
Well ID No.
34S deviation (‰) from the Canyon Diablo troilite
13C deviation (‰) from the Pee Dee Belemnite
(Data also in appendix 5)
0 10mi
0 15km
OA 7047

$\delta^{13}C$ in ground water is determined by the input with recharge water and by reaction with the rock. However, the assumption that the enriched values found in ground water in the study area can be related to longer interaction time with the host rocks is not supported by the distribution of $\delta^{13}C$ values. Old ground water in the northern part of Aquifer A has the most depleted $\delta^{13}C$ values, whereas young water with elevated tritium values in Aquifer B has enriched values. Therefore, a different mechanism controls the range and distribution of $\delta^{13}C$ in this area.

CONCLUSIONS

Lithologies underlying HU1A and HU1B are Precambrian rhyolite porphyry and Cretaceous limestone interbedded with some silty and muddy interbeds, respectively. The rhyolite porphyry is fractured. The fractures strike in many directions, dip from vertical to horizontal, and have limonite and hematite stains on the fracture surfaces. Most fractures contain no mineral fillings, indicating that they are not sealed. Cretaceous limestone at HU1B is not as fractured as the rhyolite porphyry at HU1A.

The Babb flexure is north of both sites; however, fractures away from the inferred margins of this regional structure may be related to deformation of the flexure. The flexure may be the Permian or post-Permian expression of a major pre-Permian strike-slip fault (Hodges, 1975). It is unknown if Cretaceous rocks have been warped by recurrent movement along the structure.

Flooding down Antelope Draw at HU1A may be very intense for short durations and should be considered during site selection.

Regional ground-water flow is mainly from southwest to northeast. The ground-water divide is located close to the Diablo Plateau scarp, the escarpment that defines the northern edge of the Rio Grande basin, not along the Babb flexure. In the study

area two aquifers are present; a shallow aquifer in the southwestern area with depths to water generally less than 200 ft (60 m) and a deeper aquifer through most of the region with depths to water up to 700 ft (213 m).

Recharge occurs over the entire study area and is not restricted to the updip part of the potentiometric surface in the areas of higher elevation. Tritium is found in nearly all wells regardless of their location on the regional water table, indicating rapid recharge throughout the area. Most recharge probably occurs during flooding of the arroyos that drain the plateau. Minimal recharge is expected through the interarroyo areas. Fractures are probably important pathways for recharge. Recharge along fractures is the best mechanism to move recent recharge water rapidly through a thick unsaturated section.

Ground-water flow is predominantly fracture controlled. Three separate fracture sets were identified during a pumping test. Because of the fracture control on ground-water flow, aquifer permeabilities based on seven pumping tests were found to be extremely variable, ranging from 847 gal/day/ft^2 (34.63 m/day) to 8.2 x 10^{-3} gal/day/ft^2 (6.7 x 10^{-5} m/day). Transmissivities were found to range from 49,986 gpd/ft of drawdown (6,683 ft^2/d or 621 m^2/d) to 2.39 gpd/ft of drawdown (0.32 ft^2/d or 0.03 m^2/d). Water wells in the Dell City area have reported transmissivities greater than 388,000 gpd/ft of drawdown (51,872 ft^2/d or 4819 m^2/d) (Logan, 1984). Minimum transmissivity could be determined for only three wells because the pumps installed in the water wells never adequately stressed the aquifer. All of the calculated transmissivities should be used with caution because the calculations are based on assumptions of porous media flow and not fracture flow, and they represent only seven pumping tests. The fractures may cause a very anisotropic system, and flow may not be directly down the regional potentiometric gradient. Discharge is either by evaporation on the salt flats or through pumping wells.

Total dissolved solids content ranges from 715 to 3,803 mg/L. The dominant water types are Na-SO_4 and $CaSO_4$. Many of the waters have high NO_3 concentrations, which suggests recent recharge and possible contamination by animal wastes. The chemical composition of the waters appears to be randomly distributed; there is no coherent chemical evolution of the water as it flows down the potentiometric gradient. This may be due to control of flow by fracture pathways and by local recharge across the entire Diablo Plateau.

The shallower aquifer may or may not be present at either site, although it is not used in the immediate vicinity of either site. Depth to ground water in the deeper aquifer beneath the sites is probably greater than 600 ft (180 m).

ACKNOWLEDGMENTS

We would like to thank Skeet and Jay Williams of the Williams Ranch for their hospitality, time, information, and use of their water wells during this study. We would also like to thank James Baylor of the Baylor Ranch and Gary Hebbert of the Dyer Ranch for permission and assistance during pumping and sampling tests. Appreciation is extended to Steve Hartman of the University of Texas Land Office for his assistance in obtaining permission to conduct field work. Kenneth Moore and Syd Sullenger, also of the University of Texas Land Office, were a great help in water well locations and plant identification. Richard Bowen of El Paso Natural Gas Company provided assistance in locating water well records for Pump Station No. 2. All the ranchers in the study area of Hudspeth County were true "West Texans," as shown through their daily assistance and cooperation. We owe special thanks to George and Ethyl Temple of Salt Flat, Texas, for their always open door after a hot day in the field. Thanks are also given to Alan Dutton of the Bureau of Economic Geology for his technical assistance and supervision during pumping test no. 1

operations. James Doss and Alan Standen of the Bureau performed the second phase of drilling in January 1987. Homer Logan of the Soil Conservation Service has been a valuable resource through his recharge studies in the Dell City area.

Arten Avakian and Gay Nell Gutierrez of the Bureau of Economic Geology helped with data processing, mapping, sample processing, drafting, and proofreading. Word processing was by Virginia C. Zeikus, Dorothy C. Johnson, and Rosanne M. Wilson under the supervision of Lucille C. Harrell. Figures were drafted by Don W. Thompson, Nan Minchow-Newman, T. B. Samsel III, and Annie Kubert-Kearns under the supervision of Richard L. Dillon. The report was edited by Amanda R. Masterson. Funding for this study was provided by the Texas Low-level Radioactive Waste Disposal Authority under contract no. IAC(86-87)-1061.

REFERENCES

Albritton, C. C., Jr., and Smith, J. F., 1965, Geology of the Sierra Blanca area, Hudspeth County, Texas: U. S. Geological Survey Professional Paper 479, 131 p.

Allison, G. B., and Hughes, M. W., 1978, The use of environmental chloride and tritium to estimate total recharge to an unconfined aquifer: Australian Journal of Soil Research, v. 16, p. 181-195.

Askew, B., and Algermissen, S. T., 1983, An earthquake catalog for the Basin and Range province, 1803-1977: U.S. Geological Survey Open-File Report 83-86, 21 p.

Barnes, V. E., project director, 1983, Van Horn - El Paso Sheet: The University of Texas at Austin, Bureau of Economic Geology Geologic Atlas of Texas, scale 1:250,000.

Bebout, D. G., and Loucks, R. G., 1984, Handbook for logging carbonate rocks: The University of Texas at Austin, Bureau of Economic Geology Handbook 5, 43 p.

Boersma, L., 1965, Field measurement of hydraulic conductivity above water table, in Black, L., A., ed., Methods of soil analysis: American Society of Agronomy, p. 222-234.

Boyd, F. M., and Kreitler, C. W., 1986, Hydrology of a gypsum playa, northern Salt Basin, Texas: The University of Texas at Austin, Bureau of Economic Geology Report of Investigations No. 158, 37 p.

Brune, G., 1981, The springs of Texas: Fort Worth, Branch-Smith, 566 p.

Chapman, J. E. B., 1984, Hydrogeochemistry of the unsaturated zone of a salt flat in Hudspeth County, Texas: The University of Texas at Austin, Master's thesis, 132 p.

Claypool, G. E., Holser, W. T., Kaplan, I. R., Sakai, H., and Zak, I., 1980, The age curves of sulfur and oxygen isotopes in marine sulfate and their mutual interpretation: Chemical Geology, v. 28, p. 199-260.

Correll, D. S., and Johnston, M. C., 1970, Manual of vascular plants in Texas: Renner, Texas, Texas Research Foundation, 1881 p.

Craig, H., 1961, Isotopic variations in meteoric waters: Science, v. 133, p. 1702-1703.

Dames and Moore, 1985, Siting of a low-level radioactive waste disposal facility in Texas: evaluation of State-owned lands: v. 2, Attachment C.

Dansgaard, W., 1964, Stable isotopes in precipitation: Tellus, v. 16, p. 436-469.

D'Appolonia Consulting Engineers, Inc., 1978, Phase I, ground-water recharge study, site 1; Cornudas, North and Culp Draws watershed, Site 2; Hitson, C & L and Washburn Draws watershed, Hudspeth County, Texas: United States Department of Agriculture, Soil Conservation Service, Temple, Texas, 65 p.

Dougherty, J. P., 1975, Evaporation data in Texas: Texas Water Development Board Report 192, 237 p.

Driscoll, F. G., 1986, Groundwater and wells, 2nd. ed.: St. Paul, Minnesota, Johnson Division, 1,089 p.

Dumas, D. B., 1980, Seismicity in the Basin and Range province of Texas and northeastern Chihuahua, Mexico, in Dickerson, P. W., Hoffer, J. M., and Callender, J. F., eds., Trans-Pecos region, southeastern New Mexico and West Texas: New Mexico Geological Society 31st Annual Field Conference Guidebook, p. 77-81.

Flawn, P. T., 1956, Basement rocks of Texas and southeast New Mexico: University of Texas, Austin, Bureau of Economic Geology Bulletin 5605, 261 p.

Freeze, R. A., and Cherry, J. A., 1979, Groundwater: Englewood Cliffs, New Jersey, Prentice-Hall, Inc., 604 p.

Gates, J. S., White, D. E., Stanley, W. D., and Ackermann, H. D., 1980, Availability of fresh and slightly saline ground waters in the basins of westernmost Texas: Texas Department of Water Resources Report 256, 108 p.

Goetz, L. K., 1977, Quaternary faulting in Salt Basin graben: The University of Texas at Austin, Master's thesis, 136 p.

Haley, J. F., 1971, Rb-Sr geochemistry of alkalic igneous intrusions, northern Trans-Pecos Texas: The University of Texas at Austin, Master's thesis, 62 p.

Henry, C. D., and Price, J. G., 1985, Summary of the tectonic development of Trans-Pecos Texas: The University of Texas at Austin, Bureau of Economic Geology Miscellaneous Map No. 36, 8 p.

Hodges, F. N., 1975, Petrology, chemistry and phase relations of the Sierra Prieta nepheline-analcime syenite intrusion, Diablo Plateau, Trans-Pecos Texas: The University of Texas at Austin, Ph.D. dissertation, 184 p.

Hoefs, J., 1973, Stable isotopes geochemistry: New York, Springer-Verlag, 112 p.

Hoy, R. N., and Gross, G. W., 1982, A baseline study of oxygen 18 and deuterium in the Roswell, New Mexico, groundwater basin: New Mexico Water Resources Research Institute, partial technical completion report for U.S. Department of the Interior, Office of Water Research and Technology, Project No. B-059-nmex.

King, P. B., 1948, Geology of the Southern Guadalupe Mountains, Texas: U.S. Geological Survey Professional Paper 215, 183 p.

_____ 1949, Regional geologic map of parts of Hudspeth and Culberson Counties, Texas: U.S. Geological Survey Oil and Gas Investigations Preliminary Map 90.

_____ 1965, Geology of the Sierra Diablo region, Texas: U.S. Geological Survey Professional Paper 480, 185 p.

King, P. B., and Flawn, P. T., 1953, Geology and mineral deposits of pre-Cambrian rocks of the Van Horn area, Texas: University of Texas, Austin, Bulletin 5301, 218 p.

Kreitler, C. W., Raney, J. A., Mullican, W. F., III, Collins, E. W., and Nativ, R., 1986a, Preliminary geologic and hydrologic studies of sites HU1A and HU1B in Hudspeth County, Texas: The University of Texas at Austin, Bureau of Economic Geology, report prepared for the Texas Low-Level Radioactive Waste Disposal Authority under interagency contract no. IAC(86-87)-1061, 104 p.

Kreitler, C. W., Raney, J. A., Nativ, R., Collins, E. W., Mullican, W. F., III, Gustavson, T. C., and Henry, C. D., 1986b, Final report for the Low-Level Radioactive Waste Disposal Authority: preliminary geologic and hydrologic studies of selected areas in Culberson and Hudspeth Counties, Texas: The University of Texas at Austin, Bureau of Economic Geology, report prepared for the Texas Low-Level Radioactive Waste Disposal Authority under interagency contract no. IAC(86-87)-0828, 184 p.

Kruseman, G. P., and De Ridder, N. A., 1976, Analysis and evaluation of pumping test data (3d ed.): Wageningen, The Netherlands, International Institute for Land Reclamation and Improvement, Bulletin 11, 200 p.

Larkin, T. J., and Bomar, G. W., 1983, Climatic atlas of Texas: Texas Department of Water Resources Publication LP-102, 151 p.

Logan, H. H., 1984, A ground-water recharge project associated with a flood protection plan in Hudspeth County, Texas--supportive geologic applications: Texas Christian University, Master's thesis, 110 p.

Masson, P. H., 1956, Age of igneous rocks at Pump Station Hills, Hudspeth County, Texas: American Association of Petroleum Geologists Bulletin, v. 40, no. 3, p. 501-518.

Muehlberger, W. R., Belcher, R. C., and Goetz, L. K., 1978, Quaternary faulting in Trans-Pecos Texas: Geology, v. 6, no. 6, p. 337-340.

National Weather Service, 1986a, Texas water oriented data bank--NWS maximum temperature for ID 00002012: 328 p.

_____ 1986b, Texas water oriented data bank--NWS minimum temperature for ID 00002012: 328 p.

_____ 1986c, Texas water oriented data bank--NWS precipitation for ID 00002012: 411 p.

Nativ, R., and Riggio, R., in preparation, Rain events in the Southern High Plains - their distribution and isotopic composition patterns.

Nativ, R., and Smith, D. A., 1985, Characterization study of the Ogallala aquifer, northwest Texas: The University of Texas at Austin, Bureau of Economic Geology, prepared for the U.S. Department of Energy, Office of Nuclear Waste Isolation under Contract No. DE-AC97-83WM46651, 103 p.

Nielson, P. D., and Sharp, J. M., Jr., 1985, Tectonic controls on the hydrogeology of the Salt Basin, Trans-Pecos Texas, in Structure and tectonics of Trans-Pecos Texas: West Texas Geological Society Guidebook, Publication 85-81, p. 231-234.

Orton, R. B., 1964, The climate of Texas and adjacent Gulf waters: Washington, D.C., U.S. Department of Commerce, Weather Bureau, 195 p.

Peckham, R. C., 1963, Summary of the ground-water aquifers in the Rio Grande Basin: Texas Water Commission, Circular No. 63-05, 16 p.

Reagor, B. G., Stover, C. W., and Algermissen, S. T., 1982, Seismicity map of the state of Texas: U.S. Geological Survey Miscellaneous Field Studies, map MF-1388.

Sanford, A. R., and Toppozada, T. R., 1974, Seismicity of proposed radioactive waste disposal site in southeastern New Mexico: New Mexico Bureau of Mines and Mineral Resources Circular 143, 15 p.

Scalapino, R. A., 1950, Development of ground water for irrigation in the Dell City area, Hudspeth County, Texas: Texas Board of Water Engineers, Bulletin 5004, 38 p.

Stead, F. L., and Waldschmidt, W. A., 1953, Regional significance of the Pump Station Hills, in Haigh, B. R., and others, Sierra Diablo, Guadalupe, and Hueco areas of Trans-Pecos Texas: West Texas Geological Society Guidebook, p. 70-85.

Sullins, C. J., 1971, Red Hills intrusion, northern Hudspeth County, Texas: The University of Texas at Austin, Master's thesis, 63 p.

Texas Water Development Board, 1985, Texas water oriented data bank--ground water quality system ID PD-115 for Hudspeth County, 24 p.

U. S. Department of Commerce, Economic Development Administration, 1986, Dell City Water Feasibility Study: 37 p.

U. S. Department of Housing and Urban Development, Federal Insurance Administration, 1985, Flood hazard boundary maps, Hudspeth County, Texas: Community-- Panel Nos. 480361 0400 B and 480361 0550B.

Walton, W. C., 1970, Groundwater resource evaluation: New York, McGraw-Hill, 664 p.

Wasserburg, G. J., Wetherill, G. W., Silver, L. T., and Flawn, P. T., 1962, A study of the ages of the Precambrian of Texas: Journal of Geophysical Research, v. 67, no. 10, p. 4021-4047.

Young, P. W., 1976, Water resources survey of Hudspeth County: West Texas Council of Governments, 156 p.

Appendix 1. Records of wells and springs in Hudspeth County sites.
Measurements are in feet.

BEG ID	Well name	TWC[1] ID	Coordinates		Ground-level elevation	Water-level depth	Water-level elevation	Total depth
LL106	Alamo Arroyo Spring				4,500		4,500	
LL107		48-42-1	31°22'12"	105°50'52"	3,855	335	3,550	450
LL108		48-42-404	31°18'56"	105°51'27"	3,610	90	3,520	267
LL109		48-41-618	31°17'31"	105°52'45"	3,523	10	3,513	305
LL110	Miller Feedlot	48-41-2	31°19'37"	105°54'55"	3,545	8	3,536	160
LL111		48-33-9	31°23'18"	105°53'18"	3,882	327	3,555	367
LL112	Head of Canyon Wm		31°31'42"	105°42'05"	5,059	380	4,679	720
LL113	Wilkey Well No. 1		31°23'23"	105°40'48"	4,307	600	3,707	730
LL114	Wilkey Well No. 2		31°22'48"	105°39'07"	4,346	76	4,270	200
LL115	Gunsight Well 2		31°25'03"	105°30'20"	4,780	405	4,375	480
LL116	Owen Well		31°22'31"	105°45'50"	4,014	120	3,894	300
LL126	Low Level Well		31°24'14"	105°43'32"	4,179	478	3,699	530
LL127	Gunsight Well 1		31°24'43"	105°34'45"	5,154	627	4,527	690
LL128	Temple Well	48-24-1	31°44'40"	105°05'25"	3,726	107	3,619	
LL129	Guillen E on Well	48-23-201	31°44'48"	105°12'06"	4,007	429	3,578	
LL130	Desert Inn Well	48-14-7	31°45'56"	105°21'22"	4,135			
LL131	Cornudas Cafe Well	48-13-7	31°46'45"	105°28'09"	4,304			
LL132	Williams Ranch House Well	48-20-6	31°41'31"	105°30'09"	4,334	709	3,625	
LL133	Puett Well	48-13-8	31°46'38"	105°26'53"	4,341			
LL134	Hobo Well-Deep	48-20-5	31°41'44"	105°33'07"	4,416			
LL135	Jardin Well	48-30-4	31°33'27"	105°21'25"	4,282	528	3,754	
LL136	Sparks Windmill	48-14-9	31°46'18"	105°16'45"	4,053	446	3,607	
LL137	Sparks House Pump Well	48-14-8	31°45'39"	105°18'04"	4,032	510	3,522	
LL138	Williams #4 Well	48-12-8	31°46'21"	105°33'09"	4,409	790	3,619	
LL139	Stewart #2 Well	48-12-5	31°48'30"	105°32'52"	4,447			
LL140	Adobe House Tank Well	48-21-5	31°41'10"	105°25'18"	4,200			
LL141	Bravo Well	48-29-3	31°36'14"	105°24'27"	4,278	628	3,650	
LL142	Three Sisters Well	48-29-1	31°36'10"	105°28'18"	4,362	48	4,314	
LL143	Sumrall Well	48-16-7	31°45'57"	105°05'20"	3,668	100	3,568	
LL144	Foster House Well	48-14-1	31°51'44"	105°21'44"	4,186			
LL145	Foster South Well	48-13-9	31°47'15"	105°22'47"	4,182			
LL146	Stewart #1 Well	48-12-5	31°48'29"	105°32'56"	4,445			
LL147	Beard #1 Well	48-12-7	31°46'07"	105°37'02"	4,523			
LL148	Red Well	48-23-7	31°37'47"	105°14'20"	4,075	463	3,612	
LL149	Sampson Well	48-23-1	31°42'04"	105°12'45"	3,886	262	3,625	
LL150	South Well	48-28-3	31°35'29"	105°30'08"	4,430	63	4,367	
LL151	Moon Well	48-38-1	31°29'45"	105°21'59"	4,336	160	4,176	
LL152	Gibbs Well	48-14-4	31°49'17"	105°20'17"	4,081			
LL153	Hartnutt Well	48-31°9	31°31'20"	105°09'33"	4,509			
LL154	Flattop Well- Figure 2 Ranch	48-24-9	31°37'49"	105°02'10"	3,745	294	3,451	
LL155	Frederick Well	48-39-1	31°28'16"	105°13'16"	4,368	742	3,626	
LL156	Baylor-New Well	48-37-3	31°28'05"	105°22'59"	4,408	210	4,198	
LL157	Baylor-Old Well	48-37-3	31°27'38"	105°24'51"	4,449	72	4,377	
LL158	Desert Inn Abnd. Well	48-14-7	31°45'38"	105°22'05"	4,170	549	3,622	

BEG ID	Well name	TWC[1] ID	Coordinates		Ground-level elevation	Water-level depth	Water-level elevation	Total depth
LL159	Abnd. Adobe House Tank	48-21-5	31°41'06"	105°25'15"	4,201	583	3,618	
LL160	Hobo Well-Shallow	48-20-5	31°41'48"	105°33'08"	4,415	18	4,397	
LL161	Geothermal Well (UTEP)	48-21-6	31°41'47"	105°22'40"	4,224	74	4,150	
LL162	Williams Pump Jack #1	48-21-4	31°41'18"	105°28'50"	4,303	677	3,626	
LL163	Cavender Well	48-24-4	31°42'15"	105°07'19"	3,832	310	3,522	
LL164	Graham Well	48-24-2	31°43'34"	105°03'40"	3,668	100	3,568	
LL165	Bill Crane Well	48-24-5	31°41'54"	105°02'38"	3,658	140	3,518	
LL166	Morrison Well	48-24-6	31°40'34"	105°01'48"	3,629	40	3,589	
LL167	Wesley West Well	48-24-9	31°38'20"	105°01'11"	3,659	80	3,579	
LL168	Black Mountain Well	48-23-9	31°39'39"	105°07'34"	3,993	460	3,533	
LL169	Babbs Well	48-32-6	31°34'38"	105°01'22"	3,718	123	3,595	
LL170		48-07-101	31°58'08"	105°14'39"	3,804	205	3,599	700
LL171		48-07-102	31°57'33"	105°14'40"	3,795	218	3,577	962
LL172		48-07-206	31°59'25"	105°12'02"	3,709	129	3,580	215
LL173		48-07-207	31°58'10"	105°12'01"	3,707	122	3,585	712
LL174		48-07-210	31°58'15"	105°12'27"	3,721	145	3,576	240
LL175		48-07-214	31°57'56"	105°10'57"	3,678	93	3,585	500
LL176		48-07-304	31°58'00"	105°07'55"	3,644	60	3,584	
LL177		48-07-405	31°56'17"	105°13'27"	3,755	175	3,580	230
LL178		48-07-414	31°55'13"	105°14'39"	3,795	212	3,583	680
LL179		48-07-418	31°56'17"	105°14'39"	3,805	216	3,590	886
LL180		48-07-501	31°55'37"	105°11'51"	3,688	106	3,582	
LL181		48-07-504	31°56'11"	105°12'00"	3,696	72	3,624	175
LL182		48-07-516	31°56'37"	105°12'02"	3,705	119	3,586	300
LL183		48-07-606	31°57'10"	105°09'51"	3,651	67	3,583	
LL184		48-07-607	31°55'23"	105°08'51"	3,641	59	3,582	
LL185		48-07-706	31°53'34"	105°12'38"	3,712	131	3,581	835
LL186		48-07-708	31°52'37"	105°12'32"	3,722	138	3,584	1,583
LL187		48-07-801	31°54'53"	105°10'56"	3,658	80	3,578	200
LL188		48-07-803	31°53'31"	105°12'00"	3,693	100	3,593	278
LL189		48-07-901	31°54'56"	105°07'49"	3,637	53	3,584	300
LL190		48-07-904	31°53'27"	105°09'51"	3,660	62	3,598	780
LL191		48-08-102	31°59'03"	105°07'17"	3,642	56	3,586	392
LL192		48-06-201	31°59'59"	105°17'54"	3,940	303	3,637	1,100
LL193		48-06-601	31°56'20"	105°16'15"	3,874	310	3,564	1,505
LL194		48-15-203	31°51'43"	105°11'55"	3,715	138	3,599	325
LL195		48-15-301	31°50'53"	105°09'19"	3,652	60	3,593	320
LL196		48-16-402	31°48'26"	105°05'31"	3,652	61	3,591	140
LL197	(Eclipse Well)	47-01-7	31°54'57"	104°58'24"	3,671	50	3,621	
LL198		48-08-9	31°52'37"	105°00'45"	3,635	22	3,613	
LL199		48-08-4	31°55'23"	105°06'05"	3,616	3	3,613	
LL200		48-16-8	31°45'11"	105°02'50"	3,622	23	3,599	
LL201		47-09-1	31°50'58"	104°57'21"	3,697	91	3,606	
LL202		47-09-803	31°45'19"	104°55'01"	3,790	191	3,599	
LL203		47-09-805	31°46'51"	104°56'17"	3,696	97	3,591	515
LL204		47-09-8	31°46'10"	104°56'16"	3,722	130	3,592	

BEG ID	Well name	TWC[1] ID	Coordinates		Ground-level elevation	Water-level depth	Water-level elevation	Total depth
LL205	(Black John Well)	47-17-3A	31°44'27"	104°53'57"	3,805	202	3,603	
LL206		47-17-6A	31°40'51"	104°53'50"	3,722	135	3,587	
LL207		47-17-6B	31°40'39"	104°54'06"	3,708	141	3,567	
LL208		47-17-6C	31°40'51"	104°54'59"	3,639	29	3,610	
LL209	(Hardluck Well)	47-17-3B	31°42'20"	104°54'06"	3,697	97	3,600	
LL210		47-17-3C	31°43'31"	104°54'02"	3,755	159	3,596	
LL211		47-17-2A	31°44'33"	104°56'00"	3,717	112	3,605	
LL212		47-17-2B	31°43'38"	104°56'03"	3,688	84	3,604	
LL213		47-18-4A	31°37'37"	104°52'25"	3,762	163	3,599	
LL214		48-32-3	31°36'30"	105°00'39"	3,636	39	3,597	
LL215	(Curton Well?)	47-25-4	31°32'45"	104°58'24"	3,650	48	3,602	
LL216		47-26-7	31°31'44"	104°52'30"	3,674	88	3,586	
LL217		47-26-9	31°31'18"	104°46'02"	3,786	202	3,584	
LL218	Abandoned Well	48-12-9	31°46'13"	105°30'51"	4,325	675	3,650	
LL219	Love Well	48-39-701	31°24'17"	105°13'50"	4,517	889	3,628	
LL220	Maupin Well	48-38-703	31°23'14"	105°20'37"	4,515	888	3,627	

[1]TWC well identification system has 3 sets of numbers; preliminary wells have 1 number in the last set, permitted wells have 3.

Appendix 2. Hydraulic conductivity measurements in unweathered bedrock of the unsaturated zone, Diablo Plateau.

The hydraulic conductivity of two intervals of unweathered bedrock was measured at sites HU1A and HU1B to characterize potential migration rates in the area. Procedure and interpretations follow those reported by Boersma (1965) and Freeze and Cherry (1979). The method used is referred to as the shallow well - pump-in method, the piezometric method, or the dry-auger-hole method. This method requires an uncontaminated borehole, drilled with either a hollow-stem auger or a rotary rig, and a drill bit utilizing compressed air to circulate cuttings to the surface. At site HU1A, the interval to be tested consisted of unweathered rhyolite porphyry. Attempts to core this section with air proved unsuccessful (because of tremendous heat buildup), and fresh water had to be used to circulate cuttings and cool the core bit. To a lesser extent, a similar situation existed at HU1B in Cretaceous Campagrande limestones and was also cored with fresh water. To reduce borehole contamination, the fresh water was circulated only once to keep the borehole flushed of cuttings.

Water was then supplied to the test interval and maintained at a constant level. The rate of water input was adjusted until a steady state was achieved. Hydraulic conductivity was then calculated using the following equation:

$$K = \frac{[\ln(h/r + \sqrt{(h/r)^2 - 1}) - 1]\, Q}{2\pi h^2}$$

where

K = hydraulic conductivity (cm/hr)

h = depth of water maintained as measured from the bottom of the hole (cm)

r = the radius of the test hole (cm)

Q = rate at which water flows into the test interval (cm^3)

Tests performed during this study were conducted on two different units, unweathered rhyolite porphyry at HU1A and unweathered limestone at HU1B. In previous tests in the Fort Hancock area (Kreitler and others, 1986b), uniform coarse sand was added to the test hole before adding water to stabilize the walls of the hole. This was not necessary for these tests, however, due to the competent nature of the intervals tested. Results of the two tests are presented in the following table.

Tested lithology	Depth of borehole (cm)	Length of the tested interval (cm)	Radius of the borehole (cm)	Final rate of flow into the borehole (cm^3/hr)	(cm/hr)
Rhyolite	1,524	914	3.7846	240,000	.0935
Limestone	1,524	914	4.8133	1,182,000	.4415

Hydraulic conductivity of the rhyolite at HU1A was calculated to be 26.8 ft/yr (8.19 m/yr) and that of the limestone at HU1B was 126.6 ft/yr (38.6 m/yr).

Appendix 3. Pumping test data and interpretation.

In order to determine the hydraulic properties of both aquifers A and B, seven pumping tests (PT) were conducted on water wells evenly spaced across the Diablo Plateau within the study area (fig. A3-1). The first pumping test was conducted in September 1986, and PT #2 through 7 were performed from January to March 1987. Three of the seven pumping tests resulted in only minimal, relatively instantaneous drawdown of the producing aquifer, because of inadequate production capacity of the water well required to stress the aquifer. Driscoll (1986) offers one method to determine whether or not this early drawdown is the result of wellbore storage or actual drawdown of the aquifer. In each of the three pumping tests where this was suspected, all or part of the drawdown was attributed to wellbore storage. When all or part of a very small drawdown curve is attributed to wellbore storage, no method can reliably be used to determine transmissivity. The following is a detailed discussion of each pumping test, methods used during analysis, and the resulting transmissivity. A summary of this data also appears within the hydrologic section, Water-bearing Characteristics.

PT #1

In order to determine the hydraulic parameters of the regional aquifer, PT #1 was conducted in well LL162 at Williams Ranch, Hudspeth County (fig. A3-1). The well is located 6.7 mi (10.8 km) west-northwest of the intersection between Ranch-to-Market Roads 1111 and 2317 (fig. A3-2). This well was drilled by El Paso Natural Gas Company to serve as a water supply well for their pump station #2. It was drilled into probable Victorio Peak - Bone Spring limestones of Permian age

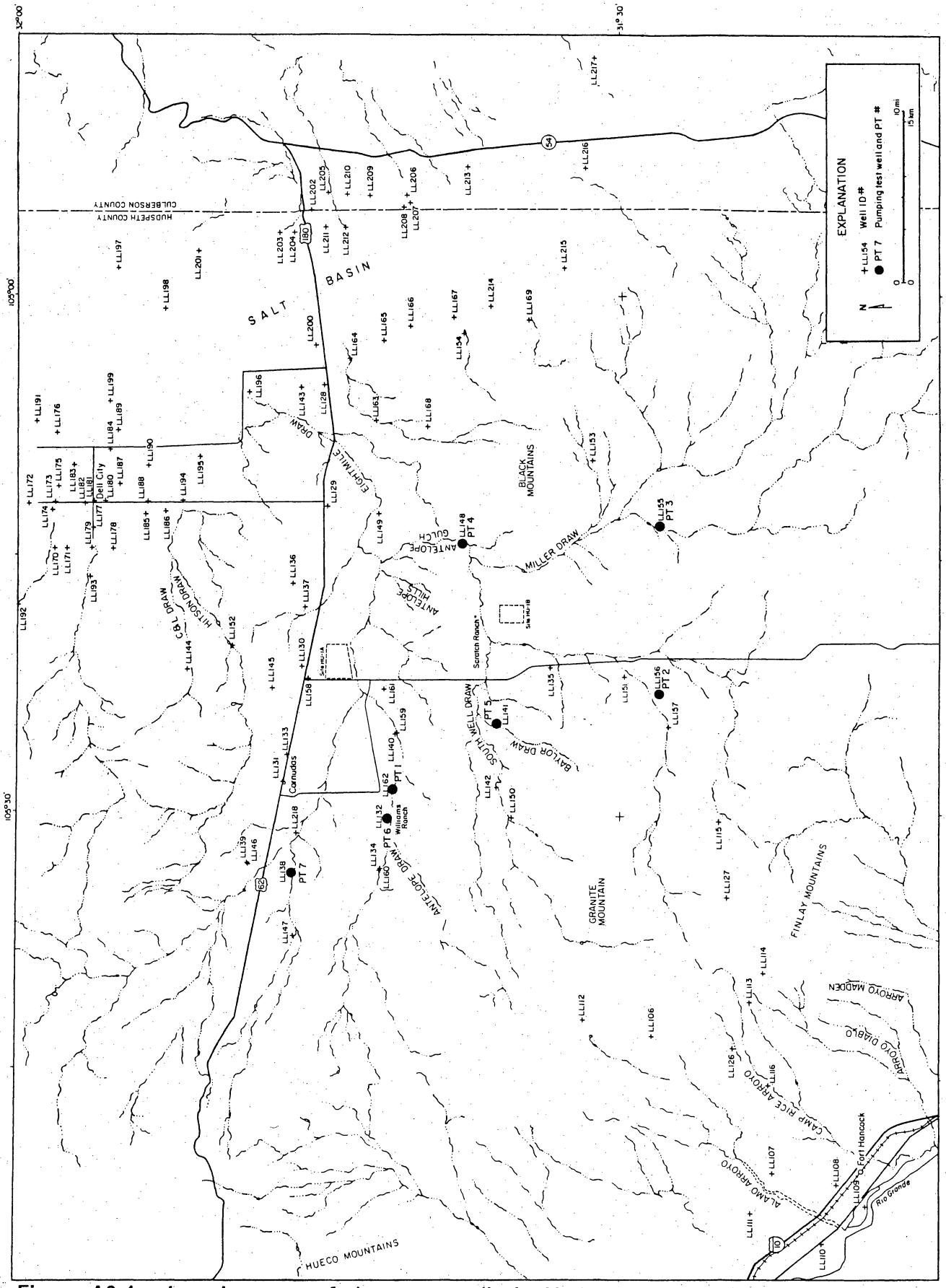

Figure A3-1. Location map of the seven wells in Hudspeth County tested during this study as part of hydrologic characterization studies.

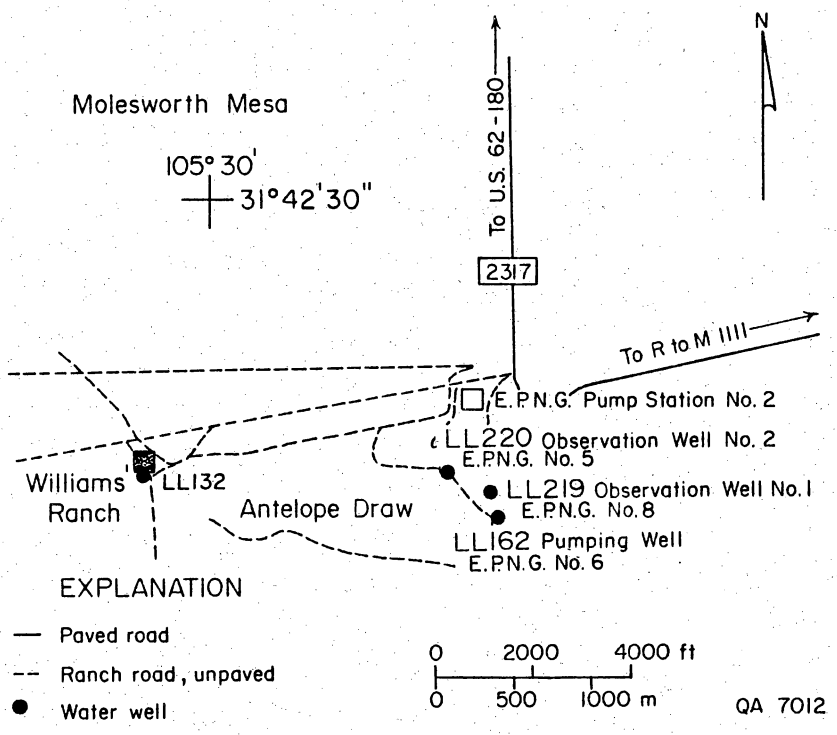

Figure A3-2. Location map of wells used in pumping test no. 1, Williams Ranch, Hudspeth County. Wells LL219 and LL220 served as observation wells the during pumping test.

to an original total depth of 1,214 ft (370 m). Wellbore diameter was 8 inches (20.3 cm). Static water level in this well was measured at 677 ft (206.3 m) below land surface, and the saturated thickness is approximately 400 ft (121.9 m). Two adjacent wells, LL219 and LL220, located 468 ft (142.6 m) north-northwest and 1,326 ft (404 m) northwest of LL162, respectively, served as observation wells for the test. Water levels in these wells were measured at 671.5 ft (204.6 m) and 682.5 ft (208.0 m), respectively, below land surface. A shallow aquifer (see Hydrologic Setting, this report) was found in observation well LL219 at a depth of about 200 ft (61 m) below land surface. Cascading ground water from this level to the bottom of the well was clearly audible in this borehole and was also observed on the electric line-probe from 200 ft (60.9 m) down to the producing aquifer.

The test started at 12:40 p.m. on September 26, 1986. Production rates were essentially constant throughout the drawdown phase at 9.7 to 10.1 gpm (table A3-1). During the pumping period, which lasted 32 hr and 50 min, the recorded water level dropped 60.5 ft (18.4 m) in the pumping well (fig. A3-3, A3-4, table A3-1), but no drawdown was detected in the observation wells. When the pump was turned off at 9:31 p.m. on September 27, the recovery of water level was monitored for another 31 hr and 30 min, until 5:00 a.m., September 28. By that time 58.4 ft (17.8 m) of the 60.5 ft (18.4 m) of drawdown had recovered (fig. A3-5, table A3-2).

Two distinct segments appear on figures A3-3 and A3-5. The change in slope of drawdown curve with time could be the result of several possible scenarios that may affect interpretation of the data.

A. The tested deep aquifer is semiconfined, and the shallow aquifer may leak into it. Considering this interpretation, the early part of the test represents nonsteady flow and nonleaky conditions. Leakage from the shallow aquifer starts at

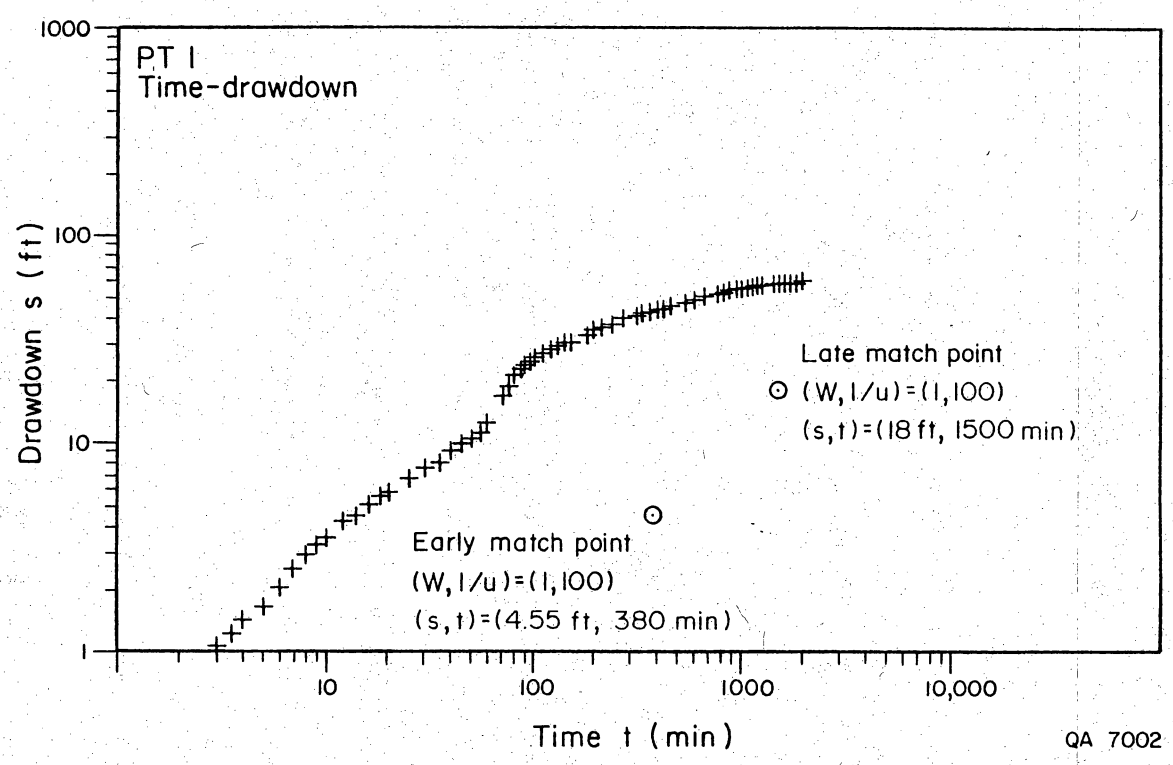

Figure A3-3. Time-drawdown curve that was matched to Walton type curves for pumping test no. 1 in well LL162. Two distinct segments appear on the curve, suggesting (1) leakage from Aquifer B to Aquifer A after a short drawdown that was caused by early pumpage or (2) dewatering of additional fracture systems as the test proceeded.

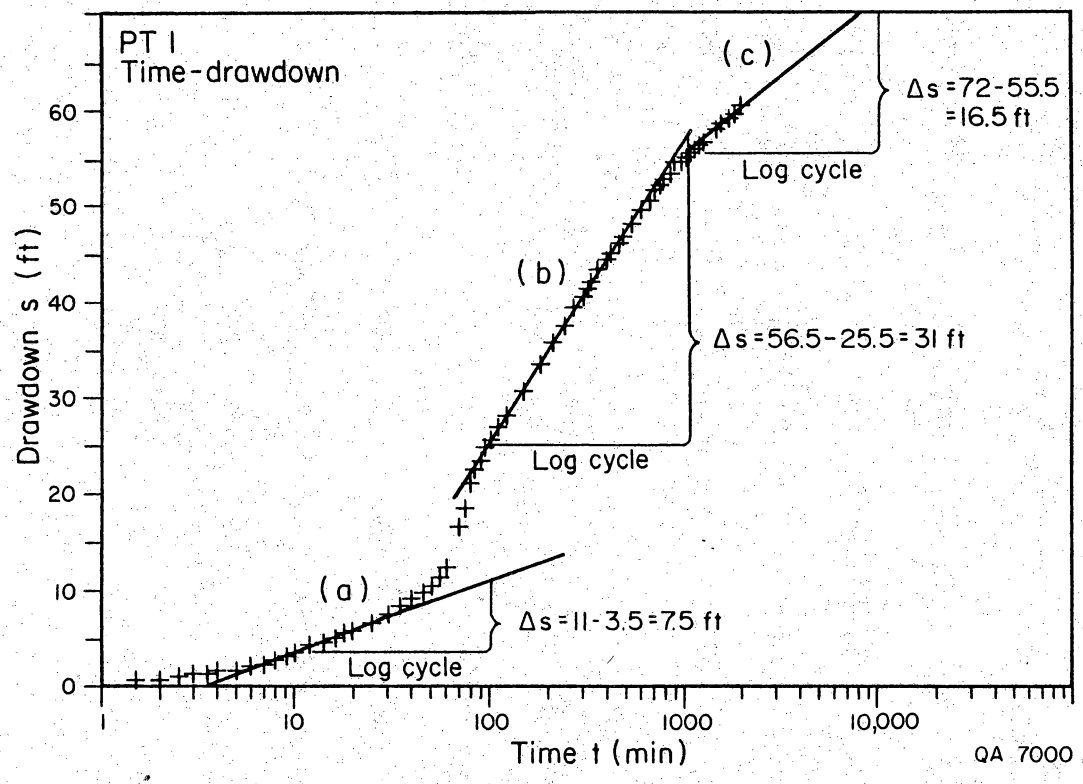

Figure A3-4. Time-drawdown plot interpreted using Jacob's method for pumping test no. 1 in well LL162. Three segments were found on the curve and may represent the dewatering of three separated fracture systems, as the cone of depression extended to greater distance from the pumping well.

Table A3-1. Drawdown data from pumping test no. 1 at well LL162.

Time (hr)	Time from beginning of pumpage (min)	Depth to water level (ft)	Water level drawdown (ft)	Flow meter reading (gal)	Well discharge (gpm)
12:40:00	0.0	680.00	0.00	3,353	0.0
12:40:30	0.5	680.00	0.00	-	-
12:41:00	1.0	680.27	0.27	3,361	8.0
12:41:30	1.5	680.625	0.625	3,365	8.0
12:42:00	2.0	680.792	0.792	3,371	12.0
12:42:30	2.5	680.917	0.917	3,378	14.0
12:43:00	3.0	681.083	1.083	-	-
	3.5	681.208	1.208	3,387	9.0
12:44:00	4.0	681.396	1.396	3,390.5	7.0
12:45:00	5.0	681.688	1.688	3,403	12.5
12:46:00	6.0	682.042	2.042	-	-
12:47:00	7.0	682.458	2.458	3,424	10.5
12:48:00	8.0	682.917	2.917	3,434	10.0
12:49:00	9.0	683.292	3.292	3,445	11.0
12:50:00	10.0	683.542	3.542	3,454	9.0
12:52:00	12.0	684.208	4.208	3,476	11.0
12:54:00	14.0	684.542	4.542	3,496	10.0
12:56:00	16.0	685.083	5.083	3,517	10.5
12:58:00	18.0	685.496	5.496	3,537	10.0
13:00:00	20.0	685.83	5.83	3,557	10.0
13:05:00	25.0	686.771	6.771	-	-
13:10:00	30.0	687.542	7.542	3,661	10.4
13:15:00	35.0	688.354	8.354	-	-
13:20:00	40.0	689.188	9.188	3,760	9.9
13:25:00	45.0	689.979	9.979	-	-
13:30:00	50.0	690.500	10.500	3,862	10.2
13:35:00	55.0	691.229	11.229	-	-
13:40:00	60.0	692.250	12.250	3,964	10.2
13:50:30	70.5	696.854	16.854	4,067	10.3
13:55:00	75.0	698.646	18.646	-	-
14:00:00	80.0	701.166	21.166	4,166	9.9
14:05:00	85.0	702.729	22.729	-	-
14:10:00	90.0	703.896	23.896	4,268	10.2
14:15:00	95.0	704.960	24.960	-	-
14:20:00	100.0	705.750	25.750	4,368	10.0
14:30:00	110	707.000	27.000	4,469	10.1
14:40:00	120	708.166	28.166	4,569	10.0
15:10:00	150	710.760	30.760	4,873	10.1
15:40:00	180	713.33	33.33	5,174	10.03
16:10:00	210	715.65	35.65	5,476.5	10.08
16:40:00	240	717.63	37.63	5,778	10.05
17:10:00	270	719.50	39.50	6,080	10.07
17:54:00	314	721.44	41.44	-	-
18:10:30	330.5	722.15	42.15	-	-
18:13:00	333			6,710	10.0
18:41:00	361	723.25	43.25	6,992	10.07
19:10:00	390	724.29	44.29	7,280.5	9.95
19:40:00	420	724.96	44.96	7,573	9.75
20:17:00	457	725.94	45.94	7,945	10.05
20:40:00	480	726.65	46.65	8,170.5	9.80

Table A3-1. (cont.)

Time (hr)	Time from beginning of pumpage (min)	Depth to water level (ft)	Water level drawdown (ft)	Flow meter reading (gal)	Well discharge (gpm)
21:40:00	540	728.00	48.00	8,761	9.84
22:10:00	570			9,045	9.80
22:40:00	600	729.33	49.33		
23:37:00	657			9,999	10.97
23:40:00	660	730.88	50.88	-	-
01:11:00	751	732.17	52.17	-	-
01:40:00	780	732.71	52.71	-	-
02:40:00	840	733.50	53.50		
02:42:00	842			11,710	9.25
03:40:00	900	734.08	54.08		
03:42:00	902			12,290	9.67
04:45:00	965	734.71	54.71	12,921.5	10.02
05:30:00	1,010			13,365.0	9.86
05:40:00	1,020	735.16	55.16		
06:47:00	1,087	735.58	55.58	14,112	9.70
07:40:00	1,140	736.0	56.00	14,637	9.91
08:40:00	1,200	736.44	56.44	15,223.5	9.78
09:40:00	1,260	736.63	56.63	15,820.0	9.78
13:23:00	1,483			18,000	9.82
13:25:00	1,485	738.17	58.17		
14:38:00	1,558			18,732	9.76
14:46:00	1,566	738.50	58.50		
16:54:00	1,694			20,065	9.80
16:56:00	1,696	739.00	59.00		
18:34:00	1,794			21,040	9.75
18:40:00	1,800	739.87	59.87		
21:08:00	1,948			22,570	9.94
21:10:00	1,950	740.35	60.35		
21:31:00	1,971	740.50	60.50	22,784.5	9.75

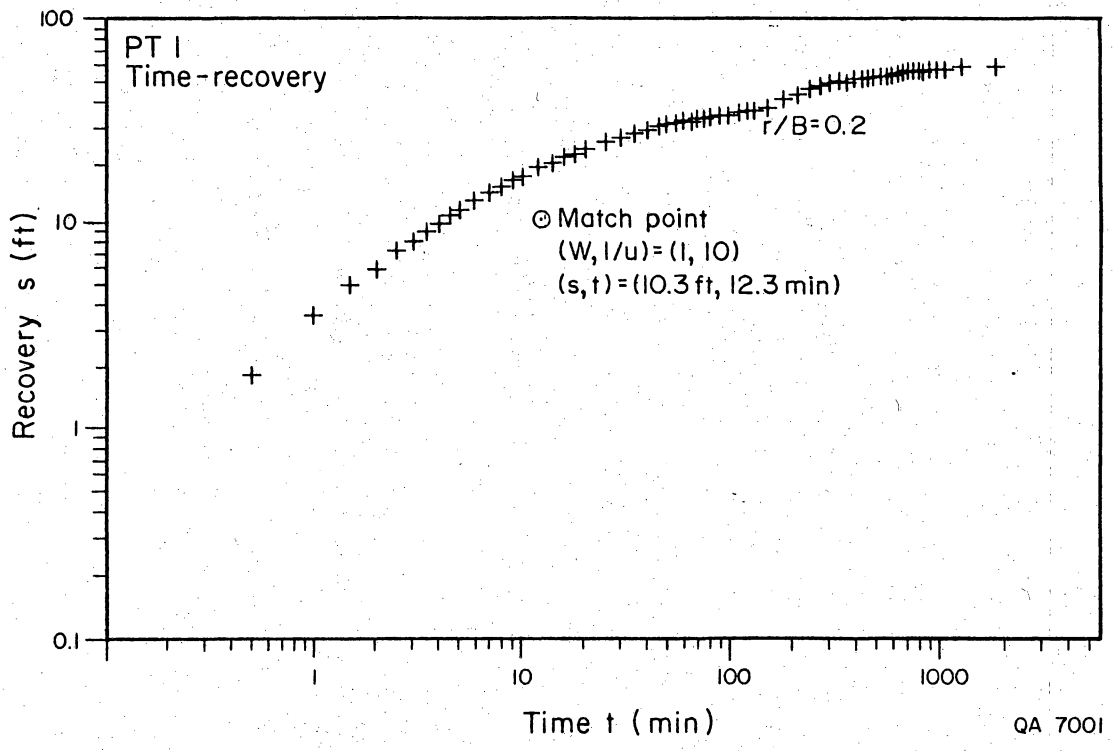

Figure A3-5. Time-recovery curve matched to Walton type curves for pumping test no. 1 in well LL162. Two distinct segments appear on the curve, similar to the time-drawdown curve.

Table A3-2. Recovery test data from pumping test no. 1 at well LL162.

Time (hr)	Time from beginning of recovery (min)	Time since pump started / Time since pump stopped (tp + Δt) / Δt	Depth to water level (ft)	Residual drawdown (s') (ft)	Water level recovery (ft)
21:31:00	0	∞	740.50	60.5	0
21:31:30	0.5	3,943	738.69	58.69	1.81
21:32:00	1.0	1,972	736.92	56.92	3.58
21:32:30	1.5	1,315	735.63	55.63	4.87
21:33:00	2.0	986.5	734.58	54.58	5.92
21:33:30	2.5	789.4	733.37	53.37	7.13
21:34:00	3.0	658.0	732.46	52.46	8.04
21:34:30	3.5	564.14	731.42	51.42	9.08
21:35:00	4.0	493.75	730.65	50.65	9.85
21:35:30	4.5	439.0	729.73	49.73	10.77
21:36:00	5.0	395.20	729.17	49.17	11.33
21:37:00	6.0	329.50	727.79	47.79	12.71
21:38:00	7.0	282.57	726.60	46.60	13.90
21:39:00	8.0	247.38	725.59	45.59	14.91
21:40:00	9.0	220.0	724.67	44.67	15.83
21:41:00	10.0	198.1	723.73	43.73	16.77
21:43:00	12.0	165.25	722.19	42.19	18.31
21:45:00	14.0	141.79	720.82	40.82	19.68
21:47:00	16.0	124.19	719.75	39.75	20.75
21:49:00	18.0	110.5	718.78	38.78	21.72
21:51:00	20.0	99.55	717.85	37.85	22.65
21:56:00	25.0	79.84	716.05	36.05	24.45
22:01:00	30.0	66.70	714.7	34.69	25.81
22:06:00	35.0	57.31	713.41	33.41	27.09
22:11:00	40.0	50.28	712.31	32.31	28.19
22:16:00	45.0	44.80	711.41	31.41	29.09
22:21:00	50.0	40.42	710.74	30.74	29.76
22:26:00	55.0	36.84	710.12	30.12	30.38
22:31:00	60.0	33.85	709.60	29.60	30.90
22:36:00	65.0	31.32	709.13	29.13	31.37
22:41:00	70.0	29.16	708.71	28.71	31.79
22:46:00	75.0	27.28	708.35	28.35	32.10
22:51:00	80.0	25.64	708.04	28.04	32.46
22:56:00	85.0	24.19	707.71	27.71	32.79

Table A3-2. (cont.)

Time (hr)	Time from beginning of recovery (min)	Time since pump started / Time since pump stopped (tp + Δt) / Δt	Depth to water level (ft)	Residual drawdown (s') (ft)	Water level recovery (ft)
23:01:00	90.0	22.90	707.40	27.40	33.10
23:06:00	95.0	21.75	707.11	27.11	33.39
23:11:00	100.0	20.71	706.83	26.83	33.67
23:21:00	110	18.92	706.35	26.35	34.15
23:31:00	120	17.43	705.89	25.89	34.61
24:01:00	150	14.14	704.23	24.23	36.27
24:31:00	180	11.95	701.28	21.28	39.22
01:01:00	210	10.39	698.17	18.17	42.33
01:31:00	240	9.21	695.85	15.85	44.65
02:01:00	270	8.30	694.34	14.34	46.16
02:31:00	300	7.57	693.10	13.10	47.40
03:01:00	330	6.97	692.25	12.25	48.25
03:31:00	360	6.48	691.46	11.46	49.04
04:01:00	390	6.05	690.98	10.98	49.52
04:34:00	423	5.66	690.35	10.35	50.15
05:01:00	450	5.38	689.90	9.90	50.60
05:31:00	480	5.11	689.37	9.37	51.13
06:31:00	540	4.65	688.59	8.59	51.91
07:01:00	570	4.46	688.20	8.20	52.30
07:34:00	603	4.27	687.83	7.83	52.67
08:10:00	639	4.08	687.42	7.42	53.08
08:31:30	660.5	3.98	687.13	7.13	53.37
09:01:00	690	3.86	686.88	6.88	53.62
10:00:00	749	3.63	686.30	6.30	54.20
11:00:00	809	3.44	685.72	5.72	54.78
12:00:00	869	3.27	685.31	5.31	55.19
13:38:00	967	3.04	684.63	4.63	55.88
15:19:00	1,068	2.85	684.03	4.03	56.47
19:00:00	1,290	2.53	683.29	3.29	57.21
05:00:00	1,890	2.04	682.08	2.08	58.42

early drawdown when water level approaches 10 to 20 ft (3.0 to 6.1 m). A similar effect can be seen on the recovery curve. When water level recovers to 10 to 20 ft (3.0 to 6.1 m) below its initial stage, a change in slope can be observed. The presence of a shallow aquifer at the adjacent observation well (LL219) may support this explanation. Interpretation of the test data based on these conditions can be done by matching Walton's (1970) set of type curves for unsteady flow in semiconfined leaky aquifers to the time-drawdown and time-recovery plots (figs. A3-3 and A3-5). Walton developed a method of solution that followed the Theis method (Kruseman and De Ridder, 1976), but, instead of one type curve, he used a family of type curves for several values of r/B (a ratio that includes the coefficient of transmissivity, permeability, and saturated thickness of the leaking aquitard). Transmissivity is calculated as follows:

$$T = \frac{114.6\ Q\ W(u,\ r/B)}{s}$$

where

T = transmissivity (gpd/ft)

Q = discharge rate (gpm)

s = drawdown or the residual recovery (ft)

W(u, r/B) = the well function (Kruseman and De Ridder, 1976) and the Y coordinate of the match point from the type curve.

The early part of the drawdown (30 min) may represent the flow in the pumped aquifer when no leakage from the upper aquifer was involved. The late part of the test may also include water contributed from the upper aquifer, as a result of the change in head in the deeper aquifer. Two transmissivity values were calculated for both parts of the drawdown. The early data set was matched to the nonleaky artesian type curve, and the match point had the coordinates (W, 1/u)=(1,100) and (s,t)=(4.55 ft, 380 min). The late part of the data curve was matched with the

curve r/B=0.2, and the match point had the coordinates (W,1/u)=(1,100) and (s,t)=(18 ft, 1500 min) (fig. A3-3). Pumpage rate used for the calculation was the mean value of 10.01 gpm. Transmissivity values calculated from both parts of the test were 252.1 gpd/ft for the early part, and 63.7 gpd/ft for the late part (33.7 ft^2/d or 3.1 m^2/d and 8.5 ft^2/d or 0.8 m^2/d), respectively.

The early recovery part of the test (120 min) was used to check on the values calculated for the pumping period that were significantly different. By matching the data to the curve r/B=0.2, we found that the match point had the coordinates (W, 1/u)=(1,100) and (s,t)=(10.3 ft and 12.3 min) (fig. A3-5), and the calculated transmissivity was 111 gpd/ft (14.9 ft^2/d or 1.4 m^2/d). This value is higher than the value estimated for the symmetric late-pumping period during the drawdown part of the test.

B. Nonsteady flow, the aquifer is confined, and the two segments on both curves represent the permeability of the area around the borehole at the early time and the more regional pattern of permeability at a later stage. In this case, Jacob's method (Kruseman and De Ridder, 1976) can be used for interpretation of the late part of the drawdown, and the Theis recovery method (Kruseman and De Ridder, 1976) can be used for evaluation of both stages of recovery.

Jacob developed a method to calculate the transmissivity based on the Theis formula for cases in which the value of u is small ($u= r^2S/4Tt$; r is the well diameter, S is the storativity, T is the transmissivity, and t is the test duration). U is small as t (test duration) increases, and therefore the later part of the drawdown is suitable for the analysis. Transmissivity is calculated as follows:

$$T = \frac{2.3\ Q}{4\pi\Delta s}$$

where

T = transmissivity (m^2/d)

Q = discharge rate (m^3/d)

s = drawdown (m).

Three segments were found on the drawdown curve and may represent the dewatering of three separated fracture systems, as the cone of depression extended further from the pumping well. For the calculation Δs were 7.5 ft/log cycle for the early phase, 31 ft/log cycle for the intermediate time, and 16 ft for the late part of the test (fig. A3-5). Calculated transmissivity values were 111, 84, and 158.6 gpd/ft (14.9 ft^2/d, or 1.44 m^2/d, 11.3 ft^2/d, or 1.05 m^2/d, and 21.5 ft^2/d, or 1.97 m^2/d), respectively.

The Theis method was used to calculate transmissivity from the time-recovery curve following the formula:

$$T = \frac{2.3\ Q}{4\pi\Delta s'}$$

where

T = transmissivity (m^2/d)

Q = discharge rate (m^3/d)

s'= residual drawdown (m)

In their calculations $\Delta s'$ values were 20 and 21.5 ft/log cycle for the early and late periods of recovery, respectively. Calculated transmissivity values for the early and late part of the recovery curve (fig. A3-6) were 130.6 gpd/ft and 121.5 gpd/ft (17.4 ft^2/d or 1.6 m^2/d and 16.2 ft^2/d or 1.5 m^2/d), respectively.

Transmissivity values calculated by the methods of Walton, Jacob, and Theis for both a semiconfined leaky aquifer and a confined nonleaky aquifer range from

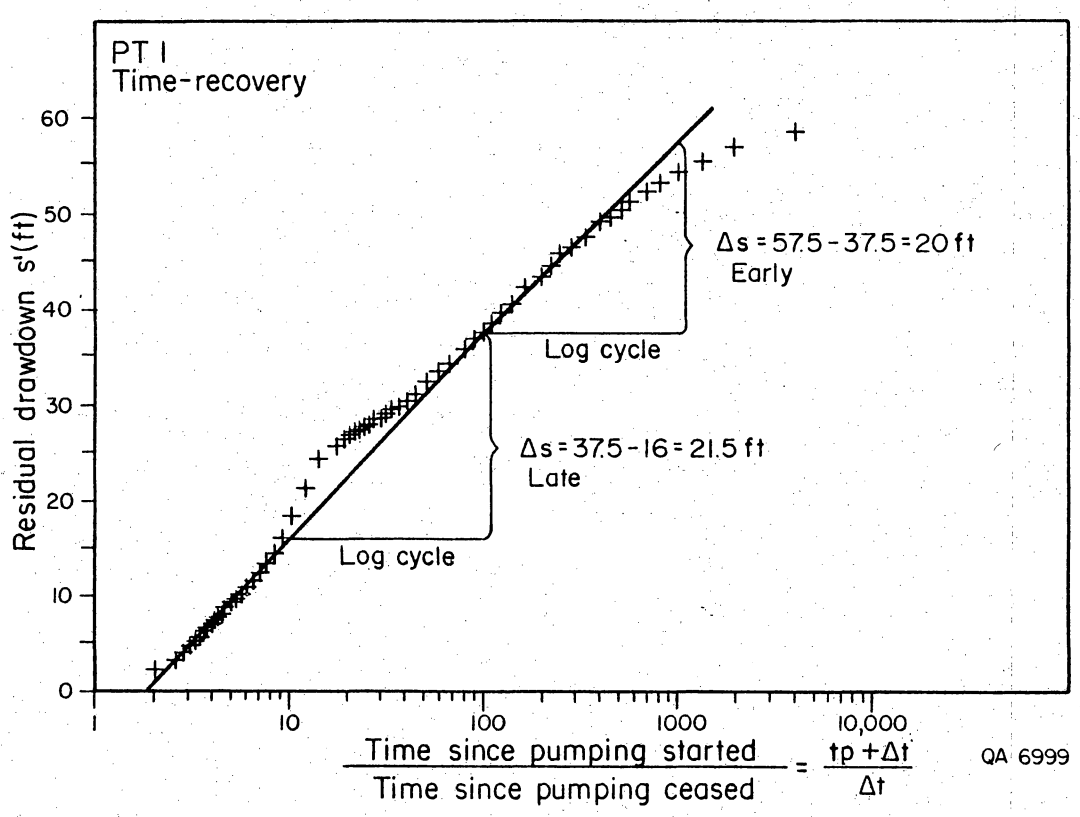

Figure A3-6. Time-recovery plot interpreted using Theis' method for pumping test no. 1 in well LL162.

63.7 gpd/ft to 252.1 gpd/ft, and the mean transmissivity calculated from all methods is 129.1 gpd/ft (17.3 ft^2/d or 1.6 m^2/d).

PT #2

PT #2 was conducted in well LL156 at the Baylor Ranch, Hudspeth County (fig. A3-1). The well is located approximately 1.9 mi (3.0 km) east-northeast of the Baylor Ranch Headquarters. The ranch road leading to this well is 20.7 mi (33.3 km) north of Sierra Blanca, Texas, and the well is 2.0 mi (3.2 km) west of Ranch to Market Road 1111. This well was drilled in the summer of 1986 by Leroy Perry of Dell City for the owner, James Baylor. It was drilled into probable Cretaceous Cox Sandstones and Campagrande Limestones, as indicated by local outcrops and by examination of cuttings by BEG personnel during the drilling of this well. Total depth of the well is approximately 265 ft (80.8 m), and wellbore diameter is 6 inches (15.2 cm). This well has 20 ft (6.1 m) of surface casing, and the producing interval was developed as an open-hole completion. Static water level in this well was measured at 206 ft (62.8 m) below land surface, and the saturated thickness in this wellbore is approximately 59 ft (17.9 m). No water wells or wellbores were available in the immediate area for use as observation wells. This well is producing $NaSO_4$ waters from aquifer B, and total dissolved solids were measured at 936 mg/L.

The drawdown phase of PT #2 was initiated at 10:30 a.m. on January 24, 1987. Although the well is equipped with a submersible pump, discharge rates varied considerably during the pumping period, from 14 gpm to 36 gpm, with a mean discharge rate of 27.5 gpm (table A3-3). During the pumping period, which lasted 50 hr, the recorded water level dropped only 1.3 ft (15.75 inches; 40.0 cm) (fig. A3-7), with 98% of the total drawdown occurring in the first 90 sec of the pumping test.

Table A3-3. Drawdown data from pumping test no. 2 at well LL156.

Time (hr)	Time from beginning of pumpage (min)	Depth to water level (ft)	Water level drawdown (ft)	Flow meter reading (gal)	Well discharge (gpm)
10:30:00	0.0	208.083	0.000	22,784	0.0
10:30:30	0.5	209.083	1.000	22,796	24.0
10:31:00	1.0	209.083	1.000	22,810	28.0
10:31:30	1.5	209.167	1.084	22,822	24.0
10:32:00	2.0	-	-	22,833	22.0
10:32:30	2.5	209.167	1.084	22,849	32.0
10:33:00	3.0	209.167	1.084	22,862	26.0
10:33:30	3.5	209.083	+1.000	22,876	28.0
10:34:00	4.0	209.083	1.000	22,892	32.0
10:34:30	4.5	209.083	1.000	22,904	24.0
10:35:00	5.0	209.083	1.000	22,911	14.0
10:36:00	6.0	209.083	1.000	22,943	32.0
10:37:00	7.0	209.083	1.000	22,975	32.0
10:38:00	8.0	209.083	1.000	23,005	30.0
10:39:00	9.0	209.083	1.000	23,033	28.0
10:40:00	10.0	209.083	1.000	23,061	28.0
10:42:00	12.0	209.083	1.000	23,115	27.0
10:44:00	14.0	209.083	1.000	23,169	27.0
10:46:00	16.0	209.083	1.000	23,229	30.0
10:48:00	18.0	209.083	1.000	23,285	28.0
10:50:00	20.0	209.083	1.000	23,339	27.0
10:55:00	25.0	209.083	1.000	23,485	29.2
11:00:00	30.0	209.083	1.000	23,615	26.0
11:10:00	40.0	209.083	1.000	23,880	26.5
11:20:00	50.0	209.083	1.000	24,130	25.0
11:30:00	60.0	209.083	1.000	24,408	27.8
11:40:00	70.0	209.083	1.000	24,705	29.7
11:50:00	80.0	209.083	1.000	25,017	31.2
12:00:00	90.0	209.083	1.000	25,315	29.8
12:10:00	100.0	209.083	1.000	25,639	32.4
12:30:00	120.0	209.083	1.000	26,292	32.65
13:00:00	150.0	209.167	1.084	27,075	26.1
13:30:00	180.0	209.167	1.084	27,860	26.167
14:00:00	210.0	209.167	1.084	28,779	30.633
14:30:00	240.0	209.167	1.084	29,778	33.3
15:00:00	270.0	209.167	1.084	30,786	36.6
15:30:00	300.0	209.167	1.084	31,816	34.333
16:00:00	330.0	209.167	1.084	32,890	35.8
16:30:00	360.0	209.167	1.084	34,032	38.067
17:30:00	420.0	209.167	1.084	36,192	36.0
18:30:00	480.0	209.167	1.084	38,324	35.533
21:00:00	630.0	209.167	1.084	43,468	34.293
23:10:00	760.0	209.250	1.167	47,480	30.862
7:30:00	1,260.0	209.250	1.167	63,419	31.878
13:30:00	1,620.0	209.250	1.167	72,680	25.725
18:30:00	1,920.0	209.250	1.167	80,130	24.833
7:30:00	2,700.0	209.250	1.167	98,120	23.064
12:00:00	2,970.0	209.250	1.167	104,553	23.826
12:30:00	3,000.0	209.167	1.083	105,292	24.633

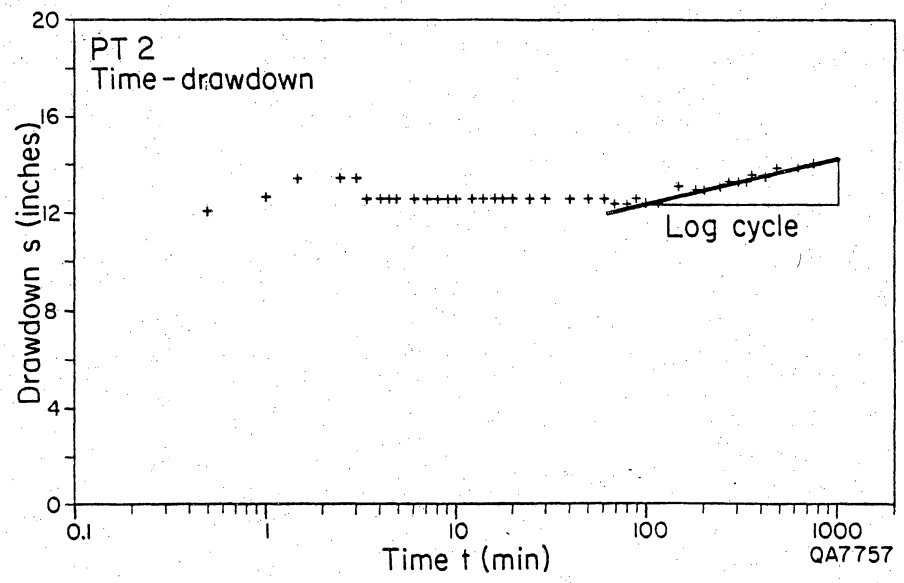

Figure A3-7. Time-drawdown plot interpreted using Jacob's method for pumping test no. 2 in well LL156, Baylor Ranch. Fluctuations in water-level decline during early phase of testing due to changes in discharge rate. Segment illustrating minor decline during late phase of test used for transmissivity calculations.

During the drawdown phase, 82,508 gal of water were produced. When the drawdown phase was terminated at 12:30 p.m. on January 26, the recovery of water level was monitored for another 20 hr until 8:30 a.m., January 27 (table A3-4). At this point, 100% of the original water level had recovered.

Figure A3-7 illustrates the limited and brief drawdown observed in this well during testing. In pumping tests where drawdown is as limited as seen in this well and basically occurs instantaneously, only general approximations of transmissivity can be calculated. Using Jacob's method for drawdown data, a small trend does appear at the end of the test. Using this late phase, a calculated transmissivity of 49,986 gpd/ft of drawdown was obtained (6,683 ft^2/d or 621 m^2/d). The mean discharge rate (Q) used in this approximation was 27.5 gpm.

PT #3

PT #3 was conducted in well LL155, the Frederick Well, which is located on the Dyer Ranch (formerly the Frederick Ranch), Hudspeth County (fig. 2; fig. A3-1). The ranch road leading to this well intersects Ranch-to-Market Road 1111 21.6 mi (34.8 km) north of Sierra Blanca. The well is 8.0 mi (12.9 km) east of the highway. No data were available concerning the age of the well, lithologies encountered while drilling, or the actual producing formation. Total depth of the well is at least 1,200 ft (365.8 m), and during this test, water intake to the pump was set at 1,137 ft (346.5 m). The wellbore diameter is 8 inches (20.3 cm) with only limited surface casing, and the producing interval is an open-hole completion. Static water level in this well was measured at 745.25 ft (227.1 m) below land surface, and the apparent saturated thickness effective during this test was 391.75 ft (119.4 m). No

Table A3-4. Recovery test data from pumping test no. 2 at well LL156.

Time (hr)	Time from beginning of recovery (min)	Time since pump started / Time since pump stopped (tp + Δt) / Δt	Depth to water level (ft)	Residual drawdown (s') (ft)	Water level recovery (ft)
12:30:00	0.0	∞	209.167	1.083	0.0
12:30:30	0.5	6001.0	208.375	0.291	0.792
12:31:00	1.0	3001.0	208.334	0.249	0.834
12:31:30	1.5	2001.0	208.334	0.249	0.834
12:32:00	2.0	1501.0	208.334	0.249	0.834
12:32:30	2.5	1201.0	208.334	0.249	0.834
12:33:00	3.0	1001.0	208.334	0.249	0.834
12:33:30	3.5	858.14	208.334	0.249	0.834
12:34:00	4.0	751.0	208.334	0.249	0.834
12:34:30	4.5	667.67	208.334	0.249	0.834
12:35:00	5.0	601.0	208.334	0.249	0.834
12:36:00	6.0	501.0	208.334	0.249	0.834
12:37:00	7.0	429.57	208.334	0.249	0.834
12:38:00	8.0	376.0	208.334	0.249	0.834
12:39:00	9.0	334.33	208.334	0.249	0.834
12:40:00	10.0	301.0	208.334	0.249	0.834
12:42:00	12.0	251.0	208.334	0.249	0.834
12:44:00	14.0	215.29	208.313	0.229	0.854
12:46:00	16.0	188.5	208.313	0.229	0.854
12:48:00	18.0	167.67	208.313	0.229	0.854
12:50:00	20.0	151.0	208.313	0.229	0.854
12:55:00	25.0	121.0	208.292	0.208	0.875
13:00:00	30.0	101.0	208.292	0.208	0.875
13:10:00	40.0	76.0	208.292	0.208	0.875
13:20:00	50.0	61.0	208.292	0.208	0.875
13:30:00	60.0	51.0	208.292	0.208	0.875
13:40:00	70.0	43.86	208.292	0.208	0.875
13:50:00	80.0	38.5	208.292	0.208	0.875
14:00:00	90.0	34.33	208.292	0.208	0.875
14:10:00	100.0	31.0	208.292	0.208	0.875
18:30:00	360.0	9.33	208.250	0.166	0.917
0:30:00	720.0	5.17	208.167	0.083	1.000
8:30:00	1200.0	3.5	208.159	0.075	1.008

other water wells or wellbores were available during this test for use as observation wells. This well is producing $NaSO_4$ waters from Aquifer A, and total dissolved solids were measured at 2,077 mg/L.

Sampling of ^{13}C, ^{14}C, and ^{3}H for replicate analyses during the drawdown phase resulted in the need to perform two pumping tests. The first pumping test of LL155 started at 9:07 a.m. on February 6, 1987. This well is equipped with a cylinder pump and maintained a relatively constant discharge rate of 3.79 gpm (table A3-5). During the pumping period, the recorded water level dropped to the level of the pump intake at 1,137 ft (346.5 m) in 720 min (12 hr) for a total drawdown of 391.75 ft (119.4 m)(fig. A3-8, A3-9). As previously stated, sampling was also in progress, therefore the pumping test recovery phase was rescheduled for a later time in order to complete sampling. Monitoring of the drawdown phase was terminated at 9:07 p.m.

After sampling had been completed, the well was turned off and allowed to recover to the original static water level. A second drawdown phase, PT #3A, was started at 11:00 a.m., February 10, 1987 (table A3-6). During this phase, 200 ft of drawdown was measured during the first 180 min of the pumping test. It was determined that this would be the maximum drawdown for this test (PT #3A) because of difficulties encountered with probe movement below this depth during previous measurements. The drawdown phase was terminated at 2:00 p.m., and recovery measurements were immediately initiated (fig. A3-10, A3-11; table A3-7). Monitoring of water level recovery continued for 42 hr until 8:00 a.m., February 12, 1987. At this point in the recovery phase, 100% of the original water level had recovered.

In contrast to well LL156, LL155 is currently being overproduced as the inflow of ground water into the borehole only begins to reach equilibrium with the discharge of ground water as maximum drawdown is being approached (fig. A3-8), which occurs after a relatively short time. Although water-bearing fracture(s) may intersect the

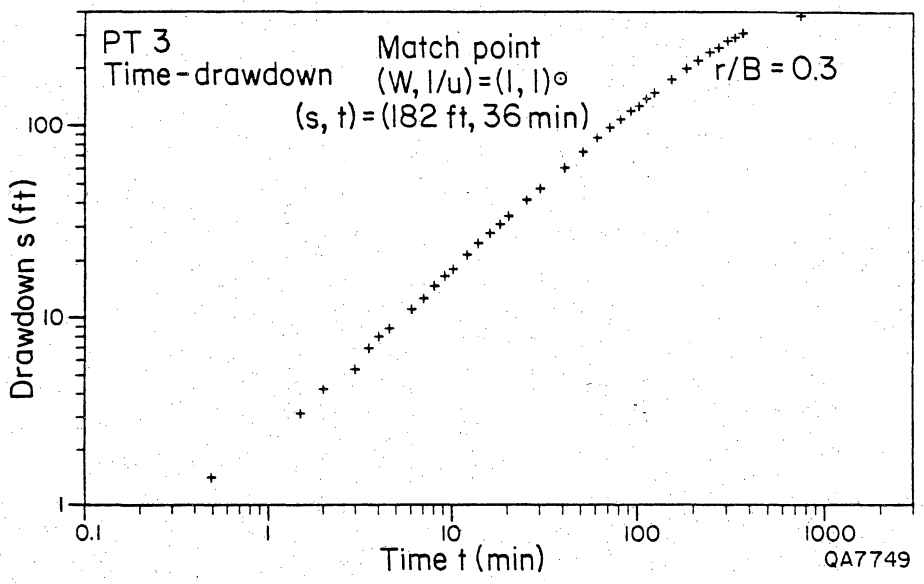

Figure A3-8. Time-drawdown curve matched to Walton type curve for pumping test no. 3 in well LL155, Dyer Ranch.

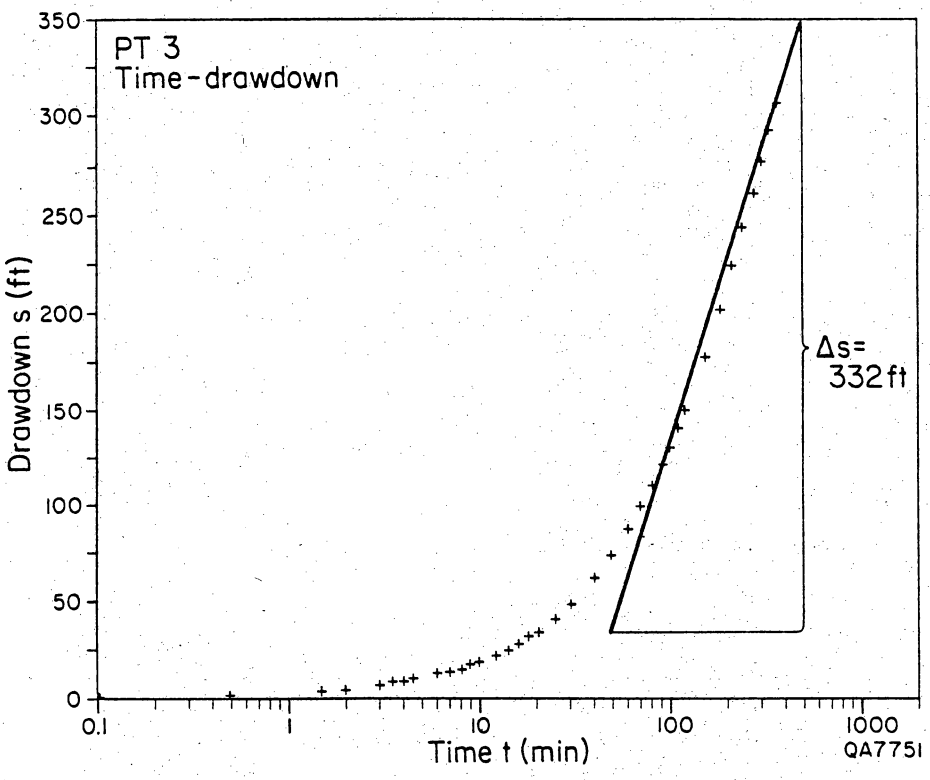

Figure A3-9. Time-drawdown plot interpreted using Jacob's method for pumping test no. 3 in well LL155, Dyer Ranch.

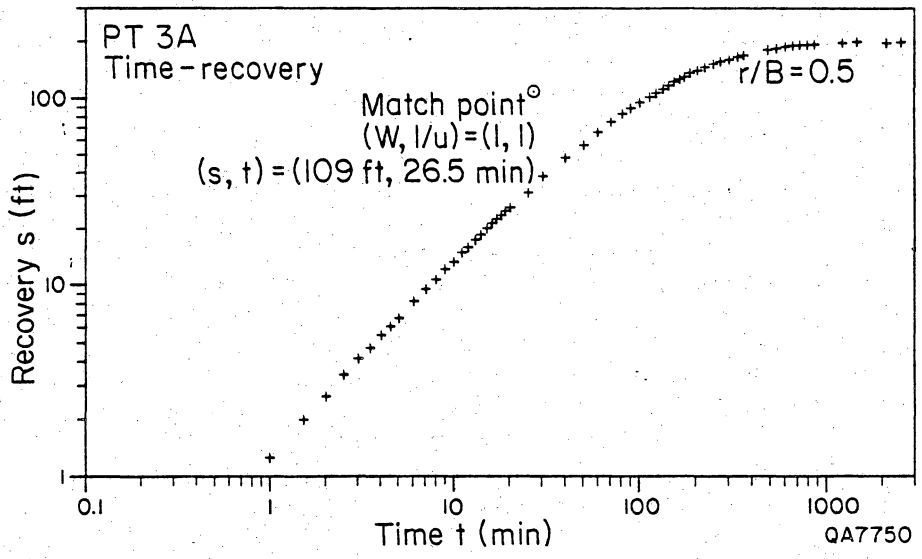

Figure A3-10. Time-recovery curve matched to Walton type curves for pumping test no. 3A in well LL155, Dyer Ranch.

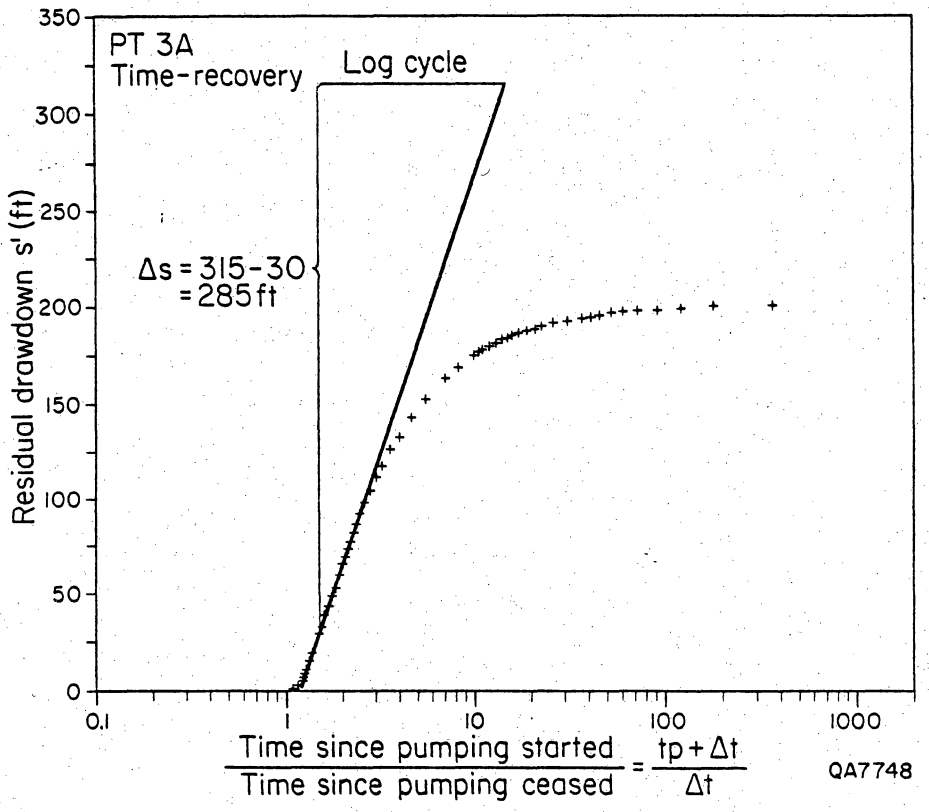

Figure A3-11. Time-recovery plot interpreted using Theis' method for pumping test no. 3A in well LL155, Dyer Ranch.

Table A3-5. Drawdown data from pumping test no. 3 at well LL155.

Time (hr)	Time from beginning of pumping (min)	Depth to water level (ft)	Water level drawdown (ft)	Flow meter reading (gal)	Well discharge (gpm)
09:07:00	0	747.917	0.000	105,393	-
09:07:30	0.5	749.333	1.416	105,393	-
09:08:00	1.0	-	-	105,395	4.0
09:08:30	1.5	751.000	3.083	105,397	4.0
09:09:00	2.0	752.000	4.083	105,398	2.0
09:09:30	2.5	-	-	105,301	6.0
09:10:00	3.0	753.083	5.166	105,303	4.0
09:10:30	3.5	754.917	7.000	105,305	4.0
09:11:00	4.0	755.833	7.916	105,306	2.0
09:11:30	4.5	756.667	8.750	-	-
09:12:00	5.0	-	-	-	-
09:13:00	6.0	759.083	11.166	105,310	2.0
09:14:00	7.0	760.833	12.916	105,315	5.0
09:15:00	8.0	762.583	14.666	105,320	5.0
09:16:00	9.0	764.750	16.833	105,327	7.0
09:17:00	10.0	765.917	18.000	105,333	5.0
09:19:00	12.0	769.333	21.416	105,345	6.5
09:21:00	14.0	772.500	24.583	105,356	5.5
09:23:00	16.0	775.333	27.416	105,367	5.5
09:25:00	18.0	778.583	30.666	105,379	6.0
09:27:00	20.0	781.417	33.500	105,390	5.5
09:32:00	25.0	788.667	40.750	105,429	7.4
09:37:00	30.0	795.667	47.750	105,448	3.8
09:47:00	40.0	809.667	61.750	105,530	5.5
09:57:00	50.0	821.667	73.750	105,569	3.9
10:07:00	60.0	835.583	87.666	-	-
10:17:00	70.0	846.167	98.250	105,735	3.9
10:27:00	80.0	857.167	109.250	-	-
10:38:00	91.0	868.667	120.750	105,725	4.1
10:47:00	100.0	877.833	129.916	-	-
10:57:00	110.0	887.833	139.916	105,804	4.2
11:07:00	120.0	897.00	149.083	105,906	4.25
11:37:00	150.0	923.917	176.000	105,956	2.90
12:07:00	180.0	948.500	200.583	106,103	3.90
12:37:00	210.0	969.833	221.916	106,200	3.90
13:07:00	240.0	989.500	241.583	106,315	3.8
13:37:00	270.0	1,007.167	259.250	-	-
14:07:00	300.0	1,024.500	276.583	106,545	3.8
14:37:00	330.0	1,040.000	292.083	106,656	4.0
15:07:00	360.0	1,055.000	307.083	-	-
21:07:00	720.0	1,137.000	389.083	-	-

Table A3-6. Drawdown data from pumping test no. 3A at well LL155.

Time (hr)	Time from beginning of pumpage (min)	Depth to water level (ft)	Water level drawdown (ft)	Flow meter reading (gal)	Well discharge (gpm)
11:00:00	0.0	744.667	0.000	108,095	--
11:00:30	0.5	745.750	1.083		
11:01:00	1.0	746.667	2.000		
11:01:30	1.5	747.667	3.000		
11:02:00	2.0	748.833	4.166		
11:02:30	2.5	749.583	4.916		
11:03:00	3.0	750.500	5.833		
11:03:30	3.5	751.500	6.833		
11:04:00	4.0	752.417	7.750		
11:04:30	4.5	753.750	9.083		
11:05:00	5.0	754.083	9.416		
11:06:00	6.0	755.667	11.000		
11:07:00	7.0	757.667	13.000		
11:08:00	8.0	759.167	14.500		
11:09:00	9.0	760.667	16.000		
11:10:00	10.0	762.500	17.833		
11:11:00	11.0	764.417	19.750		
11:12:00	12.0	765.833	21.166		
11:13:00	13.0	767.417	22.750		
11:14:00	14.0	769.000	24.333		
11:15:00	15.0	770.500	25.833		
11:16:00	16.0	771.750	27.083		
11:17:00	17.0	773.500	28.833		
11:18:00	18.0	774.833	30.166		
11:19:00	19.0	776.417	31.750		
11:20:00	20.0	777.917	33.250		
11:25:00	25.0	785.250	40.583		
11:30:00	30.0	792.333	47.666	108,125	1
11:40:00	40.0	805.583	60.916		
11:50:00	50.0	818.500	73.833		
12:00:00	60.0	830.833	86.166		
12:10:00	70.0	842.667	98.000		
12:20:00	80.0	853.750	109.083	108,330	4.02
12:30:00	90.0	864.083	119.416		
12:40:00	100.0	874.250	129.583		
12:50:00	110.0	884.167	139.500		
13:00:00	120.0	893.500	148.833	108,494	4.10
13:10:00	130.0	902.833	158.166		
13:20:00	140.0	912.000	167.333		
13:30:00	150.0	920.417	175.750		
13:40:00	160.0	929.000	184.333	108,655	3.93
13:50:00	170.0	937.000	192.333		
14:00:00	180.0	944.667	200.000	108,722	4.18

Table A3-7. Recovery data from pumping test no. 3 at well LL155.

Time (hr)	Time from beginning of recovery (min)	Time since pump started / Time since pump stopped (tp + Δt) / Δt	Depth to water level (ft)	Residual drawdown (s') (ft)	Water level recovery (ft)
14:00:00	0.0	∞	944.667	200.000	0.0
14:00:30	0.5	361.00	944.083	199.416	0.584
14:01:00	1.0	181.00	943.417	198.750	1.250
14:01:30	1.5	121.00	942.667	198.000	2.000
14:02:00	2.0	91.00	942.000	197.333	2.667
14:02:30	2.5	73.00	941.250	196.583	3.417
14:03:00	3.0	61.00	940.583	195.916	4.084
14:03:30	3.5	52.43	939.917	195.250	4.750
14:04:00	4.0	46.00	939.083	194.416	5.584
14:04:30	4.5	41.00	938.583	193.916	6.084
14:05:00	5.0	37.00	937.833	193.166	6.834
14:06:00	6.0	31.00	936.417	191.750	8.250
14:07:00	7.0	26.71	935.000	190.333	9.667
14:08:00	8.0	23.50	933.917	189.250	10.750
14:09:00	9.0	21.00	932.583	187.916	12.084
14:10:10	10.0	19.00	931.167	186.500	13.500
14:11:00	11.0	17.36	929.667	185.000	15.000
14:12:00	12.0	16.00	928.667	184.000	16.000
14:13:00	13.0	14.85	927.250	182.583	17.417
14:14:00	14.0	13.86	926.083	181.416	18.584
14:15:00	15.0	13.00	924.667	180.000	20.000
14:16:00	16.0	12.25	923.417	178.750	21.250
14:17:00	17.0	11.59	922.417	177.750	22.250
14:18:00	18.0	11.00	921.00	176.333	23.667
14:19:00	19.0	10.47	919.833	175.166	24.834
14:20:00	20.0	10.00	918.667	174.000	26.000
14:25:00	25.0	8.20	912.917	168.250	31.750
14:30:00	30.0	7.00	907.167	162.500	37.500
14:40:00	40.0	5.50	896.583	151.916	48.084
14:50:00	50.0	4.60	887.167	142.500	57.500
15:00:00	60.0	4.00	878.250	133.583	66.417
15:10:00	70.0	3.57	870.00	125.333	74.667
15:20:00	80.0	3.25	861.417	116.750	83.250

Table A3-7 (cont.)

Time (hr)	Time from beginning of recovery (min)	Time since pump started / Time since pump stopped (tp + Δt) / Δt	Depth to water level (ft)	Residual drawdown (s') (ft)	Water level recovery (ft)
15:30:00	90.0	3.00	855.250	110.583	89.417
15:40:00	100.0	2.80	848.833	104.166	95.834
15:50:00	110.0	2.64	842.667	98.000	102.000
16:00:00	120.0	2.50	836.833	92.166	107.834
16:10:00	130.0	2.38	831.417	86.750	113.250
16:20:00	140.0	2.29	826.250	81.583	118.417
16:30:00	150.0	2.20	821.750	77.083	122.917
16:40:00	160.0	2.13	817.667	73.000	127.000
16:50:00	170.0	2.06	813.833	69.166	130.834
17:00:00	180.0	2.00	810.167	65.500	134.500
17:20:00	200.0	1.90	803.917	59.250	140.750
17:40:00	220.0	1.82	798.500	53.833	146.167
18:00:00	240.0	1.75	793.750	49.083	150.917
18:30:00	270.0	1.67	787.667	43.000	157.000
19:00:00	300.0	1.60	782.667	38.000	162.000
19:30:00	330.0	1.55	778.500	33.833	166.167
20:00:00	360.0	1.50	774.833	30.166	169.834
22:00:00	480.0	1.38	764.417	19.750	180.250
23:00:00	540.0	1.33	760.917	16.250	183.750
00:00:00	600.0	1.30	757.917	13.250	186.750
01:00:00	660.0	1.27	755.333	10.666	189.334
02:00:00	720.0	1.25	753.333	8.666	191.334
03:00:00	780.0	1.23	751.583	6.916	193.084
04:00:00	840.0	1.21	750.250	5.583	194.417
10:15:00	1,215.0	1.15	746.167	1.500	198.500
13:45:00	1,425.0	1.13	745.333	0.500	199.500
00:00:00	2,040.0	1.09	745.00	0.333	199.667
08:00:00	2,520.0	1.07	744.667	0.000	200.000

borehole of this well, none of the methods used to calculate transmissivity documented or inferred their presence. Regionally, Aquifer A is unconfined although locally it may exhibit characteristics of a semiconfined aquifer. Interpretation of the test data was accomplished using four different methods (two using drawdown data and two using recovery data), as described in the discussion of PT #1.

By matching the time-drawdown and time-recovery plots from this well to Walton's set of type curves based on the Theis method for semiconfined aquifers (Kruseman and De Ridder, 1976), good agreement of calculated transmissivities resulted (figs. A3-8, A3-10). Matching the drawdown data for PT #3 with Walton's set of type curves, a calculated transmissivity of 2.39 gpd/ft of drawdown was obtained (.32 ft^2/d, or .03 m^2/d). Using the same method with recovery data from PT #3A, a transmissivity of 3.98 gpd/ft of drawdown was calculated (.53 ft^2/d, or .05 m^2/d).

Additional calculations of transmissivity were made using the Jacob method for drawdown (fig. A3-9) and the Theis method for recovery (fig. A3-11). The Jacob method is used with unsteady flow in confined aquifers. Using this method on drawdown data from PT #3, a calculated transmissivity of 3.01 gpd/ft of drawdown was obtained (.40 ft^2/d, or .04 m^2/d). The Theis recovery method may be used under the same conditions as those required for Jacob's method for drawdown. This method resulted in a transmissivity of 3.50 gpd/ft of drawdown (47 ft^2/d, or .04 m^2/d).

Averaging the four values calculated for LL155 yields a mean transmissivity of 3.22 gpd/ft of drawdown (.43 ft^2/d or .04 m^2/d) with a standard deviation of 0.68 gpd/ft. This is an extremely low value for transmissivity and, when compared to values from other wells tested in the area, may be used to infer either that only matrix permeability is contributing to the wellbore or that a considerably lower density of fractures was intersected.

PT #4

PT #4 was conducted in well LL148, the Red Well, which is located on the Baylor Lease of University of Texas Lands, Hudspeth County (fig. 2; fig. A3-1). The ranch road leading east from Ranch-to-Market Road 1111 toward Red Well is located 8.1 mi (13.1 km) south of the intersection between U. S. Highway 62-180 and Ranch-to-Market-Road 1111. East from Ranch-to-Market Road 1111, it is 4.2 mi (6.7 km) southeast to the Scratch Ranch and an additional 4.7 mi (7.5 km) east-northeast to the well. No data were available concerning the age of this well, lithologies encountered while drilling, or the actual producing formation. Total depth of this well is unknown, and during this test, water intake to the pump was set at 503 ft (153.3 m) below land surface. The wellbore diameter is 6 inches (15.2 cm) with limited surface casing because the producing interval is an open-hole completion. The static water level in this well was measured at 484.7 ft (147.7 m) below land surface, and the apparent saturated thickness effective during this test was 18.3 ft (5.6 m).

On July 31, 1986, the static water level in this well was measured during a previous phase of study at 462.7 ft (141.1 m) below land surface. Prior to this July 1986 measurement, above-average rainfall had been received in the area. Since the first measurement was taken, normal to below-normal rainfall has been recorded. The two static water level measurements record a decline in water levels between July 1986, and February 1987, of 22 ft (6.7 m). Production prior to the February measurement is not a cause of this decline in water level because the well had been inoperative for several months due to mechanical problems. No other water wells or wellbores were available during this test for use as observation wells. This well is producing NaCl waters from Aquifer A and total dissolved solids were measured at 2020.67 mg/L.

The drawdown phase of PT #4 was initiated at 4:15 p.m. on February 11, 1987. This well is equipped with a cylinder pump and maintained a relatively constant rate of discharge of 4.33 gpm (table A3-8). The pumping or drawdown phase was terminated at 8:00 a.m. on February 12, when the pumpjack pulley mounted to the gas-powered motor sheared off the motor shaft. The last measurement taken before this mechanical failure had recorded 1.1 ft (.33 m) of drawdown after 945 min (15.75 hr). Measurements of recovery rates for this portion of the test were temporarily delayed while motor and pump shutdowns were completed. The first measurement of recovery was made at 8:05 a.m. on February 12, 1987, and was terminated at 10:00 a.m., 120 min after the start of recovery (table A3-9). At this point, all but 2 inches (5.1 cm) of the original drawdown had recovered.

After the motor assembly was repaired, another pumping test was performed (PT #4A) at an increased discharge rate of 6.74 gpm in an attempt to induce better drawdown data for the calculation of transmissivity (table A3-10). PT #4A was initiated 11:05 a.m. on February 12, 1987, and was terminated at 7:05 a.m. on February 13 (fig. A3-12). Total drawdown for PT #4 was measured at 1.1 ft (13 inches or 33 cm) while total drawdown for PT #4A was 1.6 ft (19 inches or 48.3 cm). In both tests, a majority of the drawdown, 68% and 80% respectively, occurred in the first minute of production. At the request of the rancher, no recovery test was conducted for PT #4A, so that depleted water supplies could be replaced.

The results of PT #4 and 4A were both similar to the results obtained from PT #2 in that insufficient drawdown was recorded to allow accurate, reproducible calculations of transmissivity. No transmissivity value can be calculated because the drawdown occurs during the early part of the test and is probably the result of wellbore storage.

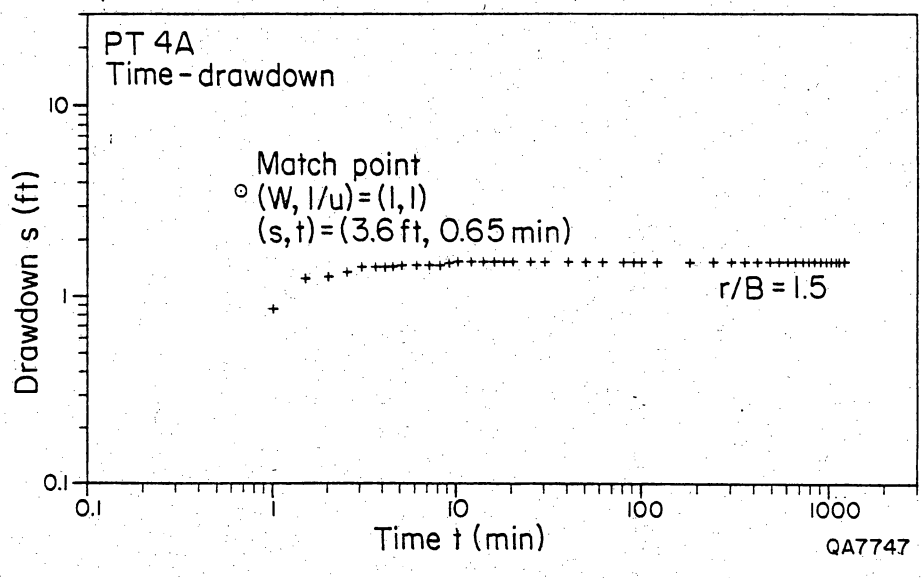

Figure A3-12. Time-drawdown curve matched to Walton-type curves for pumping test no. 4A in well LL148. All of the drawdown occurs during the early testing period and can be explained by wellbore storage. In this case, no method of transmissivity determination is available. Additional testing will be required at an increased discharge rate so that the aquifer may be reasonably stressed.

Table A3-8. Drawdown data from pumping test no. 4 at well LL148.

Time (hr)	Time from beginning of pumpage (min)	Depth to water level (ft)	Water level drawdown (ft)	Flow meter reading (gal)	Well discharge (gpm)
16:15:00	0.0	486.167	0.000		
16:15:30	0.5	486.667	0.500		
16:16:00	1.0	486.833	0.666		
16:16:30	1.5	486.917	0.750		
16:17:00	2.0	486.917	0.750		
16:17:30	2.5	486.917	0.750		
16:18:00	3.0	486.917	0.750		
16:18:00	3.5	486.917	0.750		
16:19:00	4.0	486.917	0.750		
16:19:30	4.5	487.000	0.833		
16:20:00	5.0	487.000	0.833		
16:21:00	6.0	487.000	0.833		4
16:22:00	7.0	487.000	0.833		
16:23:00	8.0	487.083	0.916		
16:24:00	9.0	487.083	0.916		
16:25:00	10.0	487.083	0.916		
16:27:00	12.0	487.083	0.916		4.3
16:29:00	14.0	487.083	0.916		4.6
16:31:00	16.0	487.083	0.916		
16:33:00	18.0	487.083	0.916		
16:35:00	20.0	487.083	0.916		4.3
16:40:00	25.0	487.083	0.916		
16:45:00	30.0	487.083	0.916		4.0
16:55:00	40.0	487.083	0.916		4.3
17:05:00	50.0	487.083	0.916		4.0
17:15:00	60.0	487.083	0.916		4.3
17:25:00	70.0	487.083	0.916		
17:35:00	80.0	487.167	1.000		4.3
17:45:00	90.0	487.167	1.000		4.3
17:55:00	100.0	487.167	1.000		
18:05:00	110.0	487.167	1.000		4.3
18:15:00	120.0	487.167	1.000		
18:45:00	150.0	487.167	1.000		4.3
19:15:00	180.0	487.167	1.000		
19:45:00	210.0	487.250	1.083		4.3
20:15:00	240.0	487.250	1.083		
20:45:00	270.0	487.250	1.083		4.3
21:15:00	300.0	487.250	1.083		
21:45:00	330.0	487.250	1.083		
22:15:00	360.0	487.250	1.083		
23:15:00	420.0	487.250	1.083		4.3
00:15:00	480.0	487.250	1.083		
01:15:00	540.0	487.250	1.083		4.3
02:15:00	600.0	487.250	1.083		
03:15:00	660.0	487.250	1.083		4.0
04:15:00	720.0	487.250	1.083		
05:15:00	780.0	487.250	1.083		4.3
06:15:00	840.0	487.250	1.083		
07:15:00	900.0	487.250	1.083		

Table A3-9. Recovery data from pumping test no. 4 at well LL148.

Time (hr)	Time from beginning of recovery (min)	$\frac{\text{Time since pump started}}{\text{Time since pump stopped}}$ $\frac{(tp + \Delta t)}{\Delta t}$	Depth to water level (ft)	Residual drawdown (s') (ft)	Water level recovery (ft)
08:00:00	0.0	∞	487.250	1.083	0
08:05:00	5.0	190.0	486.833	0.666	0.417
08:10:00	10.0	91.0	486.667	0.500	0.583
08:15:00	15.0	61.0	486.333	0.166	0.917
08:20:00	20.0	46.0	486.333	0.166	0.917
08:25:00	25.0	37.0	486.333	0.166	0.917
08:30:00	30.0	31.0	486.333	0.166	0.917
09:00:00	60.0	16.0	486.333	0.166	0.917
10:00:00	120.0	8.5	486.333	0.166	0.917

Table A3-10. Drawdown data from pumping test no. 4A at well LL148.

Time (hr)	Time from beginning of pumpage (min)	Depth to water level (ft)	Water level drawdown (ft)	Flow meter reading (gal)	Well discharge (gpm)
11:05:00	0.0	486.333	0.000		
11:06:00	1.0	487.167	0.834		
11:06:30	1.5	487.583	1.250		
11:07:00	2.0	487.625	1.292		
11:07:30	2.5	487.667	1.334		
11:08:00	3.0	487.750	1.417		
11:08:30	3.5	487.750	1.417		
11:09:00	4.0	487.750	1.417		
11:09:30	4.5	487.750	1.417		
11:10:00	5.0	487.833	1.500		
11:11:00	6.0	487.833	1.500		
11:12:00	7.0	487.833	1.500		
11:13:00	8.0	487.833	1.500		6.7
11:14:00	9.0	487.917	1.584		
11:15:00	10.0	487.917	1.584		
11:17:00	12.0	487.917	1.584		
11:19:00	14.0	487.917	1.584		
11:21:00	16.0	487.917	1.584		
11:23:00	18.0	487.917	1.584		
11:25:00	20.0	487.917	1.584		7.5
11:30:00	25.0	487.917	1.584		6.7
11:35:00	30.0	487.917	1.584		
11:45:00	40.0	487.917	1.584		
11:55:00	50.0	487.917	1.584		6.7
12:05:00	60.0	487.917	1.584		6.7
12:25:00	80.0	487.917	1.584		6.7
12:45:00	100.0	487.917	1.584		
13:05:00	120.0	487.917	1.584		6.7
14:05:00	180.0	487.917	1.584		6.7
15:05:00	240.0	487.917	1.584		6.7
16:05:00	300.0	487.917	1.584		7.5
17:05:00	360.0	487.917	1.584		6.7
18:05:00	420.0	487.917	1.584		6.7
19:05:00	480.0	487.917	1.584		
20:05:00	540.0	487.917	1.584		6.7
21:05:00	600.0	487.917	1.584		6.7
22:05:00	660.0	487.917	1.584		
23:05:00	720.0	487.917	1.584		6.7
00:05:00	780.0	487.917	1.584		6.7
01:05:00	840.0	487.917	1.584		
02:05:00	900.0	487.917	1.584		6.7
03:05:00	960.0	487.917	1.584		
04:05:00	1,020.0	487.917	1.584		6.7
05:05:00	1,080.0	487.917	1.584		
06:05:00	1,140.0	487.917	1.584		
07:05:00	1,200.0	487.917	1.584		6.7

Although other methods of analyses were attempted, including Jacob's method and Theis' method, the values obtained covered a wide range of transmissivities and were considered to be erroneous and of no real significance. As in PT #2, the discharge rate of this well will have to be increased to induce drawdown of a magnitude required for the determination of transmissivity.

PT #5

PT #5 was conducted in well LL141, the Bravo Well, which is located on the Baylor Lease of the University of Texas Lands, Hudspeth County (fig. 2; fig. A3-1). The ranch road leading west toward Bravo Well is located 10.2 mi (16.4 km) south of the intersection between U. S. Highway 62-180 and Ranch-to-Market Road 1111. West from Ranch-to-Market Road 1111, it is 2.3 mi (3.7 km) to the well. No data were available concerning the age of Bravo Well, lithologies encountered while drilling, or the producing formation. Total depth of this well is 663 ft (202.1 m) below land surface and during this test water intake was set at 661 ft (201.5 m) below land surface. The wellbore diameter is 8 inches (20.3 cm) with an unknown depth of surface casing and an open-hole completion. The static water level in this well was measured at 652.7 ft (198.9 m) below land surface, and the saturated thickness effective during this test was 9.3 ft (2.8 m).

The decline in static water level measured in LL148 (Red Well) was also recorded in LL141 (Bravo Well). On July 12, 1986, the static water level in this well was measured during a previous phase of study at 628 ft (191.4 m) below land surface. The two static water level measurements record a decline in water levels between July 1986, and February 1987 of 24.7 ft (7.5 m). Production prior to the February measurement is unlikely because arrangements had been made to allow the well

sufficient time to stabilize before testing. Both LL141 and LL148 are within the same drainage area, a series of connected arroyos. LL141 is within the drainage area of Baylor Draw, which feeds into South Well Draw, which feeds into Antelope Gulch, the arroyo within which LL148 is located. No other wells or wellbores were available during this test for use as observation wells. This well is producing $NaSO_4$ waters from Aquifer A, and total dissolved solids were measured at 1786.92 mg/L.

Currently, this well only has 9.3 ft of drawdown potential. Attempts to lower the pump to allow for additional drawdown proved to be impossible as the current total depth is 1 ft (.3 m) deeper than the intake for the pump. The most likely scenario, based on discussions with ranch personnel, is that previously this well was deeper, but a large amount of pipe had been lost in the hole and attempts to recover the lost pipe were unsuccessful. In addition to lost pipe, caving of the open borehole during fishing operations may have contributed to the loss in total depth.

The drawdown phase of PT #5 was initiated at 10:00 a.m. on February 4, 1987. This well is equipped with a submersible pump and maintained a relatively constant rate of discharge at 11.1 gpm (table A3-11). The drawdown phase was terminated at 12:00 p.m., 120 min after starting the test. Recovery rates were monitored for 90 min, which was sufficient time to record 99% recovery of the original drawdown (table A3-12). Maximum drawdown occurred (water level dropped to level of pump intake) after 60 min 10 sec of the drawdown phase. The discharge rate at this point dropped to a constant rate of 8.6 gpm.

Using the same methods of analysis that were utilized for PT #1 and #3, excellent agreement was obtained for transmissivity values in this well. Time-drawdown and time-recovery plots were constructed and matched to Walton's set of type curves for semiconfined aquifers based on Theis' method (Kruseman and De

Table A3-11. Drawdown data from pumping test no. 5 at well LL141.

Time (hr)	Time from beginning of pumpage (min)	Depth to water level (ft)	Water level drawdown (ft)	Flow meter reading (gal)	Well discharge (gpm)
10:00:00	0.0	652.7	0.00		
10:00:30	0.5	652.96	0.26		
10:01:00	1.0	653.54	0.84		12
10:01:30	1.5	654.15	1.45		
10:02:00	2.0	654.7	2.00		12
10:02:30	2.5	655.15	2.45		
10:03:00	3.0	655.5	2.80		12
10:03:30	3.5	655.8	3.10		
10:04:00	4.0	656.2	3.50		12
10:04:30	4.5	656.5	3.80		
10:05:00	5.0	656.7	4.00		10
10:06:00	6.0	657.3	4.60		
10:07:00	7.0	657.6	4.90		10
10:08:00	8.0	657.9	5.20		
10:09:00	9.0	658.2	5.50		12
10:10:00	10.0	658.5	5.80		10
10:12:00	12.0	659.0	6.30		10
10:14:00	14.0	659.4	6.70		10
10:16:00	16.0	659.8	7.10		10
10:18:00	18.0	660.1	7.40		
10:20:00	20.0	660.5	7.80		10
10:25:00	25.0	660.7	8.00		10
10:30:00	30.0	661.1	8.40		12
10:40:00	40.0	661.7	9.00		12
10:50:00	50.0	661.9	9.20		12
11:00:00	60.0	662.0	9.30		10
11:10:00	70.0				8.6
11:20:00	80.0				8.6
11:30:00	90.0				6.7
11:40:00	100.0				8.6
11:50:00	110.0				8.6
12:00:00	120.0				8.6

Table A3-12. Recovery data from pumping test no. 5 at well LL141.

Time (hr)	Time from beginning of recovery (min)	Time since pump started / Time since pump stopped (tp + Δt) / Δt	Depth to water level (ft)	Residual drawdown (s') (ft)	Water level recovery (ft)
12:00:00	0.0	∞	662.0	9.30	0.0
12:00:30	0.5	121.0	660.9	8.20	1.1
12:01:00	1.0	61.0	659.8	7.10	2.2
12:01:30	1.5	41.0	659.0	6.30	3.0
12:02:00	2.0	31.0	658.5	5.80	3.5
12:02:30	2.5	25.0	658.0	5.30	4.0
12:03:00	3.0	21.0	657.6	4.90	4.4
12:03:30	3.5	18.1	657.3	4.60	4.7
12:04:00	4.0	16.0	657.0	4.30	5.0
12:04:30	4.5	14.3	656.7	4.00	5.3
12:05:00	5.0	13.0	656.4	3.70	5.6
12:06:00	6.0	11.0	656.0	3.30	6.0
12:07:00	7.0	9.6	655.7	3.00	6.3
12:08:00	8.0	8.5	655.3	2.60	6.7
12:09:00	9.0	7.7	655.1	2.40	6.9
12:10:00	10.0	7.0	655.0	2.30	7.0
12:12:00	12.0	6.0	654.5	1.80	7.5
12:14:00	14.0	5.3	654.2	1.50	7.8
12:16:00	16.0	4.8	654.0	1.30	8.0
12:18:00	18.0	4.3	653.6	0.90	8.4
12:20:00	20.0	4.0	653.3	0.60	8.7
12:25:00	25.0	3.4	653.0	0.30	9.0
12:30:00	30.0	3.0	652.9	0.20	9.1
12:40:00	40.0	2.5	652.8	0.10	9.2
12:50:00	50.0	2.2	652.8	0.10	9.2
13:00:00	60.0	2.0	652.8	0.10	9.2
13:10:00	70.0	1.9	652.75	0.05	9.25
13:20:00	80.0	1.8	652.75	0.05	9.25
13:30:00	90.0	1.7	652.70	0.00	9.30

Ridder, 1976). The drawdown phase of this test yielded a calculated transmissivity of 410.3 gpd/ft of drawdown (54.8 ft^2/d, or 5.1 m^2/d) (fig. A3-13). Using this method for the recovery data resulted in a transmissivity value of 480 gpd/ft of drawdown (64.2 ft^2/d, or 6.0 m^2/d) (fig. A3-14).

Application of Jacob's method for drawdown data yields a calculated transmissivity of 417.9 gpd/ft of drawdown (55.9 ft^2/d, or 5.2 m^2/d) (fig. A3-15) while the Theis method for recovery resulted in a transmissivity of 517.8 gpd/ft of drawdown (69.2 ft^2/d, or 6.4 m^2/d) (fig. A3-16). Averaging the four calculated values for PT #5 on LL141 yields a mean transmissivity of 456.5 gpd/ft of drawdown (61.0 ft^2/d, or 5.7 m^2/d) with a standard deviation of 51.5 gpd/ft of drawdown (6.9 ft^2/d, or $.6^2/d$).

PT #6

PT #6 was conducted in well LL132 at the Williams' Ranch Headquarters (fig. 2; fig. A3-1). This well is located 7.8 mi (12.5 km) west-southwest of the intersection of Ranch-to-Market Roads 1111 and 2317. No precise data were available concerning the age of this well, lithologies encountered while drilling, or the producing formation. Discussions with the owner indicate that this well is probably more than 70 yr old. Total depth of this well is reported to be 1,200 ft (366 m), although this depth could not be confirmed. During this pumping test, water intake to the pump was set at 960.1 ft (292.6 m) below land surface. The wellbore diameter is 8 inches (20.3 cm) with surface casing down to an unknown depth. This well is producing from an open-hole completion. Static water level in this well was measured at 710.3 ft (216.5 m) below land surface, and apparent saturated thickness during this test was 249.8 ft (76.1 m). No other water wells or wellbores were available during this test for use as observation wells. This well is producing $NaHCO_3$ waters from aquifer A, and total dissolved solids were measured at 884.03 mg/L.

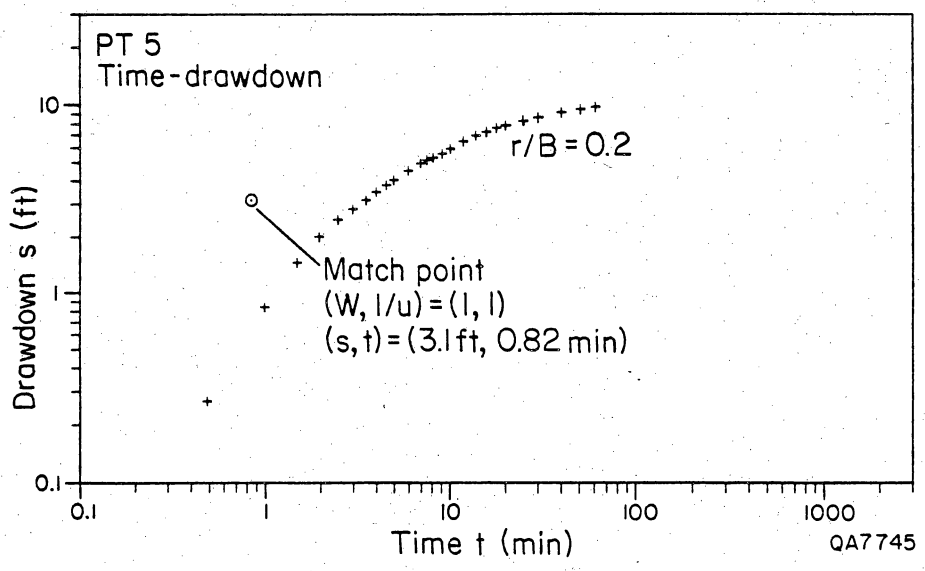

Figure A3-13. Time-drawdown curve matched to Walton type curves for pumping test no. 5 in well LL141, University Lands, Baylor lease.

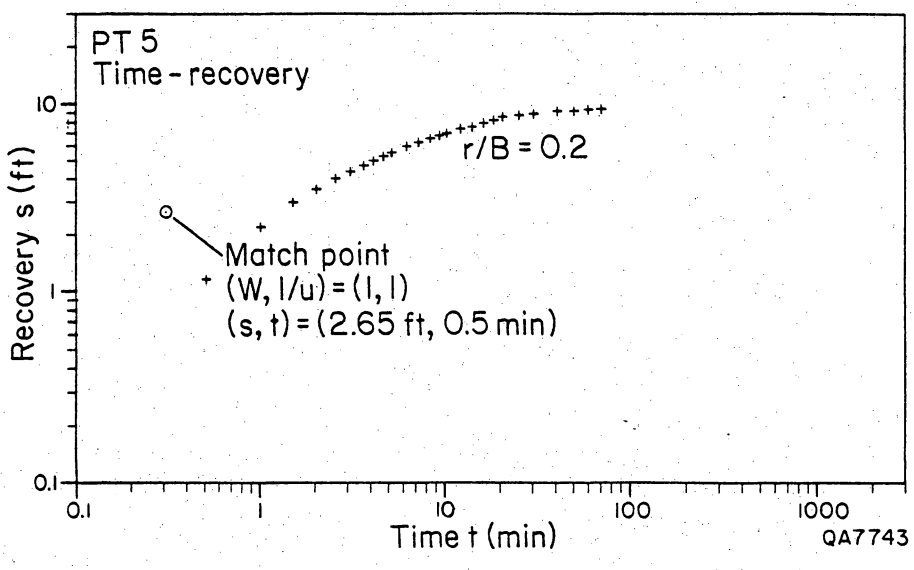

Figure A3-14. Time-recovery curve matched to Walton type curves for pumping test no. 5 in well LL141, University Lands, Baylor lease.

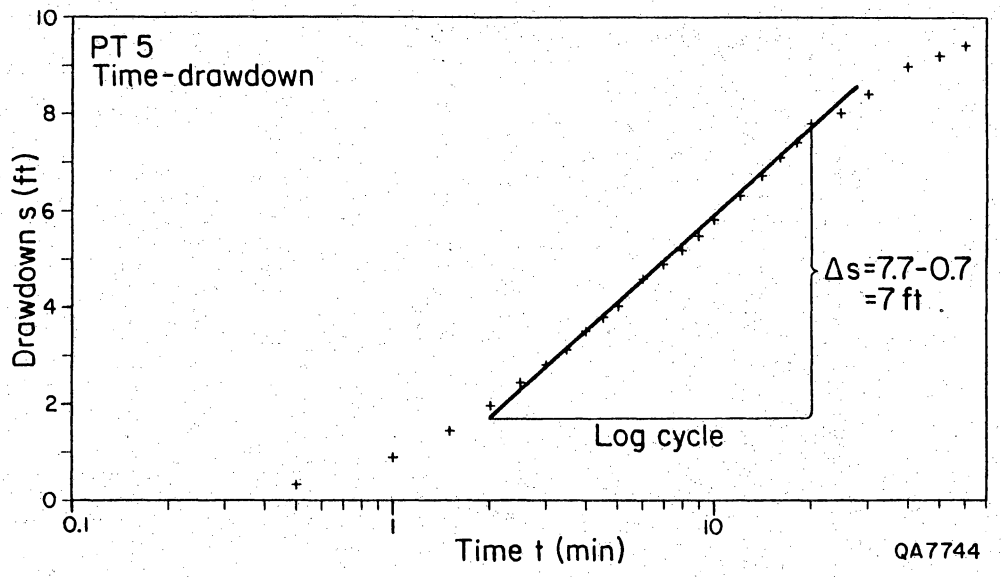

Figure A3-15. Time-drawdown plot interpreted using Jacob's method for pumping test no. 5 in well LL141, University Lands, Baylor lease.

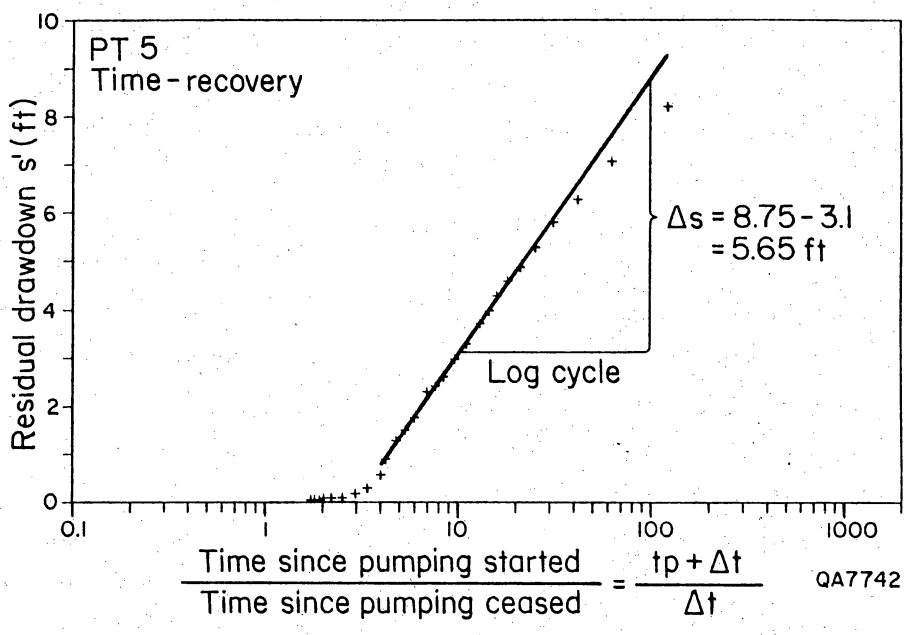

Figure A3-16. Time-recovery plot interpreted using Theis' method for pumping test no. 5 in well LL141, University Lands, Baylor lease.

After this well had reached equilibrium during the drawdown phase, rainstorms in the area caused three power failures. The water level recovery was rapid and in each case had recovered more than 50% by the time recovery procedures could be initiated. After each power failure, the well was restarted and pumped until maximum drawdown was attained. These events explain the time lapse between the termination of drawdown and the beginning of recovery.

The drawdown phase of PT #6 was initiated at 6:00 p.m. on February 24, 1987. This well is equipped with a 2.75-inch (7.0 cm) cylinder pump, which maintained a relatively constant discharge rate of 10.6 gpm (table A3-13). During the drawdown phase, which lasted 2100 min (35 hr), the recorded water level dropped 121.3 ft (37.0 m) (fig. A3-17). During the drawdown phase, 22,260 gal of water were produced. When the final drawdown phase was terminated at 11:33 p.m., February 26, the water level recovery was monitored for 2,520 min (42 hr) until 5:33 p.m. on February 28 (table A3-14). At this point, 100 % of the static water level had been recovered.

As with PT #3, PT #6 resulted in excellent agreement of transmissivity values calculated using the four methods discussed in detail for PT #1. Figures A3-17 and A3-18 represent the drawdown and recovery curves from this pumping test, which were used to match to Walton's set of type curves based on Theis' method for unsteady flow in semiconfined leaky aquifers (Kruseman and De Ridder, 1976). Based on a mean discharge rate of 10.6 gpm and a match point value for s (drawdown) of 42 ft (12.8 m) the calculated transmissivity is 28.9 gpd/ft of drawdown (3.86 ft^2/d, or .36 m^2/d). Using the same discharge rate and a match point for s of 50 results in a transmissivity of 24.3 gpd/ft of drawdown (3.2 ft^2/d, or .30 m^2/d).

The Jacob method for drawdown data in confined aquifers with unsteady flow was also used with this well and resulted in three distinct segments representing the intersection of the cone of depression with separate fractures. The early phase had a

Table A3-13. Drawdown data from pumping test no. 6 at well LL132.

Time (hr)	Time from beginning of pumpage (min)	Depth to water level (ft)	Water level drawdown (ft)	Flow meter reading (gal)	Well discharge (gpm)
18:00:00	0.0	711.958	0.0	108,703	0
18:00:18	0.3	713.333	1.375		
18:00:52	0.87	716.000	4.042		
18:01:08	1.13	716.667	4.709		
18:01:37	1.62	718.417	6.459		
18:02:00	2.00	719.750	7.792		
18:02:15	2.25	720.583	8.625		
18:02:30	2.50	721.333	9.375		
18:03:00	3.00	722.667	10.709		
18:03:26	3.43	724.083	12.125		
18:03:40	3.67	724.917	12.959		
18:04:00	4.00	725.667	13.709		
18:04:15	4.25	726.583	14.625		
18:04:45	4.75	728.750	16.792		
18:05:10	5.17	729.000	17.042		
18:05:30	5.50	729.750	17.792		
18:05:45	5.75	730.500	18.542		
18:06:05	6.08	731.417	19.459		
18:06:30	6.50	732.417	20.459		
18:07:00	7.00	733.583	21.625		
18:07:30	7.50	734.500	22.542		
18:08:00	8.00	735.583	23.625		
18:08:30	8.50	736.750	24.792		
18:09:00	9.00	737.750	25.792		
18:09:30	9.50	738.750	26.792		
18:10:00	10.00	739.917	27.959		
18:10:30	10.50	741.000	29.042		
18:11:00	11.00	742.167	30.209		
18:12:00	12.00	744.417	32.459		
18:13:00	13.00	746.417	34.459		
18:14:00	14.00	748.583	36.625		
18:15:00	15.00	750.667	38.709		
18:16:00	16.00	752.500	40.542		
18:17:00	17.00	754.417	42.459		
18:18:00	18.00	756.333	44.375		
18:19:00	19.00	757.833	45.875		
18:20:00	20.00	759.500	47.542		
18:21:00	21.00	761.500	49.542		
18:22:00	22.00	762.667	50.709		
18:23:00	23.00	764.250	52.292		
18:24:00	24.00	765.667	53.709		
18:25:00	25.00	767.083	55.125		
18:26:00	26.00	768.500	56.542		
18:27:00	27.00	769.833	57.875		
18:28:00	28.00	771.000	59.042		
18:29:00	29.00	772.250	60.292		
18:30:00	30.00	773.500	61.542		

Table A3-13. (cont.)

Time (hr)	Time from beginning of pumpage (min)	Depth to water level (ft)	Water level drawdown (ft)	Flow meter reading (gal)	Well discharge (gpm)
18:35:00	35.00	779.917	67.959		
18:40:00	40.00	783.833	71.875		
18:45:00	45.00	788.000	76.042	109,162	10.55
18:50:00	50.00	791.500	79.542		
18:55:00	55.00	794.583	82.625	109,297	10.0
19:00:00	60.00	797.417	85.459		
19:05:00	65.00	799.833	87.875	109,400	10.3
19:10:00	70.00	802.000	90.042		
19:15:00	75.00	804.083	92.125	109,505	10.5
19:20:00	80.00	805.917	93.959		
19:25:00	85.00	807.417	95.459	109,610	10.5
19:30:00	90.00	808.833	96.875		
19:35:00	95.00	810.083	98.125		
19:40:00	100.00	811.417	99.459	109,778	10.5
19:50:00	110.00	813.417	101.459		
20:00:00	120.00	815.167	103.209		
20:10:00	130.00	817.500	105.542	110,079	10.4
20:20:00	140.00	817.833	105.875		
20:30:00	150.00	818.833	106.875	110,282	10.15
20:40:00	160.00	819.667	107.709		
20:50:00	170.00	820.417	108.459		
21:00:00	180.00	821.083	109.125	110,592	10.3
21:10:00	190.00	821.750	109.792		
21:20:00	200.00	822.417	110.459	110,812	9.5
21:35:00	215.00	823.250	111.292		
21:40:00	220.00	823.667	111.709		
21:50:00	230.00	824.167	112.209		
22:00:00	240.00	824.667	112.709		
22:30:00	270.00	825.750	113.792	111,600	10.4
23:00:00	300.00	826.250	114.292		
23:30:00	330.00	826.375	114.417		
00:00:00	360.00	826.667	114.709	112,466	10.6
01:00:00	420.00	827.250	115.292		
02:00:00	480.00	827.917	115.959		
03:00:00	540.00	828.500	116.542		
04:40:00	640.00	829.833	117.875		
06:25:00	745.00	830.417	118.459	116,635	10.7
06:50:00	840.00	830.667	118.709	117,630	10.7
09:20:00	1050.00	831.583	119.625	119,875	10.7
10:33:00	1123.00	831.667	119.709	120,643	10.5
13:05:00	1275.00	831.917	119.959	122,282	10.6
15:50:00	1440.00	832.333	120.375	123,858	10.6
17:50:00	1560.00	832.833	120.875		
20:10:00	1700.00	833.250	121.292	126,815	10.7
01:05:00	1995.00	833.250	121.292	129,960	10.7
02:50:00	2100.00	833.250	121.292	130,963	10.6

Table A3-14. Recovery data from pumping test no. 6 at well LL132.

Time (hr)	Time from beginning of recovery (min)	Time since pump started / Time since pump stopped (tp + Δt) / Δt	Depth to water level (ft)	Residual drawdown (s') (ft)	Water level recovery (ft)
23:33:00	0.0	∞	828.833	121.292	0.000
23:33:30	0.5	4201.0	826.000	118.459	2.833
23:34:00	1.0	2101.0	823.833	116.292	5.000
23:34:30	1.5	1401.0	821.667	114.126	7.166
23:35:00	2.0	1051.0	819.250	111.709	9.583
23:35:30	2.5	841.0	817.417	109.876	11.416
23:36:00	3.0	701.0	815.333	107.792	13.500
23:36:30	3.5	601.0	813.750	106.209	15.083
23:37:30	4.5	467.7	809.917	102.376	18.916
23:38:00	5.0	421.0	807.917	100.376	20.916
23:39:00	6.0	351.0	804.417	96.876	24.416
23:40:00	7.0	301.0	801.250	93.709	27.583
23:41:00	8.0	263.5	798.000	90.459	30.833
23:42:00	9.0	234.3	795.000	87.459	33.833
23:43:00	10.0	211.0	792.083	84.542	36.750
23:44:00	11.0	191.9	789.417	81.876	39.416
23:45:00	12.0	176.0	786.500	78.959	42.333
23:46:00	13.0	162.5	783.833	76.292	45.000
23:47:00	14.0	151.0	781.333	73.792	47.500
23:48:00	15.0	141.0	778.583	71.042	50.250
23:49:00	16.0	132.3	776.667	69.126	52.166
23:50:00	17.0	124.5	774.333	66.792	54.500
23:51:00	18.0	117.7	772.333	64.792	56.500
23:52:00	19.0	111.5	770.083	62.542	58.750
23:53:00	20.0	106	768.750	61.209	60.083
23:55:00	22.0	96.4	764.500	56.959	64.333
23:57:00	24.0	88.5	761.083	53.542	67.75
23:59:00	26.0	81.8	757.750	50.209	71.083
00:01:00	28.0	76.0	754.917	47.376	73.916
00:03:00	30.0	71.0	752.167	44.626	76.666
00:08:00	35.0	61.0	747.333	39.792	81.500
00:13:00	40.0	53.5	742.000	34.459	86.833
00:18:00	45.0	47.7	737.833	30.292	91.000

Table A3-14. (cont.)

Time (hr)	Time from beginning of recovery (min)	Time since pump started / Time since pump stopped (tp + Δt) / Δt	Depth to water level (ft)	Residual drawdown (s') (ft)	Water level recovery (ft)
00:23:00	50.0	43.0	734.000	26.459	94.833
00:28:00	55.0	39.2	731.167	23.626	97.666
00:33:00	60.0	36.0	729.500	21.959	99.333
00:43:00	70.0	31.0	726.083	18.542	102.750
00:53:00	80.0	27.3	723.750	16.209	105.083
01:03:00	90.0	24.3	721.750	14.209	107.083
01:13:00	100.0	22.0	720.167	12.626	108.666
01:23:00	110.0	20.1	719.167	11.626	109.666
01:33:00	120.0	18.5	718.167	10.626	110.666
02:03:00	150.0	15.0	716.667	9.126	112.166
02:33:00	180.0	12.7	715.250	7.709	113.583
03:03:00	210.0	11.0	714.500	6.959	114.333
03:33:00	240.0	9.8	714.000	6.459	114.833
04:03:00	270.0	8.8	713.750	6.209	115.083
04:33:00	300.0	8.0	713.500	5.959	115.333
05:03:00	330.0	7.4	713.350	5.809	115.483
05:33:00	360.0	6.8	713.000	5.459	115.833
06:33:00	420.0	6.0	712.750	5.209	116.083
07:33:00	480.0	5.4	712.708	5.167	116.125
08:33:00	540.0	4.9	712.625	5.084	116.208
09:33:00	600.0	4.5	712.625	5.084	116.208
10:33:00	660.0	4.2	712.500	4.959	116.333
11:33:00	720.0	3.9	712.396	4.855	116.437
12:33:00	780.0	3.7	712.292	4.751	116.541
13:33:00	840.0	3.5	712.167	4.626	116.666
14:33:00	900.0	3.3	712.00	4.459	116.833
17:33:00	1080.0	2.9	711.833	4.292	117.000
20:33:00	1260.0	2.7	711.750	4.209	117.083
05:33:00	1800.0	2.2	711.667	4.126	117.166
17:33:00	2520.0	1.8	711.417	3.876	117.416

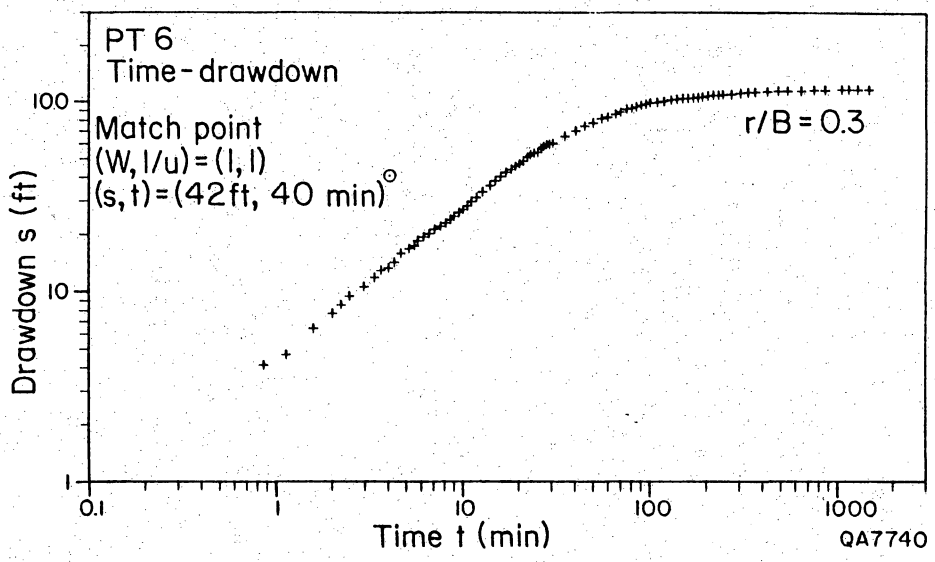

Figure A3-17. Time-drawdown curve matched to Walton type curve for pumping test no. 6 in well LL132, Williams Ranch. This well is located approximately 1.4 mi (2.3 km) west of LL162, the site of pumping test no. 1.

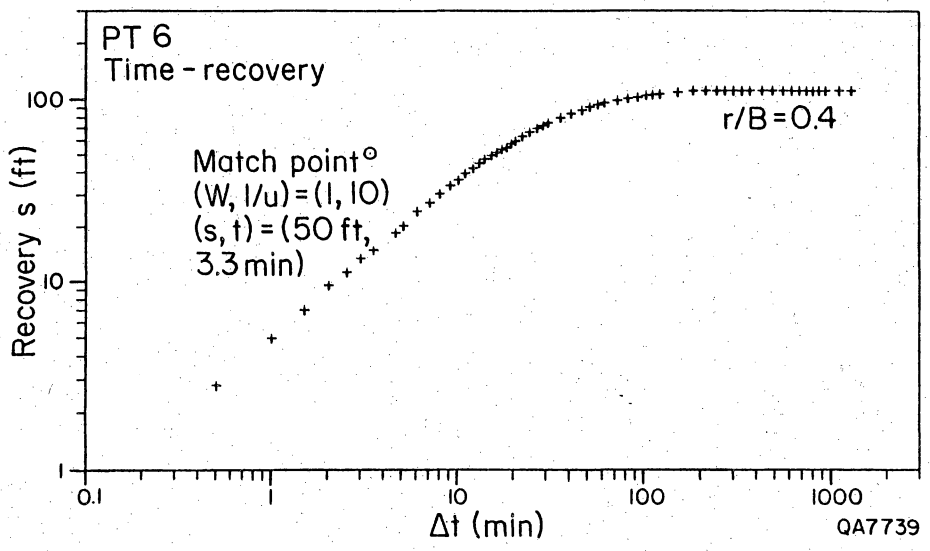

Figure A3-18. Time-recovery curve matched to Walton type curve for pumping test no. 6 in well LL132, Williams Ranch.

Δs value of 76.5 ft (23.3 m) and a transmissivity of 27.4 gpd/ft of drawdown (3.7 ft^2/d, or .34 m^2/d) (fig. A3-19). The second segment recognized recorded a Δs value of 27 ft (8.2 m) and a transmissivity of 103 gpd/ft of drawdown (13.8 ft^2 or 1.3 m^2) and the late segment before this well reached equilibrium had a Δs of 9 ft (2.7 m) with a transmissivity of 310 gpd/ft of drawdown (41.4 ft^2/d or 3.8 m^2/d). Using the Theis method for recovery data under the same aquifer conditions as required with the Jacob method, a single transmissivity of LL132 is 28.1 gpd/ft of drawdown (3.75 ft^2/d, or .35 m^2/d) (fig. A3-20). The segment observed using Jacob's method was not as apparent using Theis' method.

Averaging the six values calculated for LL132 yields a mean transmissivity of 86.95 gpd/ft of drawdown (11.6 ft^2/d, or 1.1 m^2/d) and a standard deviation of 113.4 gpd/ft of drawdown (15.2 ft^2/d, or 1.4 m^2/d). Both the drawdown data and recovery data illustrate the intersection with a fracture or fracture system during the later period of drawdown. In order to better define this occurrence, additional testing will be required and at a greater discharge rate, so that significant drawdown below this interval may be obtained.

PT #7

PT #7 was performed in well LL138, referred to as University #4 well, which is located on the Williams Ranch, Hudspeth County (fig. 2, fig. A3-1). The ranch road leading to this well is 4.7 mi (7.6 km) west of Cornudas, Texas, on U. S. Highway 62-180. The well is 1.6 mi (2.5 km) south of the highway. A USGS elevation benchmark is located at the intersection of the highway and the ranch road, where the elevation above sea level was measured at 4,408 ft (1,343.5 m). No data were available regarding the age of this well, lithologies encountered while drilling, or the producing interval. Total depth of this well is reported to be about 1,200 ft

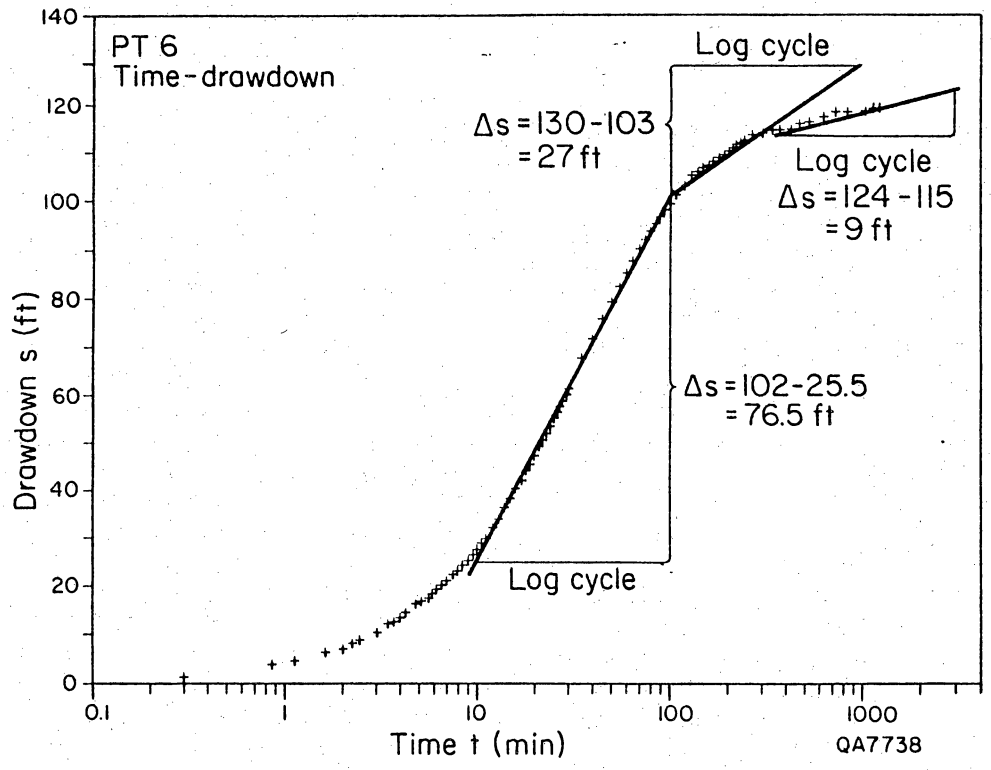

Figure A3-19. Time-drawdown plot interpreted using Jacob's method for pumping test no. 6 in well LL132, Williams Ranch. Three segments observed during drawdown similar to those recorded in pumping test no. 1, 1.4 mi (2.3 km) east of this well.

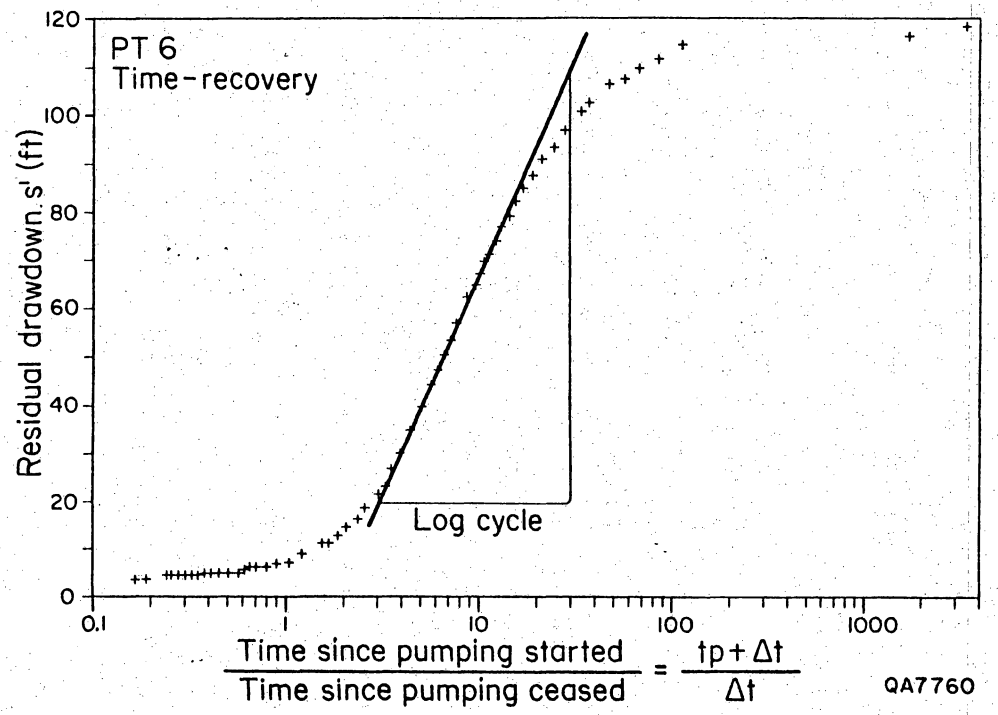

Figure A3-20. Time-recovery plot interpreted using Theis' method for pumping test no. 6 in well LL132, Williams Ranch.

(366 m), but this depth could not be confirmed. For this pumping test, water intake into the pump was set at 850 ft (259.1 m) below land surface. The wellbore diameter is 8 inches (20.3 cm) with surface casing down to an unknown depth. This well, like all the wells tested, has been completed as an open-hole completion. Static water level in this well was measured at 789.9 ft (240.8 m) below land surface. Surface elevation of this well has been mapped at 4,409 ft (1,343.9 m) above sea level, yielding a water altitude in this well of 3,619.1 ft (1,103.1 m) above sea level. Saturated thickness effective during this test was 60.1 ft (18.3 m). No other wells or wellbores were available in the immediate area for use as observation wells. This well is producing $NaSO_4$ waters from aquifer A, and total dissolved solids were measured at 1,722.28 mg/L.

The drawdown phase of PT #7 was initiated at 6:00 p.m., March 1, 1987. Well LL138 is equipped with a 2 inch (5.1 cm) cylinder pump and maintained a relatively constant discharge rate of 4.0 gpm (table A3-15). During the pumping period, which lasted 1,440 min (24 hours), the recorded water level dropped only 4.1 ft (1.25 m) (fig. A3-21), and 93% of the total drawdown occurred in the first 10 min of pumping. During the drawdown phase, approximately 5,760 gal of water were produced. The drawdown phase of this test was terminated at 6:00 p.m., March 2, 1987. Owing to problems with upward movement of the probe resulting from friction with the installed polyhose, recovery measurements proved to be unsuccessful. This resulted in transmissivity calculations based strictly on drawdown data using Logan's method, and Walton's type curves based on the Theis method for drawdown data.

Transmissivity cannot be calculated because most of the decline in water level occurred in the first 5 minutes and is attributed to wellbore storage.

Table A3-15. Drawdown data from pumping test no. 7 at well LL138.

Time (hr)	Time from beginning of pumpage (min)	Depth to water level (ft)	Water level drawdown (ft)	Flow meter reading (gal)	Well discharge (gpm)
18:00:00	0.0	790.500	0.000		
18:00:30	0.5	791.250	0.750		
18:01:00	1.0	791.833	1.333		
18:01:30	1.5	792.000	1.500		
18:02:00	2.0	792.583	2.083		
18:02:30	2.5	792.833	2.333		
18:03:00	3.0	793.083	2.583		
18:03:30	3.5	793.250	2.750		
18:04:00	4.0	793.333	2.833		
18:04:30	4.5	793.500	3.000		
18:05:00	5.0	793.667	3.167		
18:06:00	6.0	793.833	3.333		
18:07:00	7.0	794.083	3.583		
18:08:00	8.0	794.167	3.667		
18:09:00	9.0	794.250	3.750		
18:10:00	10.0	794.333	3.833		
18:11:00	11.0	794.333	3.833		
18:12:00	12.0	794.333	3.833		
18:13:00	13.0	794.417	3.917		
18:14:00	14.0	794.417	3.917		
18:16:00	16.0	794.417	3.917		
18:18:00	18.0	794.417	3.917		
18:20:00	20.0	794.417	3.917		
18:25:00	25.0	794.500	4.000		
18:30:00	30.0	794.583	4.083		
18:40:00	40.0	794.583	4.083		
18:50:00	50.0	794.583	4.083		3.75
19:00:00	60.0	794.583	4.083		4.00
19:10:00	70.0	794.583	4.083		4.00
19:20:00	80.0	794.583	4.083		4.00
19:30:00	90.0	794.583	4.083		4.00
19:40:00	100.0	794.583	4.083		
19:50:00	110.0	794.583	4.083		4.0
20:00:00	120.0	794.583	4.083		4.0
20:30:00	150.0	794.583	4.083		
21:00:00	180.0	794.583	4.083		
22:00:00	240.0	794.583	4.083		
23:00:00	300.0	794.583	4.083		4.0
00:00:00	360.0	794.583	4.083		
01:00:00	420.0	794.583	4.083		
02:00:00	480.0	794.583	4.083		
03:00:00	540.0	794.583	4.083		
04:00:00	600.0	794.583	4.083		3.75
05:00:00	660.0	794.583	4.083		
06:00:00	720.0	794.583	4.083		
18:00:00	1440.0	794.583	4.083		

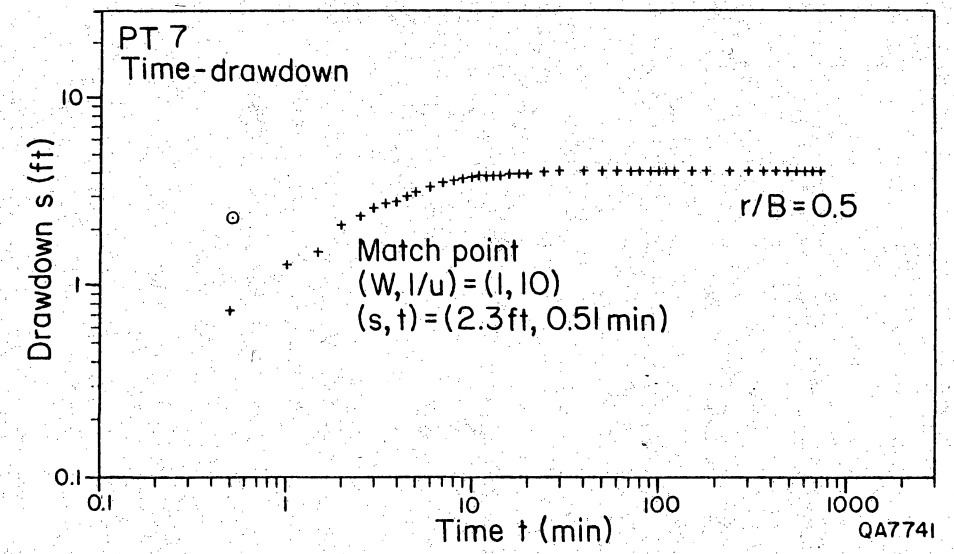

Figure A3-21. Time-drawdown curve matched to Walton-type curves for pumping test no. 7 in well LL138, Williams Ranch.

Additional testing with modifications in discharge rates and monitoring equipment would be of great value in determining a better approximation of transmissivity in this well. Once again, discharge rates should be increased by a factor of 2 or more to induce sufficient drawdown during a subsequent PT. Where a pump jack supplies lift for the water produced, discharge can often be increased simply by increasing the size of the motor pulley; this could be done at LL138 and LL148. When submersible pumps act as the lifting force, another pump of greater horsepower would have to be installed in the well; this would be required at LL156.

Appendix 4. Geologic and hydrologic data from El Paso Natural Gas Company Pump Station #2 water wells, Hudspeth County, Texas.

The following is a synthesis of operational and maintenance records for eight wells drilled by El Paso Natural Gas Company (EPNG) to supply water to Pump Station #2. This pump station, now abandoned, is located 5.8 mi (9.4 km) south of Cornudas, Texas, and 7.5 mi (12.2 km) southwest of site HU1A. Number (#) at the beginning of each section denotes the BEG ID number for EPNG documents.

Well #1

(1) History of drilling - On November 18, 1954, it was reported that well was drilled in approximately 1929. Location is NE 1/4, NE 1/4, Sec. 24, Blk. 123 PSL.

(2) Operational data - On November 29, 1954, depth of well at 1,125 ft with a static water level of 950 ft. Capacity of well reported as 7 gpm from June 1950 to present. Water level will decrease below the pump at a higher rate and also at 7 gpm if kept at that rate longer than 30 days. Pump is a rod type cylinder pump.

(3) Well water chemical analysis - On November 29, 1954, two chemical analyses were reported (mg/l).

	5/2/50	6/2/50
pH	7.3	7.6
Total hardness as $CaCO_3$	376	428
Calcium as $CaCO_3$	190	223
Magnesium as $CaCO_3$	186	205
P alkalinity as $CaCO_3$	0	0
Total alkalinity as $CaCO_3$	230	235
Chloride as Cl	188	200
Sulfate as SO_4	295	293
Silica as SiO_2	15	14
Iron as Fe	trace	0.1

(4) Water well data. Based on the November 15, 1954 report, the following well data were summarized:

Drilling completion date	1929
Total depth (TD) of well	1,200 ft
Static water level	950 ft
Pumping capacity	7 gpm
Make of pump	Jenson Brothers
Rod size	3/4 inches
Column size	2 1/4 inches
Rated HP of pump	5
Pumping column	44 rods-25 ft @ 1,100 ft with 7-ft barrel and 8-ft perforated anchor.

This well is described as having an optimum capacity of 7 gpm and that water level will decrease below the pump at a higher pumping rate. It is also noted that water level will decrease below the pump when used at 7 gpm for more than 30 days. A production screen of unknown length was installed at 791 ft, 8 inches. This well was later plugged back to 1,125 ft.

(5) This driller's log describing the encountered section of water well #1 was prepared by M. E. Hawkins on June 20, 1950. Closing statement of the document is that well was plugged back to 1,100 ft.

Interval (ft)

From	To	Lithology and comments
110	132	Tan cream and pink dense limestone
132	140	Dense cream limestone
140	160	Cream yellow-tan and deep pink limestone, partly dolomitic
160	170	Tan and cream dense limestone (partly dolomitic) partly silty, trace chert
170	180	Yellow-tan, some cream and pink partly earthy dense dolomitic limestone
180	185	Light and limestone pebbles, some fragments of reddish-brown breccia, 20% fine to coarse clear worn sand, 20% gray clay, 80% chert
185	195	Sand and limestone conglomerate including siliceous pebbles
195	200	Light tan limestone, some quartzite pebbles
200	220	Cream partly dolomitic limestone, 30% pale gray chert

220	260	Cream limestone and pale gray chert
260	290	Cream limestone, gray and trace green tuff, 20% pyrite
290	310	Dark yellow-tan, some reddish slightly granular dolomite, 20% light chert
310	320	Dark tan granular dolomite, trace red stain and chert
320	330	Dark tan granular dolomite, 20% pink chert
330	340	Dark tan and pink dolomite, 25% gray-white and pink chert
340	360	Dark tan dolomite, trace light chert
360	370	Dark tan granular dolomite, 20% dense white chert
370	390	Dark tan dolomite
390	400	Light and dark tan and dark gray dolomitic limestone
400	410	Tan brown, some gray-black limestone
410	415	Brown and brownish gray limestone, trace dark chert
415	425	Dull tan to gray-brown limestone, trace chert and black shale
425	435	Tan and light brown limestone
435	455	Tan limestone, 10% white chert
455	475	Tan limestone, 20% cream chert
475	500	Tan limestone, 10% chert
500	520	Light and dark tan limestone, trace chert
520	530	Dark gray-brown limestone, 20% black limey shale, trace dark chert
530	545	Dark brown-gray limestone, trace chert and shale
545	560	Dark brown-gray and light tan limestone, trace black shale and chert
560	575	Tan fine crystalline limestone, 20% white chert
575	625	Brown irregular textured limestone, partly mixed with some lighter limestone
625	650	Tan and light brown limestone, 20% dark chert, trace black shale
650	660	Light tan with some gray limestone, trace black shale
660	680	Tan limestone, trace light fine-grained chert
680	690	Gray-tan partly dolomitic irregular textured limestone
690	705	Irregular textured gray-tan, some cream limestone
705	715	Brown-tan mixed with some cream limestone, 20% finer, granular dull tan chert
715	720	Limestone as above

720	730	Dark tan, some brown-black shaly granular limestone
730	745	Brown, irregular textured limestone, 20% black shale
745	760	Gray-brown irregular textured limestone
760	780	Limestone similar to above
780	800	Gray-brown, some tan limestone, 10% light chert, trace black shale
800	830	Tan limestone, Show Water
830	845	Gray-brown limestone, 25% calcite
845	875	Gray-tan limestone, trace calcite, black shale and white chert
875	900	Tan, some dark gray irregular textured limestone
900	930	Gray-tan irregular textured limestone, trace black chert
930	950	Gray-tan limestone, trace black shale
950	990	Brown limestone, some darker and shaly
990	1000	Tan to brown limestone
1000	1040	Irregular textured brown-gray limestone
1040	1060	Light and gray-tan limestone, trace black shale
1060	1070	Gray-tan rather dense limestone
1070	1090	Irregular textured light and gray-tan limestone
1090	1110	Irregular textured gray-tan limestone, 25% dark gray chert
1110	1120	Gray-tan partly shaly limestone
1120	1130	Gray-tan slightly granular dolomitic limestone
1130	1150	Tan limestone, 30% dark gray shale
1150	1170	Slightly granular and dolomitic limestone, 20% dark gray shale
1170	1190	Very coarse partly worn clear sand, 20% dark gray shale, 25% gray and tan limestone, trace glauconite Water 1190
1190	1235	Slightly dolomitic gray-tan limestone, trace black shale

Wells 2, 3, 4, and 7

(6) Memorandum dated November 24, 1954, reports the following status of water wells 2, 3, 4, and 7. Wells 2 and 3 were drilled in approximately 1929 and were abandoned in approximately 1938. The casing was pulled from both wells, and remaining boreholes were then filled with dirt. Well #4 location is listed as NE 1/4, NE 1/4, Sec. 24, PSL Blk. 123, Hudspeth County, Texas. This is 1/4 mi south of the pump station. Well #4 was also abandoned, but the dates for drilling or abandonment are not given. A plate was attached to a surface nipple on top of the

casing at time of abandonment. This well was 700 ft deep. Well #7 was drilled in 1947 and was never completed. A plate was secured to the surface casing when this well was abandoned.

Well #5

(7) Location reported as NE 1/4, NE 1/4, Sec. 24, PSL Blk. 123, 900 ft south of the pump station. Well was drilled on August 18, 1936, to a total depth of 713 ft. Casing string is given as 60 ft of 10-inch pipe and 703 ft of 4-inch pipe. Pumping equipment at this time consisted of an Allis Chalmers electric motor pump jack. This borehole is reported to be crooked at 400 ft.

(8) Driller's log (source of driller's log listed as Compressor Department, El Paso Natural Gas Company):

Interval (ft)

From	To	Lithology and comments
0	4 ft	Surface
4	21	Caliche-hard
21	45	White lime
45	80	Sandy blue limestone
80	110	White lime
110	125	Sandy blue limestone
125	185	White limestone
185	198	Black limestone
198	250	Red rock-hard
250	270	White limestone
270	295	Yellow sandy limestone
295	389	Hard gray limestone
389	400	White limestone
400	402	Gray limestone
402	452	Yellow sandstone, some limestone
452	515	Yellow limestone crevis, 479-485
515	530	White limestone
530	550	Gray limestone
550	624	White limestone
624	647	Gray limestone, crevis at 637, lost drilling water
647	700	Yellow limestone, crevis 647-653, no lost returns
700	713	Corrected to 703 water sand

(9) The chemical analysis of ground-water in well #5 given below was dated November 18, 1954:

	3/49	No date
pH	8.2	7.8
Total hardness as $CaCO_3$	376	300
Calcite as $CaCO_3$	240	223
Magnesium as $CaCO_3$	136	77
P alkalinity as $CaCO_3$	0	0
Total alkalinity as $CaCO_3$	230	260
Chloride as Cl	136	170
Sulfate as SO_4	165	---
Silica as SiO_2	36	17
Iron as Fe	0.1	0
Total solids	1092	958

(10) Appropriate portions of the maintenance record for Well #5 are listed below. Drilling operations for Well #5 began July 7, 1936, and were completed on August 18, 1936. September 18, 1957 entry includes (1) total depth of hole is 697.5 ft (212.6 m); (2) static water level is at 675 ft (205.7 m); (3) initial capacity after service of well was 8.5 gpm on 13 cycles per minute of pump jack; (4) On January 21, 1958, production rate was measured at 10.0 gpm after replacing pump parts and rods; (5) On February 17, 1958, production rate still recorded at 10 gpm.

(11) Water well maintenance report dated August 12, 1965. Reports that static water level rose from 693 ft (211 m) to 684 ft (208 m) after replacing a portion of pipe string and pump. Before servicing, the production capacity fell from 11 gpm to 5 gpm, and production barrel was faulty and sanded up.

(12) Undated operational memorandum repeats that this hole is crooked at 400 ft (121.9 m) and recommends that in the future a cable tool rig be used to reclaim all of hole (from caving). This memo also reports the static water level at well #5 for August 1965 to be ranging from 693 to 684 ft (211.2 to 208.4 m) and in October 1965 to be static at 690 ft (210.3 m). Original total depth of borehole (TD) reported to be 713 ft (217.3 m).

Well #6

(13) Location of well is NE 1/4, NE 1/4, Sec. 24, PSL Blk. 123. This is located 1/4 mile south of pump station. This well was completed at a total depth of 1,209 ft (368.5 m) in 1938. Production was reported as 12 gpm through 8-inch casing.

(14) Operational record dated November 29, 1954, states that well has a total depth of 1,214 ft (370 m) and a static water level of 1,044 ft (318.2 m). Production capacity for this well is given as 20 to 30 gpm, and it is reported that water level will decrease below the pump if rates are greater.

(15) Chemical analyses reported for two consecutive days for well #6 on November 18, 1954.

	7/24/52	7/25/52
pH	7.5	7.6
Total hardness as $CaCO_3$	430	450
Calcium as $CaCO_3$	250	250
Magnesium as $CaCO_3$	180	200
P alkalinity as $CaCO_3$	0	0
Total alkalinity as $CaCO_3$	290	270
Chloride as Cl	72	64
Sulfate as SO_4	288	310
Silica as SiO_2	9	12
Iron as Fe	trace	---
Total solids	980	1000

(16) Driller's log for Well #6.

Interval (ft)		Lithology and comments
From	To	
25	35	Buff and gray lime
35	45	Buff and gray lime, scattered sand grains
45	55	Buff and gray lime, scattered sand grains
55	65	Buff gray lime, fewer sand grains
65	80	Buff gray lime, few quartz grains
80	95	Gray buff lime, rust-colored limey shale
95	105	Gray lime, few quartz grains
105	115	40% gray buff lime, 60% calcite crystals, and few pyrite inclusions
115	127	Gray and buff lime

127	136	Brown dolomite and calcitic lime, crystalline
136	140	90% gray lime, 5% black lime, 5% black limey shale
140	150	Blue lime
150	160	Blue and gray lime
160	196	Blue and gray lime
196	208	Blue and gray lime, scattered sand grains
208	218	80% blue and gray lime, 20% sand with some pyrite
218	229	Blue and gray lime, scattered sand grains
229	233	Blue and gray lime
233	237	70% buff and blue lime, 30% partly rounded quartz grains
237	240	80% buff lime, 20% sand
240	249	90% buff lime, 10% calcitic sand
249	259	Buff lime some calcitic and quartz sand
259	269	Gray buff lime
269	271	Gray buff lime
271	295	Brown dolomitic lime, few calcitic and quartz grains
295	305	Gray buff lime, few calcite grains
305	315	Light brown lime
315	320	Dark brown lime, few calcite grains, some pyrite
320	330	Blue gray lime
330	340	Dark brown lime, few calcite grains
340	360	Dark brown and gray lime
360	370	Dark brown and gray lime, few calcite grains
370	380	Dark gray and light gray lime
380	400	Dark gray and some light brown lime
400	424	Very dark gray lime
424	430	Dark brown lime, few calcite grains
430	440	Brown lime, few calcite grains
440	450	Brown and lighter brown lime
450	490	Dark brown and gray lime
490	500	Light brown and brown lime
500	530	Brown lime
530	540	Dark brown lime
540	550	Dark brown and light lime
550	560	Light brown lime and few calcite grains
560	570	Light brown and little white lime, few calcite grains
570	580	Light and dark brown lime

580	590	Brown lime, 5%-10% calcite grains
590	600	-skipped interval on log-
600	610	Light gray lime, few calcite grains
610	620	Light brown lime
620	640	Dark brown lime
640	650	Dark brown and light brown lime
650	670	Dark gray lime, few calcite grains
670	680	Dark gray and brown lime
680	690	Light brown lime
690	715	Dark brown and brown lime
715	729	Dark brown lime
729	750	Dark gray lime, few calcite grains
750	770	Brown lime, few calcite grains
770	800	Dark brown lime, few calcite grains
800	830	Dark brown lime and brown lime
830	840	Brown lime
840	850	Brown and light brown lime
850	870	Brown lime
870	900	Dark brown lime
900	930	Brown lime
930	940	Dark brown lime
940	950	Brown lime
950	960	Dark brown and brown lime
960	980	Brown lime
980	1000	Brown and light brown lime
1000	1010	Light brown lime
1010	1018	Dark brown lime
1018	1030	Brown lime
1030	1038	Dark brown lime
1038	1062	Brown lime
1062	1068	Brown and light brown lime
1068	1086	Brown lime, semi-frosted quartz grains
1086	1087	Dark brown lime
1087	1094	Light brown lime, few green limey shale flakes, few quartz grains, light brown lime contains fossil remnants
1094	1099	Dark brown lime, numerous frosted quartz grains
1099	1104	Brown lime, numerous frosted quartz grains

1104	1115	Light brown lime, few frosted quartz grains
1115	1120	Light brown lime, some pyrite inclusions
1120	1128	Dark brown lime
1128	1150	Brown lime
1150	1160	Brown lime, few frosted quartz grains
1160	1170	Brown lime, few calcite grains
1170	1175	Dark brown fossiliferous grains
1175	1180	Dark brown lime
1180	1189	Brown lime
1189	1204	Dark brown lime
1204	1209	Dark brown lime and gray lime--TD

Well #8

(17) Well data sheet gives location for this well as NE 1/4, NE 1/4, Sec. 24, PSL Blk. 123 (outside southwest corner of plant location). This well, completed on June 26, 1951, was drilled by Holland Page, Jr., to a TD of 1,288 ft (392.5 m). Well was temporarily plugged and abandoned March 28, 1956, and restored to production on January 20, 1958.

(18) This document is a memorandum to W. H. Miller from M. E. Hawkins reporting the results of pump tests on well #8.

Date	Time	Gallons per minute (gpm)
11/26/51	12:30 p.m.	start test
11/26/51	12:30-4:30 p.m.	45
11/26/51	4:30-11:30 p.m.	30
11/26-27/51	11:30 p.m.-8:30 a.m.	25
11/27/51	8:30 a.m.-10:00 p.m.	20
11/27-28/51	10:00 p.m.-6:30 a.m.	15
11/28-12/5/51	6:30 a.m. to present	12

(19) The following is a synthesis of a combined driller's log and operational report for water well #8.

Date	Interval (ft)	Lithology and comments
6/2/51	0-43	Caliche
6/3/51	43-45	Lime
	45-65	Yellow lime
	65-75	Brown lime
	75-80	Yellow lime
	80-86	Yellow lime
	86-94	Gray lime
6/4/51	94-95	Light brown hard lime
	95-100	Light brown hard lime
	100-106	Lime ballard gray lime
6/5/51	106-114	Lime gray
	114-120	Lime brown hard
	120-124	Lime brown hard
	124-134	Gray lime
	134-140	Gray lime
	140-143	Gray shale
	143-155	Gray lime shells
6/6/51	155-165	Lime, broken medium, little water at 158-160
	165-171	Lime gray hard
	171-175	Lime, broken, little more water at 171-175
	175-190	Broken lime
	190-195	Gray shale
	195-205	Gray lime
6/7/51	205-225	Lime hard sharp
	225-233	Lime hard sharp
	233-239	Sand, report increase in water
	239-240	Hard gray lime
6/8/51	240-245	Lime gray hard
	245-253	Lime broken
	253-270	Lime-sand medium
	270-276	Lime-sand
	276-295	Yellow lime hard

6/9/51	295-310	Lime gray brown hard
	310-325	Brown lime hard
6/10/51	325-340	Lime brown hard
	340-348	Lime
6/17/51	348-355	Lime hard
	355-358	Lime hard
6/18/51	358-360	Lime hard
	360-370	Lime hard
	370-377	Black lime
6/19/51	377-383	Hard lime
	383-397	Hard lime, testing water, 1.5 bailers per hour
6/20/51	397-401	Hard lime
	401-410	Brown lime
	410-421	Brown lime
6/21/51	421-443	Brown lime
	443-450	Brown lime
6/24/51	450-455	Brown lime hard
	455-464	Brown lime hard
	464-480	Brown lime
6/25/51	480-493	Brown lime
	493-513	Brown lime
6/26/51	513-525	Brown lime hard
	525-557	Brown lime
6/27/51	557-571	Lime shells
	571-607	Brown lime
6/28/51	607-618	Broken lime hard
	618-649	Black lime, tested production at 0.5 bailer per hour
6/29/51	649-685	Lime
6/30/51	685-698	Lime
7/1/51	698-710	Lime hard
	710-743	Black lime
7/3/51	743-760	Black lime

7/4/51	760-771	Lime black
	771-777	Gray lime
	777-790	Brown lime
	790-804	Black lime
7/5/51	804-825	Gray lime
	825-843	Blue lime
7/6/51	843-875	Gray lime
7/7/51	875-885	Gray lime hard
	885-908	Gray lime
7/8/51	908-920	Gray lime
	920-933	Gray lime hard
	933-940	Gray lime, tested water production, rate at 1.5 bailers per hour
7/9/51	940-952	Gray lime
	952-963	Hard gray lime
	963-973	Hard gray lime
7/10/51	973-983	Gray lime
7/13/51	983-985	Black lime
7/14/51	985-997	Black lime
	997-1021	Blue gray lime
7/15/51	1021-1051	Blue gray lime hard
7/16/51	1051-1070	Black lime
	1070-1093	Blue gray lime
7/17/51	1093-1131	Blue gray lime
7/18/51	1131-1150	Shale-gray lime
7/19/51	1150-1180	Blue gray lime, possible water from 1170 to 1180, begin testing water-no results
	1180-1200	Black lime
7/20/51	1200-1217	Blue gray lime, testing production-initial rate of 2.5 bailers per hour, increased to 10 bailers per hour
7/21/51	1217-1235	Blue gray lime, tested 5 bailers per hour, hit small crevice at 1225
7/22/51	1235-1266	Shale and lime

7/23/51	1266-1288	Shale and lime, recorded 400 ft (121.9 m) of fluid in the hole, bailed from 11:30 a.m. to 5:30 p.m. (75 bailers full), during one hour delay for equipment repair-water level rose 100 ft, at 530 ft, 65 bailers water 500 ft
7/24/51	1288	Continued bailing, water rose approximately 25 ft (7.6 m) averaged bailing 15 bailers per hour-lowered the water level 40 ft (12.2 m) -shut down 45 minutes and water level rebounded to original level of 250 ft (76.2 m) (Note-the water level of 250 ft mentioned in this entry is unclear because the last entry noted water level of approximately 530 ft (161.5 m)
7/25/51	1288	Started production test. Before starting-water level measured at 590 ft (179.8 m), recovered 23 bailers in 1 hour, water level at 948 ft (288.9 m), after bailing 1,640 gallons bailed (6207.4 L)-bailed 23 to 24 gallons per hour-maximum drawdown measured was 200 ft (60.9 m)
7/26/51	1288	420 ft (128.0 m) of fluid in the hole at beginning of production test-recovered 21 bailers containing 1,425 gal (5393.6 L) lowering water table 100 ft (30.4 m) unable to lower water table below 200 ft (60.8 m)-end of test.

(20) The following chemical analysis as prepared for water well #8 by D. C. Kelly is dated November 18, 1954.

	7/24/51	12/--/51
pH	7.6	7.4
Total hardness as $CaCO_3$	400	405
Calcium as $CaCO_3$	230	240
Magnesium as CaCO3	170	265
P alkalinity as $CaCO_3$	0	0
Total alkalinity as $CaCO_3$	215	230
Chloride as Cl	80	104
Sulfate as SO_4	108	336
Silica as SiO_2	18	17
Iron as Fe	trace	---
Total solids	---	1578

(21) An operational report dated March 1952 provides information about water found in the following intervals in water well #8:

158 ft- 165 ft
171 ft- 175 ft
1170 ft-1190 ft

Static water level is recorded at 626.5 ft (190.9 m). Other remarks in this memo include (1) well does not have a sand trap, (2) is not gravel packed, (3) does have a foot valve, and 4) well does not pump sand.

Appendix 5. (cont.)

Trace ions (mg/L) and isotopic composition.

Aquifer A+

BEG ID	Well name	TWC[1] ID	As	Cd^{2+}	Li^{+}	Fe^{2+}	Sr^{2+}	Ba^{2+}	Br^{-}	F^{-}	$\delta^{18}O$**	δD**	Tritium	$\delta^{34}S$**	$\delta^{13}C$**	PMC†	^{14}C Age††
LL128	Temple Well	48-24-1	<0.05	<0.03	0.07	*0.02	8.04	0.06	0.5	3.0	-9.18	-68.8	4.1	16.11	-5.77	13.47	7,639
LL129	Guillen Exxon Well	48-23-201	<0.05	<0.03	*0.05	0.08	8.25	0.06	0.5	5.2	-9.19	-72.7	2.7	12.11	-5.78	9.56	10,488
LL130	Desert Inn Well	48-14-7	<0.05	<0.03	0.08	0.04	6.14	0.03	0.7	5.1	-9.17	-70.3	3.8	5.56	-8.49	6.74	16,556
LL131	Cornudas Cafe Well	48-13-7	<0.05	<0.03	0.10	<0.02	4.49	0.05	0.7	5.0	-9.18	-69.8	3.5	4.53	-6.07	10.54	10,084
LL132	Williams Ranch House Well	48-20-6	<0.05	<0.03	*0.04	0.03	3.77	0.61	0.6	5.0	-6.90	-50.9	13.7	8.61	-8.00	21.02	6,660
LL133	Puett Well	48-13-8	<0.05	<0.03	0.16	1.62	5.58	0.03	1.0	5.0	-10.21	-81.1	2.3	5.71	-6.36	5.36	16,061
LL134	Hobo Well-Deep	48-20-5	<0.05	<0.03	0.09	1.42	0.09	0.02	0.8	7.2	-8.01	-64.2	2.3	7.70	-8.92	18.46	8,635
LL135	Jardin Well	48-30-4	<0.05	<0.03	0.45	6.97	0.45	0.08	1.4	9.0	-9.15	-67.4	2.8	15.72	-6.79	5.08	17,046
LL136	Sparks Windmill	48-14-9	<0.05	<0.03	0.14	16.3	0.14	0.03	0.7	6.6	-10.53	-81.5	3.3	11.29	-3.64	5.99	10,529
LL137	Sparks House Pump Well	48-14-8	<0.05	<0.03	0.14	2.24	0.14	*0.01	0.7	6.2	-9.53	-71.3	3.2	10.37	-4.67	11.32	7,328
LL138	Williams #4 Well	48-12-8	<0.05	<0.03	0.09	11.8	0.09	0.08	0.8	6.3	-7.91	-65.1	6.8	10.12	-9.65	13.98	11,583
LL139	Stewart #2 Well	48-12-5	<0.05	<0.03	0.10	0.25	0.10	0.03	0.8	5.7	-10.44	-79.6	<0.8	-1.24	-10.35	4.34	21,832
LL140	Adobe House Tank Well	48-21-5	<0.05	<0.03	0.11	5.24	0.11	0.04	0.9	8.5	-9.73	-76.0	8.2	7.05	-5.67	13.02	7,775
LL141	Bravo Well	48-29-3	<0.05	<0.03	0.15	<0.02	0.15	0.02	1.9	9.0	-2.72	-35.3	3.4	5.84	-7.99	46.52	84
LL142	Three Sisters Well	48-29-1	<0.05	<0.03	0.11	0.17	0.11	0.12	1.9	7.7	-8.16	-66.5	<0.8	7.23	-6.27	23.50	3,725
LL143	Sumrall Well	48-16-7	<0.05	<0.03	0.09	<0.02	0.09	0.04	0.39	1.3	-9.26	-64.8	<0.8	11.13	-6.80	19.64	5,880
LL144	Foster House Well	48-14-1	<0.05	<0.03	0.12	0.10	0.12	0.10	0.75	2.7	-9.47	-69.1	2.2	7.81	-7.54	49.5	modern
LL145	Foster South Well	48-13-9	<0.05	<0.03	0.08	0.07	0.08	0.02	0.81	3.0	-9.82	-75.4	4.5	4.26	-7.59	9.71	12,610
LL146	Stewart #1 Well	48-12-5	<0.05	<0.03	0.08	13.0	0.08	0.04	0.93	3.0	-9.79	-73.2	1.9	-0.72	-10.04	4.84	20,678
LL147	Beard #1 Well	48-12-7	<0.05	<0.03	0.13	0.11	0.13	0.09	0.92	3.0	-8.36	-63.8	3.0	6.58	-8.01	6.31	16,618
LL148	Red Well	48-23-7	<0.05	<0.03	0.22	3.10	0.22	0.06	0.96	3.3	-9.71	-75.0	4.5	5.91	-7.46	13.13	9,974
LL149	Sampson Well	48-23-1	<0.05	<0.03	0.11	0.05	0.11	0.03	0.63	2.3	-8.99	-68.6	1.4	9.28	-6.38	16.70	6,691
LL152	Gibbs Well	48-14-4	<0.05	<0.03	0.13	0.03	0.13	0.11	0.69	2.7	-9.69	-72.9	1.2	6.74	-7.58	7.60	14,628
LL153	Dyer #2 Black Mountain South Well	48-31-9	<0.05	*0.03	0.16	0.07	0.16	0.04	0.82	2.7	-8.42	-61.8	<0.8	5.58	-7.09	10.96	11,047
LL154	Flattop Well - Figure 2 Ranch	48-24-9	<0.05	<0.03	0.09	0.35	0.09	0.12	0.50	1.5	-8.90	-61.8	8.1	11.04	-7.40	25.54	4,406
LL155	Dyer #3 Well	48-39-1	<0.05	<0.03	0.19	0.65	0.19	0.07	1.46	3.0	-7.31	-54.8	21.4	2.91	-6.76	9.08	12,210

Appendix 5. Chemical and isotopic composition of ground-water samples, HU1A and HU1B sites, Hudspeth County.

Major ions (mg/L) and temperatures (°C).

Aquifer A+

BEG ID	Well Name	Coordinates		Ca^{2+}	Mg^{2+}	Na^{+}	K^{+}	HCO_3^{-}	SO_4^{2-}	Cl^{-}	NO_3^{-}	TDS	Temp.
LL128	Temple Well	31°44'40"	105°05'25"	320	116	278	11.3	236	820	530	40	2363	22
LL129	Guillen Exxon Well	31°44'48"	105°12'06"	193	79.7	113	5.2	178	680	117	24	1404	25
LL130	Desert Inn Well	31°45'56"	105°21'22"	178	73.5	269	7.0	345	553	305	2.7	1745	24
LL131	Cornudas Cafe Well	31°46'45"	105°28'09"	146	63.7	325	10.0	293	580	312	3.8	1744	24
LL132	Williams Ranch House Well	31°41'31"	105°30'09"	95.1	37.1	100	2.7	299	170	78	92	884	25
LL133	Puett Well	31°46'38"	105°26'53"	199	86.6	462	12.7	332	950	405	<1.0	2462	23
LL134	Hobo Well-Deep	31°41'44"	105°33'07"	157	73.2	308	5.8	352	710	202	<1.0	1827	22
LL135	Jardin Well	31°33'27"	105°21'25"	169	60.9	964	40.5	412	580	1300	<1.0	3552	23
LL136	Sparks Windmill	31°46'18"	105°16'45"	605	193	259	11.7	243	2210	245	<1.0	3803	22
LL137	Sparks House Pump Well	31°45'39"	105°18'04"	497	121	310	9.2	263	1470	401	<1.0	3095	20
LL138	Williams #4 Well	31°46'21"	105°33'09"	176	80.5	238	5.9	283	740	172	<1.0	1722	22
LL139	Stewart #2 Well	31°48'30"	105°32'52"	358	133	303	5.8	430	1490	122	2.4	2859	21
LL140	Adobe House Tank Well	31°41'10"	105°25'18"	111	48.6	249	7.9	328	510	147	26	1445	22
LL141	Bravo Well	31°36'14"	105°24'27"	95.2	69.8	381	5.9	177	690	275	76	1787	25
LL142	Three Sisters Well	31°36'10"	105°28'18"	118	60.1	290	3.7	251	570	209	99	1616	22
LL143	Sumrall Well	31°45'57"	105°05'20"	252	95.2	303	9.1	290	660	500	10	2126	23
LL144	Foster House Well	31°51'44"	105°21'44"	213	86.8	340	8.4	300	730	410	1.3	2103	26
LL145	Foster South Well	31°47'15"	105°22'47"	141	59.4	182	4.3	340	530	110	7.0	1384	21
LL146	Stewart #1 Well	31°48'29"	105°32'56"	258	102	225	4.9	400	1040	91	<1.0	2145	19
LL147	Beard #1 Well	31°46'07"	105°37'02"	166	87.6	408	7.1	400	840	340	6.0	2267	22
LL148	Red Well	31°37'47"	105°14'20"	153	60.4	416	18.3	320	540	490	10	2021	20
LL149	Sampson Well	31°42'04"	105°12'45"	216	86.2	267	9.0	280	590	410	30	1898	22
LL152	Gibbs Well	31°49'17"	105°20'17"	203	82.9	328	10.3	310	700	380	1.0	2027	21
LL153	Dyer #2 Black Mountain South Well	31°31'20"	105°09'33"	113	52.8	324	14.6	370	290	400	9	1581	22
LL154	Flattop Well-Figure 2 Ranch	31°37'49"	105°02'10"	218	80.4	265	9.7	290	550	420	16	1857	24
LL155	Dyer #3 Well	31°28'16"	105°13'16"	150	77	400	14.5	370	700	340	13	2077	19

Appendix 5. (cont.)

Major ions (mg/L) and temperatures (°C).

Aquifer B+

BEG ID	Well Name	Coordinates		Ca^{2+}	Mg^{2+}	Na^{+}	K^{+}	HCO_3^{-}	SO_4^{2-}	Cl^{-}	NO_3^{-}	TDS	Temp.
LL150	South Well	31°35'29"	105°30'08"	97	50.7	247	4.3	240	470	140	63	1322	20
LL151	Dyer #1 Ranch House	31°29'45"	105°21'59"	89.3	58	519	6.7	400	830	230	105	2247	21
LL156	Baylor - New Well	31°28'05"	105°22'59"	66.3	36.6	164	3.3	200	230	130	99	936	22
LL157	Baylor - Old Well	31°27'38"	105°24'51"	85.2	22.4	87.3	3.3	240	110	61	100	715	20

Aquifer B+

BEG ID	Well name	TWC[1] ID	As	Cd^{2+}	Li^{+}	Fe^{2+}	Sr^{2+}	Ba^{2+}	Br^{-}	F^{-}	$\delta^{18}O$**	δD**	Tritium	$\delta^{34}S$**	$\delta^{13}C$**	PMC†	^{14}C Age††
LL150	South Well	48-28-3	<0.05	<0.03	0.10	0.06	0.10	0.16	1.74	3.7	-8.27	-63.0	0.9	6.87	-5.40	35.77	modern
LL151	Dyer #1 Ranch House	48-38-1	<0.05	<0.03	0.14	0.03	0.14	0.02	2.06	3.7	-8.19	-64.7	<0.8	6.34	-5.65	11.82	8,544
LL156	Baylor-New Well	48-37-3	<0.05	<0.03	0.07	<0.02	0.07	0.04	1.31	3.0	-7.38	-57.4	9.5	6.65	-4.73	39.43	modern
LL157	Baylor-Old Well	48-37-3	<0.05	<0.03	0.06	0.19	0.06	0.14	0.60	3.0	-7.04	-46.4	32.0	9.00	-4.75	90.77	modern

+ see fig. 7 for distribution
< less than indicated value
* reported value near detection limit
** $\delta^{18}O$ and $\delta^{2}H$ are defined relative to SMOW. $\delta^{34}S$ is given as deviation from the Canyon Diablo Meteorite standard. $\delta^{13}C$ is defined relative to Pee Dee Belemnite carbonate.
† PMC is percent of modern carbon
†† ^{14}C age was corrected by using $\delta^{13}C$ values (Kreitler and others, 1986b; their Appendix 5)

[1]TWC's well identification system has 3 sets of numbers; preliminary wells have only one number in the last set, permitted wells have 3.

Appendix 6.

A. Chemical and isotopic composition of ground-water samples, Fort Hancock site (Kreitler and others, 1986a).

Major ions (mg/L) and temperatures (°C).

BEG ID	Well name	Coordinates		Ca^{2+}	Mg^{2+}	Na^{+}	K^{+}	HCO_3^{-}	SO_4^{2-}	Cl^{-}	NO_3^{-}	TDS	Temp.
LL107	48-42-1 Windmill	31°22'12"	105°50'52"	169.0	35.3	1250	7.7	161	2270	520	1.3	4422	24.5
LL108	48-42-404 Well	31°18'56"	105°51'27"	34.7	11.9	410	4.5	263	395	259	5.1	1388	22.5
LL109	48-41-618 Well	31°17'31"	105°52'45"	23.8	23.9	486	14.6	96	315	555	<0.5	1517	
LL110	48-41-2 Well	31°19'37"	105°54'55"	387.0	91.7	881	12.8	495	770	1450	<0.5	3604	19
LL111	48-33-9 Windmill	31°23'18"	105°53'18"	26.8	10.5	327	4.2	242	360	168	11.4	1154	21
LL112	Head of Canyon WM	31°31'42"	105°42'05"	61.6	19.3	177	5.4	282	168	116	26.5	862	14
LL113	Wilkey Well no. 1	31°23'23"	105°40'48"	77.1	43.1	237	3.4	336	438	88	11.8	1241	20
LL114	Wilkey Well no. 2	31°22'48"	105°39'07"	131.0	24.6	55	1.5	284	275	10	11.3	801	11
LL115	Gunsight Windmill no. 1	31°25'03"	105°30'20"	37.3	22.1	454	7.4	411	570	137	<0.5	1649	19
LL116	Owens Well	31°22'31"	105°45'50"	48.4	15.3	362	3.5	278	525	128	<0.5	1369	14
LL126	Low Level Well	31°24'14"	105°43'32"	70.7	6.9	549	4.4	60	710	416	18.3	1850	17
Springs:													
LL106	Thaxton Sp	31°28'11"	105°42'57"	26.8	22.9	475	4.6	501	520	148	11.3	1718	9

Trace ions (mg/L) and isotope composition[1] in ground-water samples.

BEG ID	Well name	Coordinates		As	Cd^{2+}	Li^{+}	Fe^{2+}	Sr^{2+}	Ba^{2+}	Br^{-}	F^{-}	$\delta^{18}O$	$\delta^{2}H$	Tritium	$\delta^{34}S$	$\delta^{13}C$	PMC[2]	^{14}C Age[3]
LL107	48-42-1 Windmill	31°22'12"	105°50'52"	0.012	<0.03	0.26	0.04	3.20	0.02	2.66	1.05	-8.0	-59	<0.8	1.0	-16.8	16.6	14,748
LL108	48-42-404 Well	31°18'56"	105°51'27"	0.017	<0.03	0.10	0.05	1.01	0.04	1.25	2.37	-6.9	-48	<0.8	3.8	-9.6	61	Modern
LL109	48-41-618 Well	31°17'31"	105°52'45"	<0.01	<0.03	0.21	0.02	1.43	0.01	0.59	0.39	-7.4	-71	27.2	16.9			
LL110	48-41-2 Well	31°19'37"	105°54'55"	<0.01	<0.03	0.26	1.35	6.69	0.06	2.27	0.61	-8.8	-74	21.8	4.7	-12.0	116	Modern
LL111	48-33-9 Windmill	31°23'18"	105°53'18"	<0.01	<0.03	0.10	0.49	0.81	0.02	1.01	2.03	-7.3	-51	<0.8	7.2	-10.1	21.8	8,288
LL112	Head of Canyon Windmill	31°31'42"	105°42'05"	<0.01	<0.03	0.06	0.10	1.72	0.02	1.14	2.79	-7.1	-50	11.8	5.8	-8.0	43	833
LL113	Wilkey Well no. 1	31°23'23"	105°40'48"	<0.01	<0.03	0.05	0.71	3.90	0.03	0.77	1.60	-7.7	-58	3.74	5.2	-9.4	36	3,529
LL114	Wilkey Well no. 2	31°22'48"	105°39'07"	<0.01	<0.03	0.03	<0.02	7.50	0.03	0.44	0.90	-7.5	-54	20.67	10.9	-11.3	60	868
LL115	Gunsight Windmill no. 1	31°25'03"	105°30'20"	<0.01	<0.03	0.12	2.15	3.32	0.03	1.15	3.10	-10.7	-83	0.5	-0.5	-7.9	9.6	13,071
LL116	Owens Well	31°22'31"	105°45'50"	<0.01	<0.03	0.07	0.20	2.87	0.12	1.10	4.30	-8.0	-62	1.52	7.0	-7.8	8.9	13,520
LL126	Low Level well	31°24'14"	105°43'32"	<0.05	<0.03	0.10	0.13	8.30	0.19	2.10	4.30	-8.3	-61	3.0	4.1	-18.1	3.3	27,400
Springs:																		
LL106	Thaxton Sp	31°28'11"	105°42'57"	<0.01	<0.03	0.13	0.02	1.63	0.02	1.34	5.57	-7.5	-58	<0.8	-1.8			

Appendix 6. (cont.)

B. Chemical composition (mg/L) of ground water from selected wells (Texas Water Development Board [TWDB], 1985).

BEG ID	TWDB ID	Ca^{2+}	Mg^{2+}	Na^{+}	K^{+}	HCO_3^{-}	SO_4^{2-}	Cl^{-}	F^{-}	NO_3^{-}	TDS
LL170	48-07-101	324	139	168	-	193	1,300	145	-	31.0	2,220
LL171	48-07-102	598	164	250	-	214	2,142	267	2.0	8.7	3,555
LL172	48-07-206	459	225	640	-	172	2,230	594	3.1	286.0	4,563
LL173	48-07-207	364	136	119	-	227	1,220	156	1.8	14.1	2,140
LL174	48-07-210	326	158	267	-	240	1,180	405	1.8	51.0	2,520
LL176	48-07-304	332	124	175	-	248	860	408	1.8	7.0	2,045
LL177	48-07-405	435	219	471	-	195	1,630	800	2.4	110.0	3,779
LL178	48-07-414	324	134	481	-	260	1,120	750	1.9	29.5	2,983
LL180	48-07-501	358	264	510	-	138	1,670	890	2.1	39.0	3,817
LL183	48-07-606	368	220	338	-	259	1,230	670	2.1	42.0	3,011
LL184	48-07-607	350	137	121	-	238	910	415	1.5	3.5	2,070
LL185	48-07-706	264	82	392	1.2	294	703	667	1.1	4.87	2,276
LL187	48-07-801	538	306	952	-	231	2,117	1,512	1.8	44.20	5,603
LL188	48-07-803	500	199	820	-	123	2,110	1,120	2.6	42.0	4,869
LL189	48-07-901	215	87	160	-	95	700	320	1.4	3.50	1,548
LL190	48-07-904	522	248	773	-	255	1,646	1,400	1.6	22.60	4,757
LL192	48-06-201	560	166	40	-	229	1,910	20	2.7	0.40	2,831
LL193	48-06-601	520	178	58	-	201	1,900	27	2.7	0.40	2,804
LL194	48-15-203	266	77	378	1.1	293	681	615	1.1	5.01	2,184
LL195	48-15-301	280	81	326	-	293	720	550	1.6	7.00	2,125
LL202	47-09-803	222	99	156	-	279	660	256	-	3.50	1,549
LL203	47-09-805	171	70	82	-	283	439	126	1.0	0.10	1,044

1) $\delta^{18}O$ and $\delta^{2}H$ are defined relative to SMOW. $\delta^{34}S$ is given as deviation from the Canyon Diablo Meteorite standard. $\delta^{13}C$ is defined relative to Pee Dee Belemnite carbonate.
2) PMC is percent of modern carbon.
3) ^{14}C age was corrected by using $\delta^{13}C$ values (Kreitler and others, 1986b), except for sample LL126.

Appendix 7. Lithologic and structural descriptions of test holes.

Two boreholes drilled as part of this study were continuously cored from the top of bedrock to a total depth of 150 ft (46 m). Lithologic logs for both boreholes are presented below.

HU1A (fig. A7-1)

Bedrock was encountered in HU1A-BEG #1 at a depth of 8 ft (2.4 m). Alluvial cover from 0 to 5 ft (0 to 1.5 m) consisted of tan to brown, sand to silty sand, with minor occurrences of caliche. From 5 ft (1.5 m) to 8 ft (2.4 m) the alluvium became increasingly coarser with gravels of predominantly rhyolite composition. The dark-red rhyolite porphyry has pink feldspar and clear glassy quartz phenocrysts that range in size from 0.1 to 0.4 inches (0.2 to 1.0 cm). Chlorite is a common alteration product. Limonite and hematite stains also occur on fracture surfaces in the core. Fifty percent of the rhyolite porphyry core from site HU1A is fractured. Lithologic descriptions, fractured intervals, and fracture orientations are presented below.

HU1B (fig. A7-2)

Bedrock was encountered in HU1B-BEG#1 at a depth of 18 ft (5.4 m). Alluvial cover at this site consisted of tan to brown sand with abundant caliche nodules from 0 to 8 ft (0 to 2.4 m); tan to yellow clay with variable amounts of brown sandstone gravels and minor inclusions of interbedded silts and sands from 8 to 18 ft (2.4 to 5.4 m). Cretaceous bedrock encountered at 18 ft (5.4 m) consisted of a limestone breccia to 20.3 ft (6.2 m). Cretaceous Cox sandstone consists at

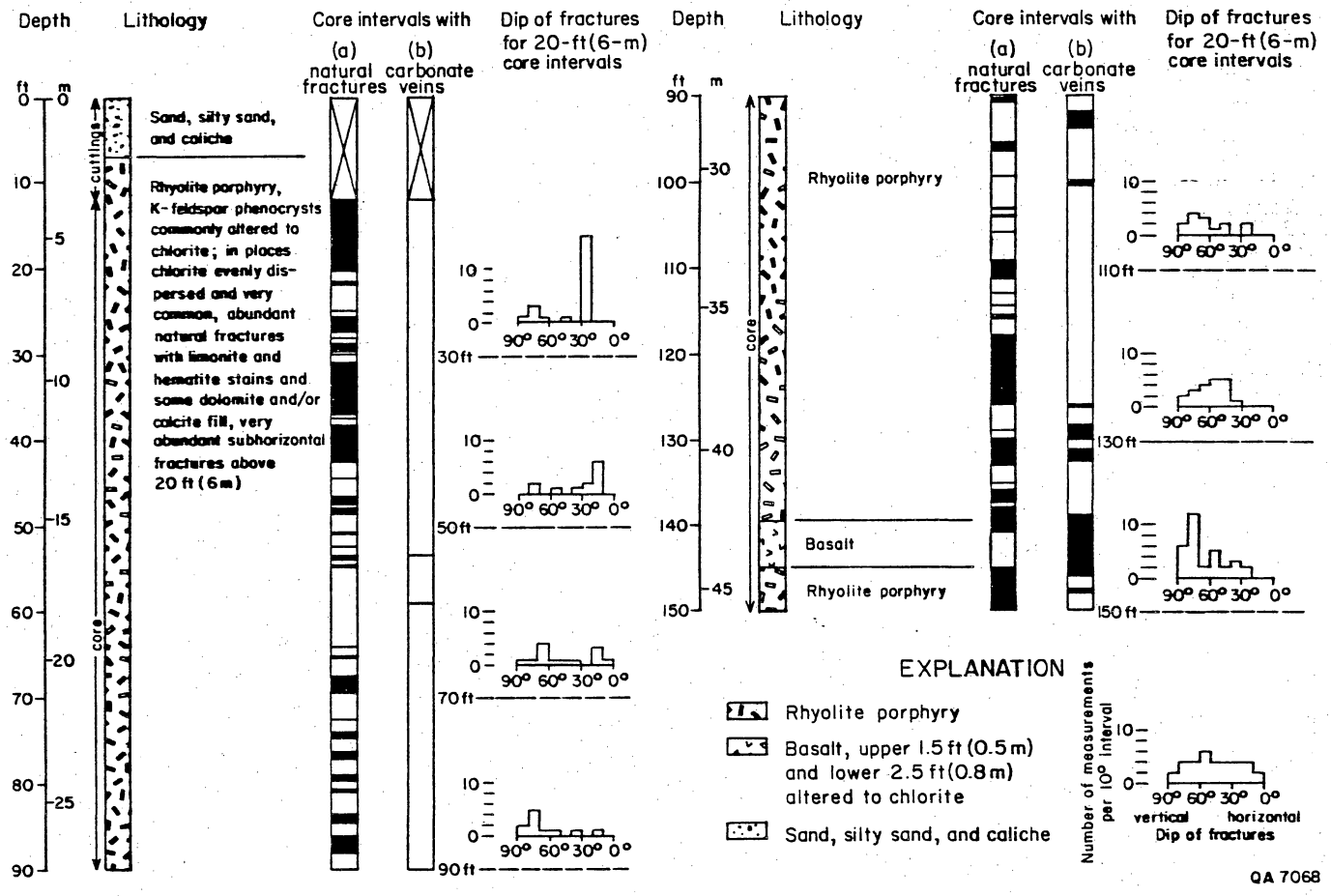

Figure A7-1. Lithologic log for the rhyolite core from HU1A site.

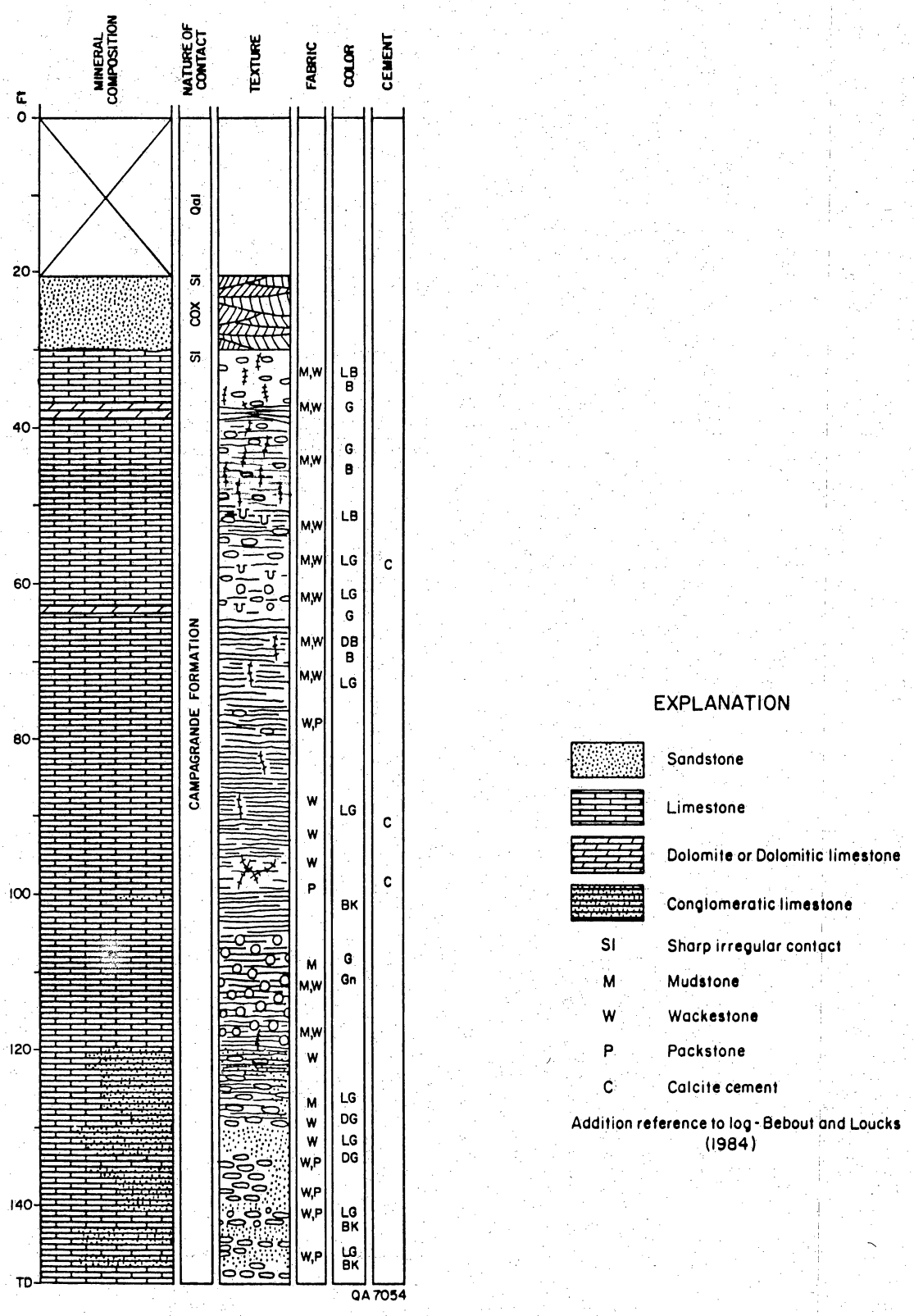

Figure A7-2. Lithologic log for the limestone core from HU1B site.

this location of a predominantly gray crossbedded sandstone interbedded with thin purple layers of quartz grains, and was recorded from 20.3 ft (6.2 m) to 30.8 ft (9.3 m). This interval recorded variable amounts of fracturing. Oxidation of iron minerals in this interval was prevalent.

From 30.8 ft (9.2 m) to total depth at 150 ft (45.7 m) the stratigraphic interval was Cretaceous Campagrande limestones. This interval is dominated by nodular limestones in the upper section, becoming more conglomeratic in the lower section. Logging descriptions used are based on the system of Bebout and Loucks (1984).

Appendix 8. Climate and vegetation controls on surface recharge.

Differences in annual rates of precipitation, evaporation, temperature, and dominant plant ecosystems between sites HU1A and HU1B on the Diablo Plateau and the Fort Hancock site in the Hueco Bolson may influence the potential for surface recharge. Distinct differences between the two areas in climate, surface and near-surface lithologies, and vegetation have been reviewed to determine how they may affect surface recharge. Further study is required to quantify actual levels of evapotranspiration at both areas before final conclusions are drawn.

Trans-Pecos Climate

Regional climatic data for Hudspeth and El Paso Counties have been previously discussed (Kreitler and others, 1986a). The region has a subtropical arid climate (Larkin and Bomar, 1983) characterized by (1) high mean temperatures and marked fluctuations over broad diurnal and annual ranges and (2) low mean precipitation with widely separated annual extremes (Orton, 1964). Rainfall in this climate is inadequate to support vegetation other than desert and semi-desert types.

Precipitation and temperature (minimum and maximum) data were selected for five monitoring stations in the area (fig. A8-1; table A8-1) (National Weather Service, 1986a, b, c). Three of these are located within the Hueco Bolson at the El Paso Airport, in Fabens, and in Fort Hancock. Two stations on the Diablo Plateau were also monitored. They are at Sierra Blanca, south of the study area, and at Cornudas, northwest of the study area. Only the El Paso Airport station had complete records for extended lengths of time. Data from the other four stations are incomplete.

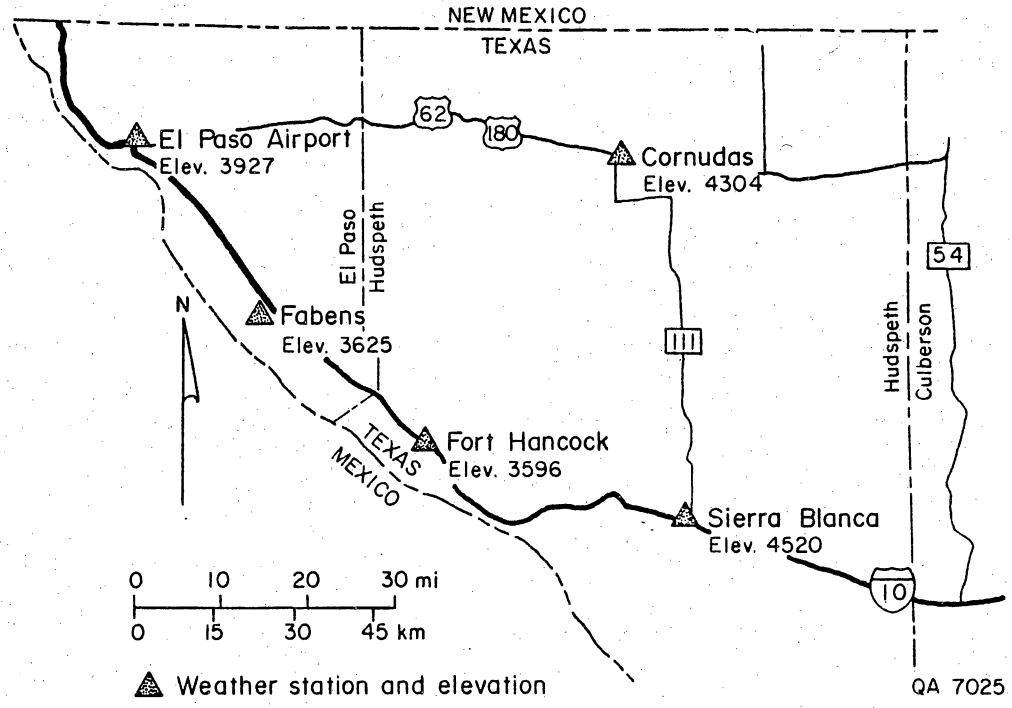

Figure A8-1. Weather stations location map. Three stations (El Paso, Fabens, and Fort Hancock) are in the Hueco Bolson area, whereas two stations (Sierra Blanca and Cornudas) are in the Diablo Plateau.

Table A8-1. Climatic data for Hueco Bolson and Diablo Plateau in the study area.

Monitor Station (Elevation in ft)	Latitude/ Longitude	Annual Average			Summer Average (June - Sept.)		
		Rainfall (inches)	Minimum Temperature (°F)	Maximum Temperature (°F)	Rainfall (inches)	Minimum Temperature (°F)	Maximum Temperature (°F)
Cornudas Service Station (4304)	31°47'00" 105°28'00"	10.2	42.5	77.7	6.24	59.1	91.9
El Paso WSO AP (3927)	31°48'00" 106°24'00"	9.53	49.0	77.9	5.56	65.5	94.0
Fabens (3625)	31°30'00" 106°09'00"	9.65	45.2	77.8	6.96	62.5	91.6
Fort Hancock (3596)	31°17'00" 105°51'00"	10.27	44.1	79.8	6.48	61.9	95.0
Sierra Blanca (4520)	31°11'00" 105°21'00"	13.45	43.9	77.3	9.28	59.7	90.2

National Weather Service (NWS) records were used to describe the climate of the study area. Monthly totals for precipitation and monthly averages for minimum and maximum temperatures were recorded at the above-mentioned five stations. No year with incomplete data was used; data from some stations represent different years. Ten complete years of data were assembled for each station except Fort Hancock, which had only 7 years of precipitation data. Mean annual, monthly, and summer (June to September) values for precipitation and temperatures were calculated along with their standard deviation. The results are presented in table A8-1.

Most annual precipitation occurs as afternoon thundershowers from June to September. These thundershowers are the result of moist air from the Gulf of Mexico moving northwest into the Trans-Pecos area during the hurricane season. At the Cornudas service station, annual precipitation has averaged 10.2 inches (25.9 cm) and average summer precipitation is 6.24 inches (15.8 cm) or 61% of the annual total over 33% of the time. Similar values were observed at the other stations.

Changes in elevation have a direct effect on both temperature and precipitation patterns. The difference in elevation between Cornudas and Fort Hancock is approximately 708 ft (215 m), and the difference in average temperatures is 2.1°F for maxima and 1.6°F for minima. Average precipitation totals for both Cornudas and Fort Hancock are 10.2 inches (25.9 cm) and do not reflect the difference in elevations. Sierra Blanca, however, records a greater average annual precipitation of 13.45 inches (34.1 cm).

The degree to which an increase in temperature within the Hueco Bolson affects potential evaporation, and thus evapotranspiration changes between the bolson and plateau are unknown. Quantitative data on potential evaporation in the area are from two stations in Ysleta, both of which are in the bolson east of El Paso. The adjusted annual mean evaporation for these stations ranges from 93.1 inches (2.4 m) in 1944 to 116.4 inches (3 m) in 1956 (Dougherty, 1975). Scalapino (1950)

reported that the annual potential evaporation in the Dell City area is nine times greater than the annual precipitation. If the only variables in the two systems were precipitation and temperature, the potential for evapotranspiration in the bolson would be greater, and, thus, the potential for surface recharge to the water table would be more probable on the Diablo Plateau.

Fort Hancock Area - Hueco Bolson Plant Ecosystems

Common plant ecosystems in the Hueco Bolson north of Fort Hancock are representative of desert shrublands (taxonomic identification assisted by Kenneth Moore, personal communication, 1986; Correll and Johnston, 1970). Most of the annual vegetative production is from woody plants with running mesquite (*Prosopis sp.*) dominant in areas of rolling sandy loams and the creosote bush (*Larrea tridentata*) more dominant in gravelly areas. Annual plant production from herbaceous plants is low, averaging 500 pounds per acre (ppa). Commonly, bare land surface exists between woody plants, a controlling factor in the low plant production. Annual grasses may also constitute a large part of the plant production.

Other woody plants common in the area are javelina bush (*Condalia ericoides*), yucca (*Yucca sp.*), and cactus (Cactaceae family). Minor populations of four-wing salt bush (*Atriplex canescens*) and broomweed or snakeweed (*Xanthocephalum sp.*) are also present. Perennial grasses in the area include bush muhly (*Muhlenbergia porteri*), dropseed (*Sporobolus sp.*), fluffgrass (*Erioneuron pulchellum*), and burro grass (*Scleropogon brevifolius*).

The area on the Diablo Plateau in the vicinity of HU1A and HU1B is a desert grassland. Numerous annual and perennial grasses may be found in the area but only sparse occurrences of woody vegetation. Annual plant production from desert grasslands may be considerably higher than has been reported for desert shrublands, ranging from 1,000 to 5,000 ppa. Dominant annual grasses of the area include blue grama (*Bouteloua gracilis*), black grama (*Bouteloua eriopoda*), tobosa grass (*Hilaria mutica*), plains bristlegrass (*Setaria macrostachya, S. texana,* and *S. leucopila* collectively), and side-oats grama (*Bouteloua curtipendula*).

Perennial grasses may also represent a large segment of the desert grassland ecosystem. Several of these species are *Muhlenbergia, Sporobolus*, along with vine-mesquite (*Panicum obtusum*), burro grass (*Scleropogon brevifolius*), and fluffgrass *(Erioneuron pulchellum*). In local areas that receive additional water from runoff, such as in draws, Cane bluestem (*Andropogon sp.*) and Sacaton grass (*Sporobolus sp.*) may also be dominant part of the ecosystem.

Woody vegetation is rare in the desert grassland, except where the soil is sandy or gravelly. Woody vegetation that occasionally dominates the draws includes vine ephedra (*Ephedra pedunculata*), several species of the cactus family, the creosote bush (*Larrea tridentata*), desert sumac (*Rhus microphylla*), yucca (*Yucca sp.*), and the javelina bush (*Condalia cricoides*).

Discussion

The correlation between temperature, precipitation, and dominant plant ecosystem discussed above influences evapotranspiration rates and potential for surface recharge. High tritium levels in several sampled wells on the Diablo Plateau indicate surface

recharge activity significantly higher than that measured in the Hueco Bolson, north of Fort Hancock (fig. 14, this report; Kreitler and others, 1986b). Greater rainfall and lower temperatures may be directly related to active surface recharge on the Diablo Plateau. However, increases in precipitation may not affect surface recharge in the Diablo Plateau because the denser plant populations may absorb more water, whereas shrublands lose water during runoff infiltration due to less extensive or less efficient root systems. There is a large difference between plant production in the bolson (500 ppa) and on the plateau (up to 5,000 ppa). Quantification of evapotranspiration rates in both areas would facilitate a better understanding of recharge mechanism and recharge potential in the bolson and on the plateau.

Appendix 9. Chloride and annual recharge data at HU1B.

Borehole I.D.	Total depth (ft) [A^+ top of bedrock]	Total number of chloride samples collected	Test hole geological setting	Bulk density of soil at surface (gm/cm^3)	Cl_s	Calculated Recharge to Cretaceous Bedrock (inch/year)		
						Clp = 3.71 mg/l San Angelo	Clp = 0.6 mg/l Amarillo	Clp = 0.79 mg/l Midland
C1	23.5	4	Arroyo	1.37	135.5	.3230	.0522	.0688
C2	30.5	6	Interarroyo	1.41	10,226.6	.0043	.0007	.0009
C3	21.0	4	Interarroyo	1.33	11,536	.0038	.0006	.0008
C4	26.0	6	Minor arroyo	1.29	2,286	.0191	.0031	.0041
C5	13.0	3	Interarroyo	1.36	4,901	.0089	.0014	.0019
C6	18.0	4	Arroyo	1.39	3,292	.0133	.0021	.0028
C7	23.0	5	Interarroyo	1.42	6,093	.0072	.0012	.0015
C8	14.0	3	Interarroyo	1.41	4,211	.0104	.0017	.0022
C9	16.0	4	Interarroyo	1.42	5,326	.0082	.0013	.0017
C10	19.0	4	Interarroyo	1.23	5,020	.0087	.0014	.0018
C11	5.5	2	Closed depression	1.27	186	.2353	.0381	.0501

P (average annual precipitation) = 11.8 inches, the average of Cornudas (10.2 inches) and Sierra Blanca (13.45 inches).